

**Exploring CRISPR/Cas9 as a tool to
investigate the role of Androgen
Receptor in basal to luminal cell
differentiation using human
prostate cell lines**

Georgina Lucy Kathleen McDonald

MSc (by Research)

University of York

Biology

December 2018

Abstract

The prostate epithelium is defined in terms of a hierarchical structure, where each cell type can differentiate into the next cell in the lineage until terminally differentiated luminal cells are formed. Androgen receptor (AR) appears to be essential for differentiation of basal to luminal cells. However previous research was predominantly conducted on mouse models, which have a different epithelial structure and therefore this project focussed on 3D models of human prostate cell lines. This project aims to knockout (KO) *AR* in BPH-1 PPmO cells (benign cell line with fluorescent differentiation indicator) and P4E6 cells (localised cancer cell line) using CRISPR/Cas9, then to generate tools with which to investigate the effects of AR KO on prostate differentiation. The hypothesis was that AR expression is essential for cell differentiation during prostate cancer (PCa) development. Copy number analysis determined that BPH-1 PPmO contains three copies of AR, whilst P4E6 contains one copy. This allowed for the generation of P4E6 homozygous and BPH-1 PPmO heterozygous clones. The CRISPR/Cas9 lentivirus successfully created edits in both cell lines, with the highest efficiency occurring in P4E6 cells. Analysis via qRT-PCR confirmed that AR was successfully knocked out in both the BPH-1 PPmO and P4E6 clones. Growing prostate basal cells in 3D culture induces differentiation and the expression of *AR*, by mimicking the prostate *in vivo*. The differentiation indicator only fluoresced in wild-type (WT) BPH-1 PPmO spheroids, indicating AR may indeed be required for differentiation. However the survival of ARKO clones demonstrated that AR is not essential for basal cell survival. Future work should focus on further optimising differentiation via the addition of retinoic acid (RA) to spheroids and engrafting the edited cell lines into immunocompromised mouse models. This project has generated a wide selection of ARKO models which are suitable for the investigation of the role of AR during PCa development.

Table of Contents

Abstract.....	2
List of Tables.....	8
List of Figures	9
Acknowledgements.....	11
Declaration.....	12
1. Introduction	13
1.1 The Prostate Gland	13
1.1.1 Development of the Prostate	15
1.1.2 The Adult Prostate Epithelium	18
1.2 Prostate Cancer.....	22
1.2.1 Premalignancies of prostate cancer	22
1.2.2 Epidemiology	24
1.2.3 Diagnosis	24
1.2.4 Treatment of localised tumours	25
1.2.5 Treatment of metastatic tumours	26
1.2.6 Treatment of castrate resistant prostate cancer	27
1.2.7 Clonal evolution model.....	28
1.2.8 Cancer stem cell model.....	28
1.2.8.1 Evidence luminal cells are the cell of origin	30
1.2.8.2 Evidence Basal Cells are the Cell of Origin	31
1.3 Androgen Receptor.....	31
1.3.1 Gene structure.....	31
1.3.2 Genomic and non-genomic signalling pathways.....	35
1.3.3 The role of AR in PCa.....	37
1.3.4 Adaptations of AR signalling in CRPC.....	37
1.3.5 The role of AR in differentiation.....	38

1.4 Genetic Engineering Technologies Using Programmable Nucleases	40
1.4.1 ZFNs.....	41
1.4.2 TALENs.....	42
1.4.3 CRISPR/Cas9.....	44
1.4.3.1 Applications of CRISPR/Cas9.....	46
1.5 Models Used to Study Prostate Cancer.....	47
1.5.1 Culture of cell lines in 2D.....	47
1.5.2 Culture of cell lines in 3D.....	50
1.5.3 Culture of patient primary cells.....	50
1.5.4 Mouse models.....	50
1.6 Research Aims.....	53
2. Materials and Methods	54
2.1 Mammalian cell culture.....	54
2.1.1 Cell culture of cell lines.....	54
2.1.2 Live cell counting using a haemocytometer.....	54
2.1.3 Cryopreservation of cell cultures.....	55
2.2 Generation and Identification of AR Knock-Out Clones.....	55
2.2.1 Minimal lethal dose of puromycin.....	55
2.2.2 CRISPR/Cas9 transduction.....	56
2.2.3 Ring cloning.....	56
2.2.4 Dilution cloning.....	56
2.2.5 Sanger sequencing.....	57
2.3 Isolation and Analysis of Genomic DNA.....	57
2.3.1 DNA extraction.....	57
2.3.2 PCR.....	58
2.3.2.1 AR master mix and PCR programme.....	58
2.3.2.2 EMX1 master mix and PCR programme.....	58
2.3.4 PCR Purification.....	59

2.3.5 Gel electrophoresis.....	59
2.3.6 Copy number analysis of genomic <i>AR</i>	59
2.4 Isolation and Analysis of Protein Expression	60
2.4.1 Protein extraction.....	60
2.4.2 Bicinchoninic acid assay (BCA) for protein concentration determination	60
2.4.3 SDS-PAGE gel electrophoresis.....	61
2.4.4 Western blotting.....	61
2.5 <i>In vitro</i> Differentiation of Prostate Epithelial Cells.....	62
2.5.1 Development of an epithelial bilayer	62
2.5.2 3D co-Culture of prostate spheroids.....	62
2.5.2.1 Quantification of mOrange Expression.....	63
2.6 Detection of <i>AR</i> Expression.....	63
2.6.1 Spheroid cell recovery.....	63
2.6.2 RNA extraction	64
2.6.3 cDNA synthesis.....	64
2.6.4 Quantitative reverse transcriptase (qRT-PCR) detection of <i>AR</i> mRNA.....	65
2.7 Paraffin-embedding and Sectioning of Prostate Spheroids.....	66
2.7.1 Collection and preparation of spheroids	66
2.7.2 Paraffin-embedding spheroids	66
2.7.3 Sectioning spheroids	67
2.8 Immunohistochemistry of spheroids.....	67
2.9 Cell Viability Assay	69
2.10 Statistical Analyses	70
3. Results.....	71
3.1 Generation of <i>AR</i> Knock-Out in Basal Prostate Cells.....	71
3.1.1 Basal cell lines contain one or more copies of <i>AR</i>	71
3.1.2 Determination of minimal lethal dose of puromycin.....	73

3.1.3 PCR Optimisation of <i>AR</i> primers.....	75
3.1.4 CRISPR/Cas9 successfully produced <i>AR</i> KO clones in basal prostate cell lines.....	77
3.2 Inducing Differentiation of Basal Cells into Luminal Cells	89
3.2.1 Basal cell lines do not express <i>AR</i>	89
3.2.2 Growth in DHT for 24 hr is insufficient to induce full length <i>AR</i> expression.....	91
3.2.3 Culturing cell lines into a bilayer is insufficient to induce differentiation	93
3.2.4 Co-culturing basal cells with stroma to form 3D spheroids induces differentiation and <i>AR</i> expression	96
3.2.4.1 The effects of calcium on differentiation and <i>AR</i> expression.....	98
3.2.4.2 <i>AR</i> expression is reduced in <i>ARKO</i> clones	101
3.3 Characterising Differentiated <i>ARKO</i> Clone Spheroids	103
3.3.1 Cell viability assay optimisation.....	103
3.3.2 Spheroid morphology and structure varies between cell lines.....	105
3.3.3 Optimisation of <i>AR</i> and <i>NKX3.1</i> IHC antibodies	107
3.3.4 <i>BPH-1 PPMO</i> and <i>P4E6</i> spheroids display heterogeneous expression of differentiation markers	109
3.3.5 <i>AR</i> is potentially required for differentiation	116
4. Discussion	118
4.1 CRISPR/Cas9 is a successful tool to generate gene KO models.....	118
4.1.1 Therapeutic relevance of CRISPR/Cas9.....	120
4.2 The role of <i>AR</i> in the prostate epithelium	121
4.2.1 <i>AR</i> may be required for differentiation	121
4.2.2 Terminally differentiated luminal cells undergo apoptosis	124
4.2.3 <i>AR</i> is not required for basal cell survival.....	125
4.2.4 Identification of <i>AR</i> splice variants	126
4.3 Immortalisation of cell lines results in genomic instability	127
4.4 Future work and concluding remarks.....	128
Appendix.....	131

Abbreviations	146
References.....	154

List of Tables

Table 1.1: Cell types found in prostate epithelia and their known expressed markers.	21
Table 1.2: A list of prostate epithelial cells and their respective AR expression and responsiveness to androgen.....	33
Table 1.3: Comparison of different genetic engineering technologies using programmable nucleases.....	41
Table 1.4: Comparison of available prostate cell lines.....	49
Table 2.1: A summary of the human prostate cell lines used	55
Table 2.2: Primers for PCR.....	59
Table 2.3: Primers for copy number analysis	60
Table 2.4: Primary and secondary antibodies for AR and GAPDH western blots	61
Table 2.5: cDNA synthesis master mixes	65
Table 2.6: Primers for qRT-PCR.....	66
Table 2.7: Antibodies used for IHC	69
Table 3.1: Summary of AR CRISPR/Cas9 clones	77
Table 3.2: Summary of spheroid morphology in BPH-1 PPMO and P4E6 WT and ARKO clones.....	105
Table 3.3: Expression levels of different differentiation markers in prostate spheroids	110

List of Figures

Figure 1.1: The prostate gland	14
Figure 1.2: Predicted models for prostate development.	17
Figure 1.3: The human prostate epithelium forms a hierarchical pathway	20
Figure 1.4: The phenotypic and molecular changes that result in prostate cancer ..	23
Figure 1.5: The AR gene and protein structure.....	34
Figure 1.6: AR signalling via the genomic and non-genomic pathways	36
Figure 1.7: ZFN and TALEN programmable nucleases.....	43
Figure 1.8: CRISPR-Cas9 genetic editing system.....	45
Figure 1.9: A comparison of different prostate cancer models.	52
Figure 3.1: <i>AR</i> and <i>DMD</i> copy number varies in different prostate cell lines.....	72
Figure 3.2: Minimum lethal dose of puromycin for BPH-1 and BPH-1 PPMO cells...74	
Figure 3.3: Optimisation of PCR conditions for <i>AR</i> primers.....	76
Figure 3.4 A work flow of the CRISPR/Cas9 experimental set up	78
Figure 3.5 The use of CRISPR/Cas9 to KO <i>AR</i> in prostate cell lines.....	81
Figure 3.6: BPH-1 cell line <i>AR</i> CRISPR/Cas9 experiment.	83
Figure 3.7: BPH-1 PPMO cell line <i>AR</i> CRISPR/Cas9 experiment	86
Figure 3.8: P4E6 cell line <i>AR</i> CRISPR/Cas9 experiment.....	88
Figure 3.9: Basal cell lines do not express <i>AR</i> protein when undifferentiated.....	90
Figure 3.10: Addition of DHT to induce differentiation in BPH-1 cells.....	92
Figure 3.11: Growing cells into a bilayer does not push cells into differentiation	95
Figure 3.12: Optimisation of prostate spheroids in co-culture with stroma.	97

Figure 3.13: Growing cells into spheroids induces the expression of AR without the presence of calcium	100
Figure 3.14: AR expression is reduced in CRISPR/Cas9 AR KO clones.....	102
Figure 3.15: Optimisation of the CellTiter-Glo [®] assay	104
Figure 3.16: Spheroid morphology is heterogeneous between cell lines and differs in ARKO clones.	106
Figure 3.17: Optimisation of AR and NKX3.1 antibodies for IHC.....	108
Figure 3.18: Expression of CK5 in spheroids.....	111
Figure 3.19: Expression of p63 in spheroids	112
Figure 3.20: Expression of CK18 in spheroids.....	113
Figure 3.21: Expression of NKX3.1 in spheroids	114
Figure 3.22: Expression of AR in spheroids	115
Figure 3.23: AR is required for differentiation in BPH-1 PPMO cells	117
Figure 4.1: Proposed future experiments to determine the role of AR during epithelial differentiation.....	130

Acknowledgements

This project is dedicated to my dad, everything I do is for you. Thank you to my mum for supporting my dreams no matter what.

Thank you to Norman and Charity Soul for allowing me to be part of such a wonderful lab and extending my stay.

Thank you to everyone in the CRU for their support and guidance, especially to Hannah for helping me get started.

Thank you to Fiona supporting me during my first conference, for being a soundboard for ideas and an excellent tour guide around Edinburgh.

Thank you to Anne for your advice and expertise that guided me through the difficult aspects of my project.

Thank you to all my friends at the University Barbell Club, for lifting me up every day.

Last, but not least, a huge thank you goes to Leanne. I would not have made it through this year without your pep talks, hugs and constant supply of oreos. You will forever be my best friend, thank you for always believing in me.

Declaration

I declare that this thesis presented is original work and I am the sole author unless otherwise stated. This work has not previously been presented for an award at this, or any other, University. All sources are acknowledged as references.

This work has been presented at the following conferences:

Androgens Meeting, The University of Edinburgh, Sept 2018

BACR Student Conference, The Francis Crick Institute, Nov 2018

1. Introduction

1.1 The Prostate Gland

The prostate is a male exocrine gland that is situated around the urethra and beneath the bladder. The prostate is composed of epithelial acini that are surrounded by a fibromuscular stromal network. Its primary role is to produce prostatic fluid, which contributes to the formation of semen. It consists of three main areas; the central zone, the peripheral zone and the transitional zone (Figure 1.1). The peripheral zone is where 70% of prostate cancer (PCa) arises, with 20% occurring in the transitional zone, and 10% in the central zone (Levine & Haggitt, 1989). The transitional zone is also where the majority of benign prostatic hyperplasia (BPH) occurs (McNeal, 1981).

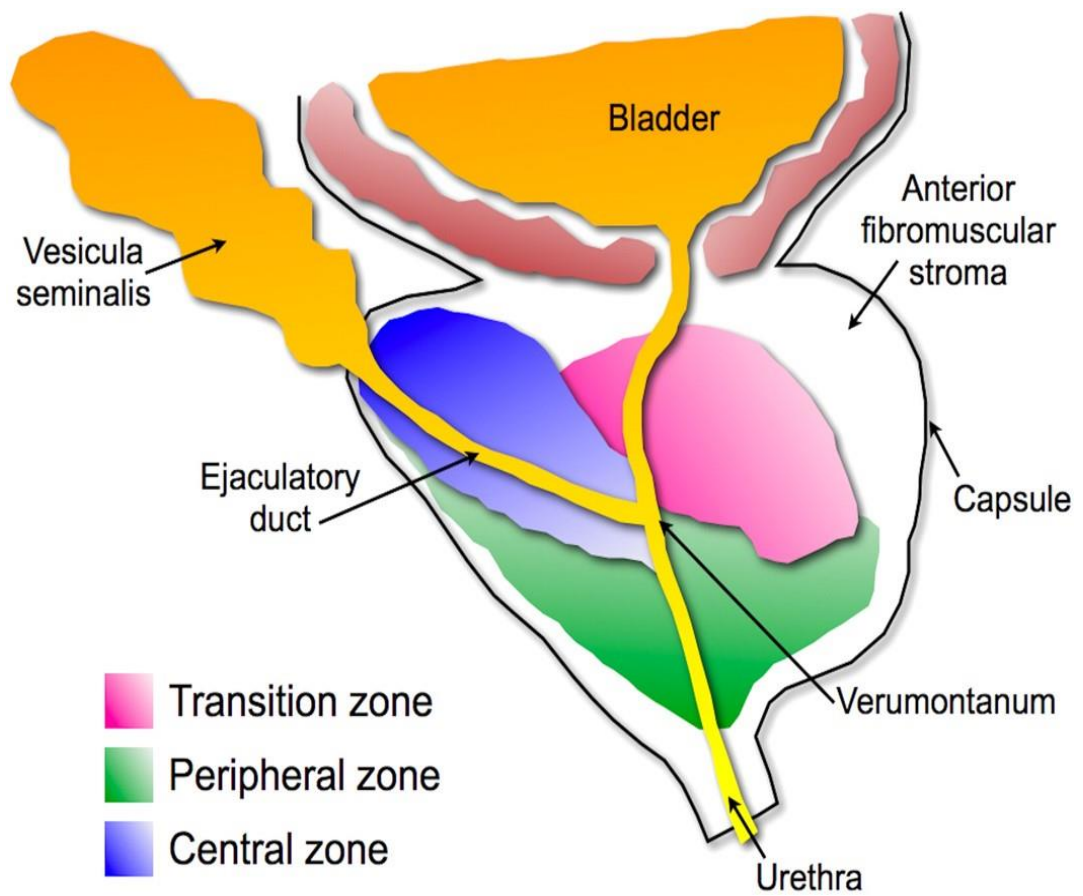


Figure 1.1: The prostate gland. The prostate consists of three zones: the transition, peripheral and central zones. It is found below the bladder and surrounding the urethra (Adapted from Oldridge *et al.*, 2012).

1.1.1 Development of the Prostate

The urogenital sinus in embryos can differentiate into either the prostate in males, or the vagina in females, at approximately 9 weeks of gestation in humans (Toivanen and Shen, 2017). This sexual dimorphism is controlled by the presence of androgens which trigger epithelial budding to form the prostate (Bryant et al., 2014). Androgen signalling from the urogenital sinus mesenchyme (UGM) to the urogenital sinus epithelium (UGE) initiates the formation of ducts, which then mature to form a ductal network. Currently there are two main hypotheses to suggest how androgens are able to initiate epithelial induction and budding: the smooth muscle model and the andromedin model (Toivanen and Shen, 2017).

The smooth muscle model suggests that androgen signalling controls the differentiation of smooth muscle around the prostate ducts; hence stopping epithelial budding in these areas. Therefore, in this model, androgens from the mesenchyme have an indirect effect on the development of epithelial tissue. The andromedin hypothesis, on the other hand, suggests that a signalling factor called an andromedin binds to the androgen receptor (AR) found within the UGM, and this directly triggers epithelial budding in the UGE (Figure 1.2). Currently it is thought that andromedins could be fibroblast growth factor (FGF) or Wnt, however there is currently not enough evidence to confirm the possibility of either of these ligands to be related to androgens (Toivanen and Shen, 2017).

As well as androgen signalling, retinoic acid (RA) can also initiate bud development in the UGS. RA is a ligand that binds to a RA receptor (RAR), which is found in the nucleus. RAR then binds to retinoic acid response elements (RARE) in DNA, along with retinoic X receptors (RXR), to control gene expression. Interestingly, if androgens are not present, RA is still able to induce prostate development. Also, if aldehyde dehydrogenase (ALDH), which catalyses the formation of RA, is inhibited, prostate buds cannot form in UGS explants, despite the presence of dihydrotestosterone

(DHT). This suggests that both androgens and RA work together to initiate bud formation and prostate development in the UGE (Bryant et al., 2014, Rivera-Gonzalez et al., 2012).

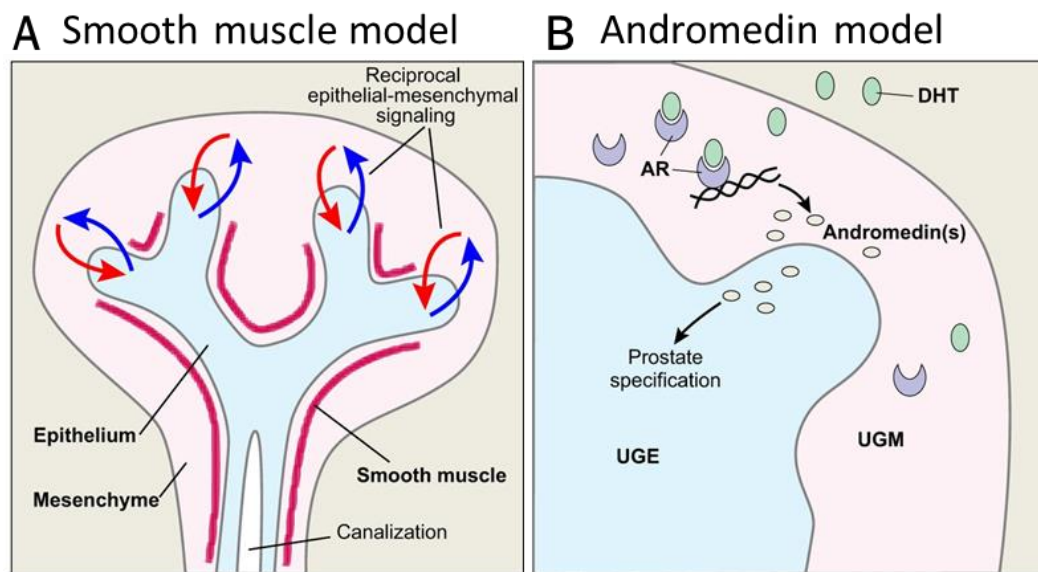


Figure 1.2: Predicted models for prostate development. (A) The smooth muscle model suggests androgens have an indirect effect on epithelial budding by controlling the development of the smooth muscle. (B) The andromedin model suggests andromedins bind to AR in the UGM to directly induce epithelial budding (Adapted from Toivanen and Shen, 2017).

1.1.2 The Adult Prostate Epithelium

The epithelium contains a variety of cell types: prostate stem cells (SC), neuroendocrine cells, transit amplifying (TA) cells, committed basal (CB) cells and luminal cells. The basal compartment is formed of SCs, TA and CB cells which are attached to the basement membrane (BM) (Figure 1.3A) (Maitland, 2013). The prostate epithelium can be described in terms of an hierarchical pathway, in which each type of cell can differentiate into the next cell in the lineage until the terminally differentiated luminal cells are formed (Figure 1.3B). However, there is a degree of plasticity within this hierarchy, because TA cells are potentially able to maintain multipotency and cycle back to form SCs (Isaacs and Coffey, 1989).

Luminal cells make up the majority of adult prostate epithelium (60%) (Packer and Maitland, 2016). They are secretory and terminally differentiated cells that are dependent on androgen signalling for survival. They secrete prostate specific antigen (PSA) and prostatic acid phosphatase (PAP) (Myers and Grizzle, 1996). Luminal cells can be characterised by high expression of AR (Table 1.2) (Prins et al., 1991) the presence of cytokeratins CK8 and CK18 (Sherwood et al., 1990), NKX3.1 (He et al., 1997) and CD57 (Liu et al., 1997) (Table 1.1).

Basal SCs asymmetrically divide, allowing for the differentiation into two groups of basal cells: CB cells and TA cells (also referred to as intermediate cells) (Oldridge et al., 2012). Together they make up 40% of the epithelium (Packer & Maitland, 2016). Both CB and TA cells do not rely on androgen signalling for survival and hence express either no, or low levels of AR (Table 1.2) (Kyprianou and Isaacs, 1988). Despite this, some TA cells have been shown to be androgen responsive which enables them to increase the number of AR dependent luminal cells (Collins et al., 2005). CB cells express different cytokeratins (CK5 and CK14) to luminal cells (Sherwood et al., 1990) as well as p63 (Liu et al., 1997) (Table 1.1). Some TA cells display both luminal and CB cell markers, resulting in an intermediate phenotype (Table 1.1) (Verhagen et al., 1992,

Xue et al., 1998, Hudson et al., 2001). These differing markers can help to distinguish between the basal and luminal cell types in prostate epithelium.

Similar to basal cells, neuroendocrine cells are insensitive to androgen, but like luminal cells they are terminally differentiated (Table 1.2). There are very few within the epithelium, and their role is still largely unknown (Bonkhoff and Remberger, 1993). They secrete many different growth factors and hormones which help to stimulate proliferation and differentiation in the epithelium (Di Sant'Agnese, 1998, Li et al., 2016). They can be identified by their markers; neuron-specific enolase (NSE) and chromogranin A (CGA) (Yao et al., 2011, Mjones et al., 2017) (Table 1.1).

The stromal tissue contains extracellular matrix (ECM), blood vessels and a myriad of cell types, including fibroblasts, smooth muscle cells and immune cells (Livermore et al., 2016, Packer and Maitland, 2016). It is separated in normal prostate from the epithelium by the BM. A proportion of stromal cells express AR and are androgen-sensitive. Stromal androgen signalling regulates the expression of growth factors, including keratinocyte growth factor, FGFs and insulin-like growth factor (IGF), which diffuse into the epithelium to promote growth and differentiation (Planz et al., 1998, Kwabi-Addo et al., 2004, Lai et al., 2012, Yu et al., 2012). Various studies also show that stromal AR plays a key role in the development and growth of BPH, primary prostate tumours and metastasis (Henshall et al., 2001, Lucia and Lambert, 2008, Lai et al., 2012).

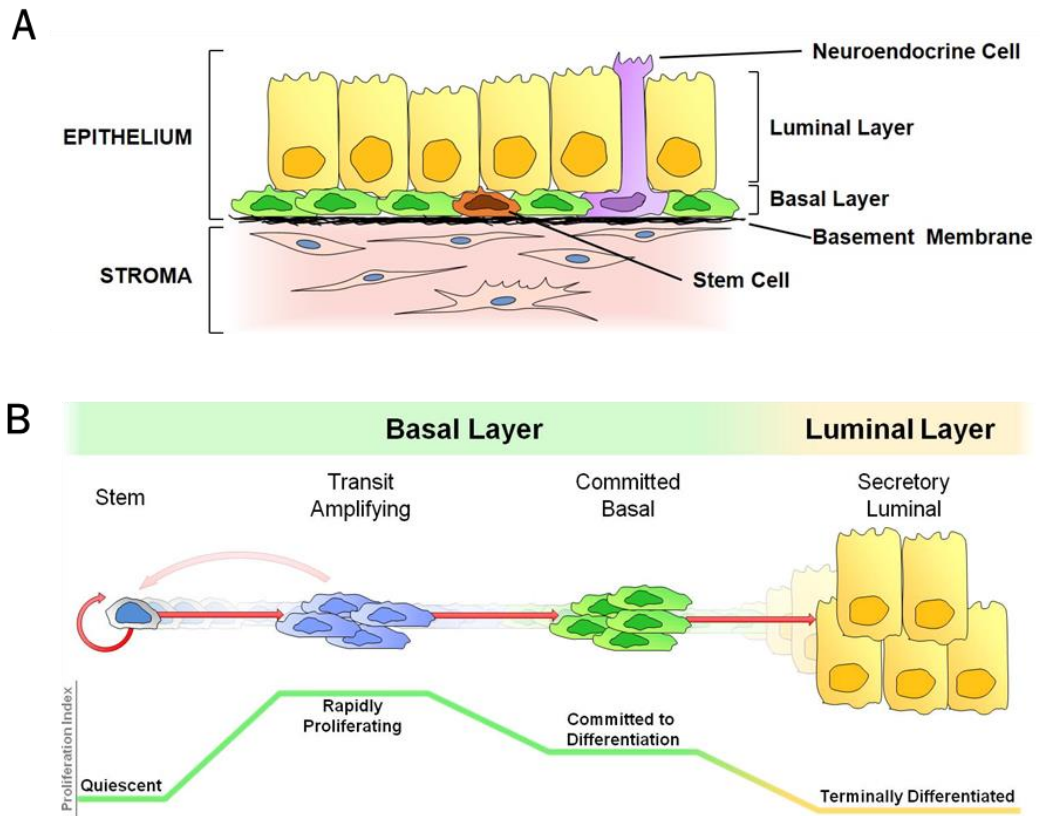


Figure 1.3: The human prostate epithelium forms a hierarchical pathway. (A) The majority of the epithelium consists of terminally differentiated luminal cells, followed by undifferentiated basal cells and a few neuroendocrine cells and stem cells. The epithelium sits on top of the basement membrane which is surrounded by the stroma. (B) Quiescent stem cells differentiate into rapidly dividing transit amplifying cells. Transit amplifying cells differentiate into committed basal cells which are on track to differentiate into the final cell type, secretory luminal cells (Adapted from Oldridge, Pellacani et al. 2012).

Table 1.1: Cell types found in prostate epithelia and their known expressed markers.

Cell Type	Marker	Reference
Luminal Cell	PSA	(Myers and Grizzle, 1996)
	PAP	(Myers and Grizzle, 1996)
	CK18	(Sherwood et al., 1990)
	CK8	(Sherwood et al., 1990)
	NKX3.1	(He et al., 1997)
	AR	(Prins et al., 1991)
Committed Basal Cell	CK5	(Sherwood et al., 1990)
	CK14	(Sherwood et al., 1990)
	p63	(Liu et al., 1997)
Transit Amplifying Cell	CD49b ^{high}	(Guzman-Ramirez et al., 2009)
	CD133 ^{low}	(Grey et al., 2009)
	CK5	(Sherwood et al., 1990)
	CK14	(Sherwood et al., 1990)
	p63	(Liu et al., 1997)
Neuroendocrine Cell	CGA	(Yao et al., 2011)
	NSE	(Mjones et al., 2017)
	Synaptophysin	(Wiedenmann et al., 1986)
Stem Cell	CD44 ^{high}	(Collins et al., 2005)
	CD133 ^{high}	(Collins et al., 2005)
	$\alpha 2\beta 1$ integrin ^{high}	(Collins et al., 2005)
	CD166	(Jiao et al., 2012)
	Sca-1	(Xin et al., 2005)

1.2 Prostate Cancer

1.2.1 Premalignancies of prostate cancer

Proliferative inflammatory atrophy (PIA) is an abnormality in the prostate that is thought to be a precursor to PCa. It occurs in the peripheral zone like PCa, and it involves the atrophy of prostate tissue as well as inflammation (Putzi and De Marzo, 2000). The molecular signatures of prostate cancer start to appear at this stage, such as downregulation of tumour suppressors like *NKX3.1*, *CDKN1B* and *PTEN* (Figure 1.4) (Ruska et al., 1998).

It is thought that PIA then goes on to develop into prostatic intraepithelial neoplasia (PIN) which also occurs in the peripheral zone of the prostate. Low-grade PIN consists of a few abnormal cells in the prostate, whereas high-grade PIN consists of hyperproliferative luminal cells, shortened telomeres, reactive stroma and a *TMPRSS2-ERG* fusion, the most common genetic abnormality in PCa (Tomlins et al., 2005, Polson et al., 2013). Due to high-grade PIN cells having many similar characteristics to PCa cells, it implies that the development of prostate cancer is likely. When prostate cancer develops, not only is there hyperproliferation of luminal cells, but also the loss of the basal epithelial cells and BM (Barsky, 1983, Lang et al., 2000). Immune cells also start infiltrating the tumour, telomerase becomes activated and the tumour suppressor genes *PTEN*, *RB1* and *NKX3.1* are deleted (Figure 1.4) (Wymenga et al., 2000, Kunderfranco et al., 2010, Baca et al., 2013). Even though telomerase is active to extend the life span of cancerous cells, PCa cells have abnormally short telomeres in comparison to other cancers (Sommerfeld et al., 1996). It has been suggested by von Zglinicki that high oxidative stress from cancer can result in telomeric DNA being poorly repaired as well as accelerating telomere loss (von Zglinicki, 2002).

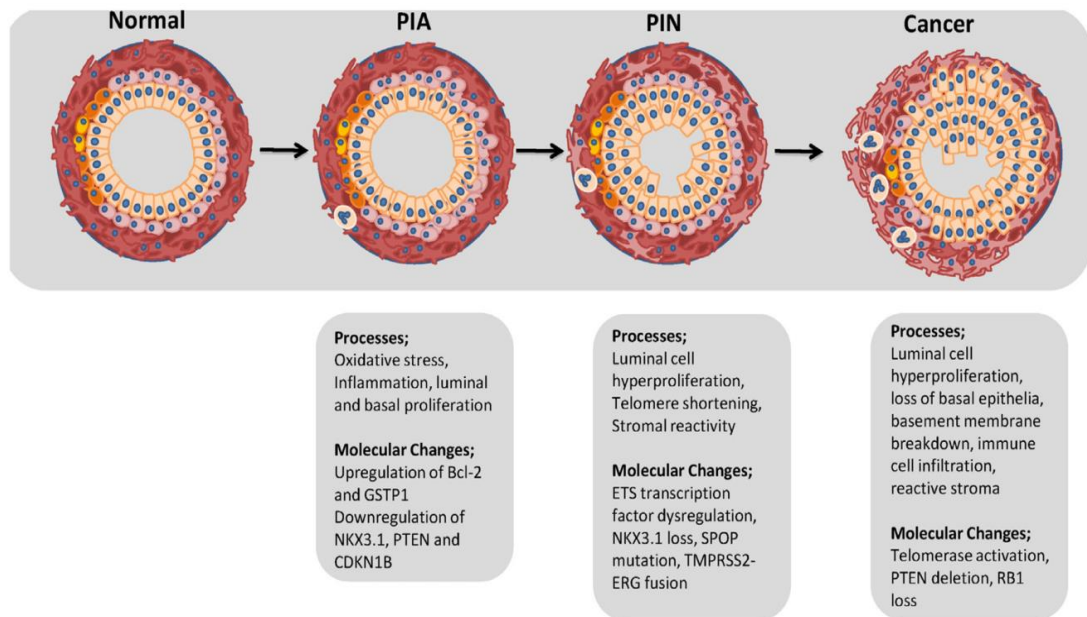


Figure 1.4: The phenotypic and molecular changes that result in prostate cancer. Prostate cancer possibly develops from proliferative inflammatory atrophy (PIA) and prostatic intraepithelial neoplasia (PIN) via a series of molecular and phenotypic changes. Luminal secretory cells (orange cells) hyperproliferate resulting in PIN and cancer. Molecular changes include *NKX3.1* and *PTEN* deletion and *TMPRSS2-ERG* fusion (Adapted from Packer and Maitland, 2016).

1.2.2 Epidemiology

PCa is the most common cancer detected in males, and overall the second most common cancer in the UK. It is likely that 1 in 8 men will be diagnosed with prostate cancer, with more than half of those being diagnosed being aged 70 and over. In 2015, there were 47,151 cases reported and 11,918 deaths. The number of deaths from PCa now surpasses breast cancer which makes it the third biggest killer in the UK after lung and bowel cancer (Cancer Research UK).

1.2.3 Diagnosis

Men over the age of 50 can be regularly screened for PCa via blood PSA testing. However, raised blood PSA is not mutually exclusive to PCa; it can increase due to old age, BPH, infection and prostatitis (Obort et al., 2013). Despite PSA being termed as a prostate-specific antigen, it can also be expressed in other tissues such as the ovary, salivary glands, lung and breast (Smith et al., 1995). PSA testing has been found to have a sensitivity of 86% and specificity of 33% when PSA levels were 4 ng/ml or below (Hoffman et al., 2002). Therefore, PSA testing can often result in false positives and hence results in treating patients unnecessarily.

If high PSA levels are detected, the patient then undergoes multiple transrectal ultrasound (TRUS) biopsies and MRI scans. The presence and progression of PCa can then be defined by its tissue architecture via the Gleason grading system (Gleason, 1966). Biopsies which are graded Gleason 3 to 5 are considered to be cancerous, with grade 5 having the least differentiated glands. It is likely that there will be multiple Gleason grades within the cancer biopsy, which results in the addition of Gleason grades, totalling up to Gleason grade 10. For example, Gleason grade 7 can be comprised of 3+4 tumours (with the majority being Gleason grade 3) or 4+3 tumours (with the majority being Gleason grade 4) (Chen and Zhou, 2016). The Gleason grading system helps determine the most successful treatment option and hence improves the patient's prognosis. However, it only partially takes into account the

heterogeneous nature of PCa and the fact that it is a multifocal disease (Clark et al., 2007). Therefore, a more specific PCa biomarker is required to avoid overtreatment and introduce a more personalised treatment regime for patients.

1.2.4 Treatment of localised tumours

Localised prostate tumours are often slow growing and have low chances of spreading. In these cases, active surveillance of PSA levels and regular biopsies is required, as treatment might not be necessary (Kollmeier and Zelefsky, 2012). This prevents overtreatment of these men, and improves their quality of life. However, it requires an accurate classification of the Gleason grade of the tumour (Gleason, 1966).

If the tumour is localised but has a higher risk of metastasising, the patient has several options for treatment; a radical prostatectomy (RP), radiotherapy, or focal therapy. RP is a surgical treatment whereby the entire prostate is removed. This is a successful treatment option if the cancer is completely contained within the prostate. However, it comes with a host of side effects including incontinence and impotence. It is also only suitable if the patient has no other health problems.

There are two forms of radiotherapy which are available to treat local and locally advanced PCa: external beam radiation therapy (EBRT) or directed brachytherapy. Both forms of radiotherapy kill cancer cells by stopping them from growing and spreading throughout the body. Often radiotherapy is paired with hormone therapy to shrink the tumour as much as possible, so it is easier to target. EBRT includes image-guided intensity-modulated radiation therapy (IMRT) and 3D-dimensional conformal radiation therapy (3D-CRT) (Heidenreich et al., 2014). The advantage of IMRT over 3D-CRT is that the intensity of the radiation beams can be controlled and therefore toxicity to surrounding tissues is reduced, while still maintaining a high dosage of radiation to the tumour (Bauman et al., 2012). Brachytherapy on the other hand is considerably more localised than EBRT due to using implanted radioactive seeds

directly into the prostate. This greatly minimises the amount of radiation to nearby healthy tissues (Koukourakis et al., 2009).

Focal therapy is used as a form of treatment for patients' whose tumour is restricted to one lobe. For high-intensity focused ultrasound (HIFU) a probe is inserted transrectally to kill cancer cells using high-frequency ultrasound. HIFU is a new treatment, and therefore the side effects and long-term success rates are still unknown. The advantages of the treatment include a short recovery time, no surgery and the ability to have HIFU again if the cancer regresses (Madersbacher et al., 1995). Photodynamic therapy (PDT) involves the intravenous delivery of photo-sensitive drugs which upon activation with light, cause cell death within prostate tissue (Koudinova et al., 2003). This is more sensitive than other focal therapies. However the photo-sensitive drugs stay in the patient's bloodstream for weeks after which requires them to protect themselves from the sun (Moore et al., 2009). Cryotherapy destroys cells subjecting them to freezing and thawing cycles and extremely low temperatures (de la Taille et al., 2000). Argon gas or liquid nitrogen is administered to specific regions in the prostate under TRUS (Nomura and Mimata, 2012). Cryoablation can also be used as a salvage therapy after relapse, however it requires protection of surrounding tissues from the low temperatures (Cohen and Miller, 1994).

1.2.5 Treatment of metastatic tumours

Metastasis is classified as one of the hallmarks of cancer (Hanahan and Weinberg, 2011). Up to 40% of men will develop metastatic PCa despite local treatment, and 90% of these metastases will occur in the bone (Beltran et al., 2011). In order to invade the BM and stroma, primary tumour cells undergo epithelial-to-mesenchymal transition (EMT). This involves a switch from an epithelial to a mesenchymal phenotype, including a loss in cell polarity, cell adhesion and low levels of E-cadherin (Valastyan and Weinberg, 2011).

Metastatic and high-grade PCa are both treated with drugs which inhibit the growth of the tumour cells by depriving them of androgens. This form of treatment is referred to as androgen deprivation therapy (ADT), and there are four main categories:

1. **Anti-androgen therapy:** AR is blocked to prevent the activation of androgen target genes, e.g. bicalutamide (Iversen et al., 2000)
2. **Gonadotropin-releasing hormone (GnRH) antagonist:** blocks GnRH receptor to stop the production of testosterone, e.g. degarelix (Steinberg, 2009)
1. **Luteinising hormone releasing hormone (LHRH) agonist:** inhibition of LH resulting in the decrease in testosterone and DHT production, e.g. leuprorelin acetate (Persad, 2002)
2. **Oestrogen treatment:** inhibits 5- α reductase to stop testosterone production, e.g. diethylstilbestrol (Clemons et al., 2013)

1.2.6 Treatment of castrate resistant prostate cancer

Patients which undergo ADT therapy for high grade prostate tumours initially show regression of the tumour, however they eventually become hormone resistant. The cancer is then referred to as castration-resistant prostate cancer (CRPC). The mechanisms by which CRPC arises are discussed in section 1.3.4. It is estimated that 28% of PCa patients develop CRPC and these patients have a mean survival of 13.5 months after CRPC diagnosis (Hirst et al., 2012). Therefore a major focus of current PCa research is the development of more successful next generation androgen deprivation therapies and CRPC chemotherapy agents. Current drugs that are able to prolong a patient's survival but are not curative, include:

1. **Enzalutamide:** 2nd generation antiandrogen which inhibits AR binding to DNA to activate AR target genes (Scher et al., 2012)

2. **Apalutamide:** 2nd generation antiandrogen which blocks translocation of AR to the nucleus via competitive binding to the ligand binding domain (Clegg et al., 2012)
3. **Cabazitaxel:** 3rd generation taxane which has a lower affinity to p-glycoprotein compared to other taxanes, and it also targets microtubules and AR trafficking (Paller and Antonarakis, 2011)
4. **Radium-223 dichloride:** α -emitting radionuclide which targets bone metastases by mimicking calcium (Deshayes et al., 2017)
5. **Abiraterone acetate:** an inhibitor of the enzyme CYP17A to prevent the synthesis of androgen from the adrenal glands and testes (De Bono et al., 2011)
6. **Sipuleucel-T:** immunotherapy treatment for early asymptomatic metastatic CRPC (Kantoff et al., 2010)
7. **Docetaxel:** 2nd generation taxane which inhibits cell division and AR trafficking by targeting microtubules (James et al., 2015)

1.2.7 Clonal evolution model

The clonal evolution model (also known as the stochastic model) is the traditional view by which a tumour arises. It suggests that any cell has the potential to initiate a tumour when a mutation occurs in a tumour suppressor or oncogene. From here the founder cell will grow via mitosis to form a tumour. The tumour can then become heterogeneous via further mutations in the progeny of the founder cell (Nowell, 1976). Recently, it has been shown that a minimum of one to ten driver mutations is all that is required in a founder cell to result in cancer (Martincorena et al., 2017).

1.2.8 Cancer stem cell model

Adult SCs are present in the majority of human tissues where they aid regeneration, repair and tissue homeostasis. Unlike totipotent embryonic SCs, they are limited in their differentiation potential and are therefore referred to as being multipotent. Adult

SCs are largely quiescent cells, but they are triggered into division when damage occurs (Ojeh et al., 2015). This causes the SCs to give rise to their daughter TA cells, which subsequently commit to producing highly differentiated cells to replenish the cells after damage.

The cancer stem cell (CSC) model suggests that a small population of cells within a tumour are able to initiate and maintain tumour growth, and hence without these cells the tumour would regress. Like adult SCs, they are multipotent and are able to undergo self-renewal. However, they have dysregulated differentiation and proliferation, allowing a heterogeneous population of cells to occur within the tumour. In this model, it is considered that the other cells in the bulk of the tumour are non-tumour initiating, which means that CSCs need to be targeted directly to prevent further cancer growth and relapse (Archer et al., 2017, Batlle and Clevers, 2017). The clonal evolution model and CSC model for tumour development may not be mutually exclusive but rather, in reality, tumours might form due to a combination of both.

CSCs have been identified in many cancers such as: glioblastomas (Singh *et al*, 2003), acute myeloid leukemia (Bonnet and Dick, 1997), colon (Ricci-Vitiani et al., 2007), lung (Eramo et al., 2008), breast (Al-Hajj et al., 2004), bladder (Li et al., 2016) and pancreatic (Li et al., 2007, Frame et al., 2017, Frame et al., 2013) cancers. Isaacs and Coffey (1989) were the first to suggest that cancerous SCs could be present in PCa. Their model predicts that androgen-independent SCs are able to differentiate into androgen-independent TA cells. The TA cells are androgen-responsive which allows them to give rise to androgen-dependent secretory luminal cells (Table 1.2). This model came about from a series of androgen cycling experiments in male rats; whereby after castration the prostate gland can be fully restored when androgen levels are replaced (Isaacs and Coffey, 1989).

Since then, CSCs have been successfully identified in PCa (Collins *et al.*, 2005). They form a rare (0.1%) and treatment-resistant population within prostate tumours, which enables them to 'hide' within the bulk of the tumour away from chemotherapy and radiotherapy treatments (Packer & Maitland, 2016). This is due to CSCs not expressing AR and therefore they cannot be targeted by ADT (Table 1.2). Also, they undergo self-renewal as well as differentiation into TA, and hence CB and luminal cells, to regenerate the tumour and cause a relapse. It has been discovered that CSCs are resistant to radiation and the chemotherapy drug, epirubicin (Frame *et al.*, 2017, Frame *et al.*, 2010). Therefore it is currently thought that to treat PCa, the CSCs themselves need to be directly targeted to prevent regrowth of the tumour (Maitland and Collins, 2008). The PCa CSCs can be selected using the putative markers: CD133, CD44 and $\alpha 2\beta 1$ integrin^{high} (Table 1.1) (Collins *et al.*, 2005).

1.2.8.1 Evidence luminal cells are the cell of origin

The cell of origin in a tumour is the cell which has been targeted for mutation that results in the formation of a cancerous tumour. This could be the SCs themselves, but there also remains a debate over whether basal or luminal cells are the cell of origin in PCa.

The majority of cells within a prostate tumour are thought to be luminal cells, due to the expression of luminal specific markers: CK8, CK18, AR, PSA and PAP (Table 1.1). Luminal progenitor cells have been found in prostate tumours within mice, however the mouse prostate is structurally different to the human prostate Liu *et al.* (2011), (Agarwal *et al.*, 2015). Wang *et al.*, has also identified a subpopulation of luminal cells in mice that are able to survive after androgen deprivation, called castration resistant NKX3.1 expressing cells (CARNs) (Wang *et al.*, 2009). These cells are present in PIN and carcinoma lesions after a *PTEN* deletion, which suggests that they could be the origin of PCa (Wang *et al.*, 2009). As of yet, a luminal CSC has not been successfully

isolated from primary human prostate tumours, and therefore it cannot be confirmed whether luminal cells are the source for PCa.

1.2.8.2 Evidence Basal Cells are the Cell of Origin

There is a large amount of evidence to suggest that CSCs originating from basal cells could give rise to PCa. A small population of basal cells has been found to express known SC markers, CD133 and $\alpha_2\beta_1^{\text{high}}$. This population also demonstrates known SC attributes: high proliferative potential *in vitro* and the ability to reform prostate-like acini *in vivo* (Richardson et al., 2004). This population of CD133⁺/ $\alpha_2\beta_1^{\text{high}}$ cells also shows cancer cell characteristics, and is able to differentiate into AR⁺ luminal cells, similar to the formation of primary prostate tumours (Collins et al., 2005). The RNA signature of basal CSC population has been associated with a more aggressive type of prostate cancer (Smith et al., 2015). Finally, Goldstein et al., discovered that potentially basal cells could form a luminal phenotype tumour within NOD/SCID/IL2Ry^{null} mice after ERG, AKT and AR expression (Goldstein et al., 2010).

1.3 Androgen Receptor

1.3.1 Gene structure

Androgens are a group of steroid hormones which are major regulators in the differentiation and development of the prostate epithelium (Oldridge et al., 2012). AR is a nuclear receptor in the subfamily 3, group C, member 4 and is located on Xq12 and it contains 8 exons, spanning approximately 180 kb (Hu et al., 2017). AR is found to be expressed all over the body and not just in the prostate. For example, expression is seen in the bone marrow, spleen, thymus and the brain (Dart et al., 2013). Androgen has a repressive effect on AR mRNA indicating that AR has a self-limiting expression (Olsen et al., 2016). This ensures a context dependent expression of AR and hence androgen regulated genes.

AR is a large 110 kDa protein, and is organised into four sections: The N-terminal transcriptional activation domain (NTD), DNA binding domain (DBD) with two zinc finger motifs, a hinge region and ligand-binding domain (LBD) (Hu et al., 2017, Berry et al., 2008). NTD is encoded by exon 1 and it helps regulate the transcription of AR (Hu et al., 2017). DBD determines how AR binds to the androgen response element (ARE) in the DNA promoter regions, and it is encoded in exons 2 and 3. The hinge region regulates the dimerization of AR when it moves into the nucleus. LBD binds to an androgen ligand in the cell cytoplasm, which results in specific downstream effects within the target cell. Exons 4-8 encode for both the LBD and hinge region (Livermore et al., 2016, Hu et al., 2017). Despite the presence of the LBD, AR can be activated without a ligand. This occurs via the hormone-independent activation function (AF1) within the NTD and it allows CRPC to develop. The hormone-dependent activation function 2 (AF2) is located within the LBD and does require a ligand (Figure 1.5) (Livermore et al., 2016).

At the end of exon 1 there is a series of CAG repeats. The length of the repeat sequence is inversely correlated with the transcription promoting activity of AR; hence the longer the polymorphism repeat the less AR activity. CAG repeat length has been shown to vary in different ethnic populations. For example, those of Afro-Caribbean lineage have the shortest mean repeat length (19.6 ± 3.2) and those of Thai lineage have the longest mean repeat length (23.1 ± 3.3) (Ackerman et al., 2012). The research around whether the repeat length has an association with the risk of prostate cancer has been controversial up until recently. A meta-analysis shows that short polymorphic CAG repeats may increase the susceptibility of developing PCa (Qin et al., 2017).

Table 1.2: A list of prostate epithelial cells and their respective AR expression and responsiveness to androgen (Adapted from Oldridge *et al*, 2012).

Cell Type	AR Expression	Androgen responsiveness
Stem Cells	AR ⁻	Non-responsive
Transit Amplifying Cells	AR ⁻	Responsive
Committed Basal Cells	AR ⁻	Responsive
Luminal Cells	AR ⁺	Dependent

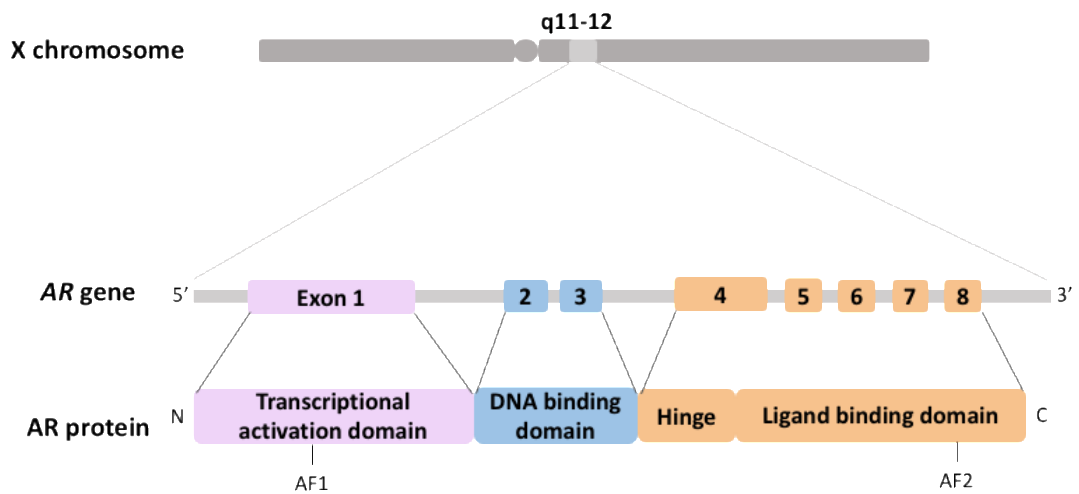


Figure 1.5: The AR gene and protein structure. The locus is located at Xq11-12 and it contains eight exons. These exons encode a protein with four domains: the N-terminal transcription activation domain (NTD), the C-terminal ligand binding domain (LBD), the central DNA binding domain (DBD) and the hinge region. AR can be activated without a ligand via AF1 domain. It can also be activated with a ligand via AF2 domain.

1.3.2 Genomic and non-genomic signalling pathways

The genomic signalling pathway is the common way by which AR transduces a signal when androgens bind to AR. Firstly, the androgen testosterone moves into the cell where it is converted into DHT by 5 α -reductase at the plasma membrane. DHT binds to the LBD of AR and induces a conformational change, causing AR to dissociate from heat shock proteins (Hsp) and chaperones within the cytoplasm. From here AR is phosphorylated, enabling its translocation to the nucleus. Once it reaches the nucleus, it dimerizes with another activated AR and binds to a series of coactivators (Livermore et al., 2016). The dimerized AR binds to ARE in the promoter regions of the androgen target genes, including those linked with prostate disease (Berry et al., 2008) (Figure 1.6A). This activates multiple genes and promotes functions such as cell survival and proliferation (Livermore et al., 2016). For example, the *PSA* gene contains three AREs which demonstrates that luminal cells are responsive to androgen signalling (Berry et al., 2008).

Unlike the genomic signalling pathway that takes several hours to complete, the non-genomic signalling pathway can occur within minutes. This non-genomic signalling pathway does not require AR to translocate into the nucleus and bind to DNA. Instead, activated AR binds to a series of intracellular signalling molecules such as PI3K, Src and Ras/Raf-1. This then triggers the activation of the MAPK/ERK pathway which induces cell proliferation (Livermore et al., 2016) (Figure 1.6B). This pathway does not occur in non-cancerous luminal cells since they are terminally differentiated, so that they are no longer able to proliferate.

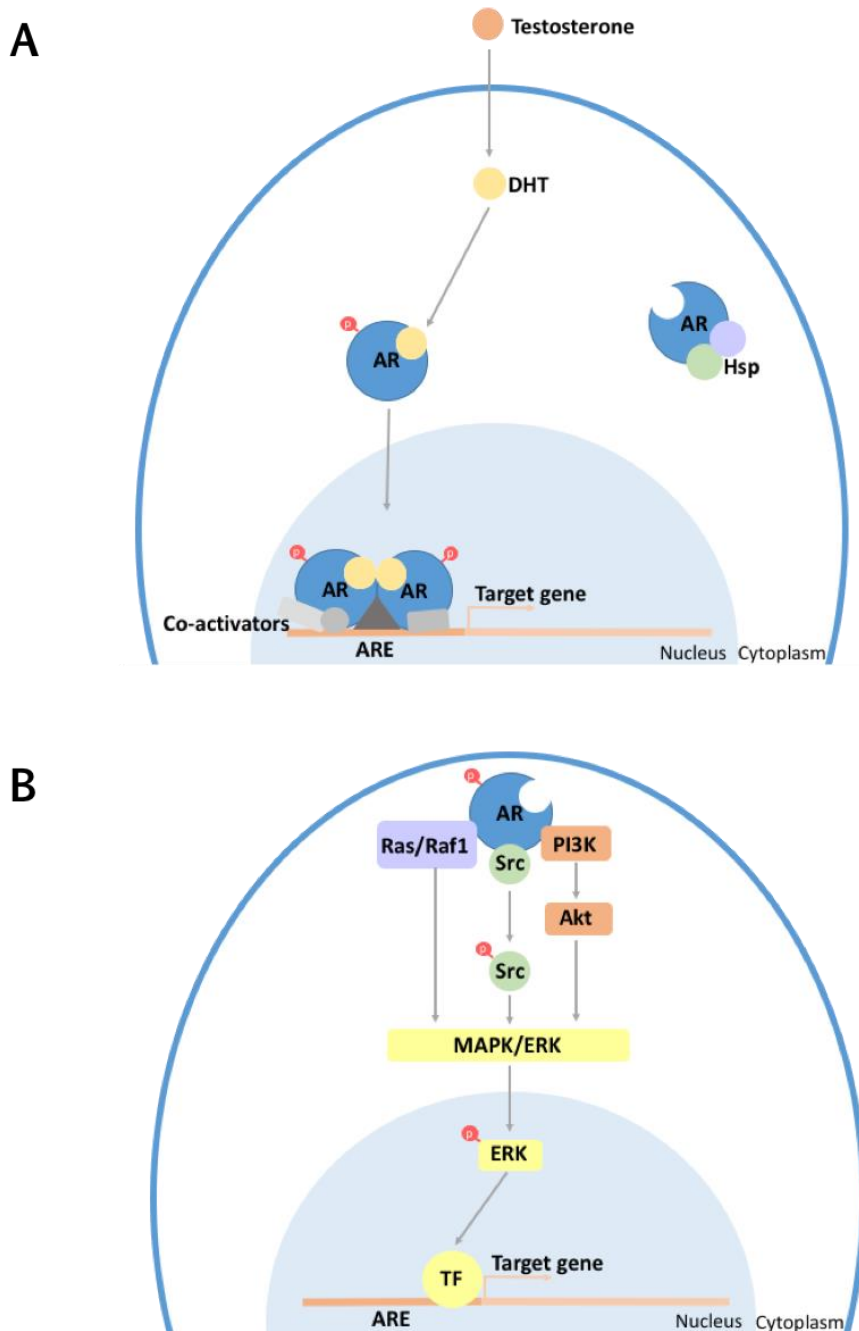


Figure 1.6: AR signalling via the genomic and non-genomic pathways. (A) Testosterone is converted to DHT that binds to AR in the cytoplasm. AR moves into the nucleus and dimerizes on an ARE in DNA, upstream from androgen regulated genes. (B) AR is activated without the presence of androgens and it does not translocate into the nucleus. Target genes are activated via the MAPK/ERK pathway that can be initiated by signalling molecules (PI3K, Src, Ras/Raf1) binding to phosphorylated AR.

1.3.3 The role of AR in PCa

It has been known that PCa is an androgen-sensitive disease since 1941 from the research of Huggins and Hodges (Huggins, 1941). ADT targets the androgen-responsive luminal cells within the tumour to stop growth (Table 1.2). However, the inevitable development of CRPC, has increased the demand for novel therapeutics (see section 1.2.6) (Karantanos et al., 2013). Therefore, continued understanding and investigation of the role of AR in prostate cancer should help elucidate possible ways to tackle CRPC.

1.3.4 Adaptations of AR signalling in CRPC

Even though androgen levels are low in patients undergoing ADT, AR signalling is still able to be reactivated resulting in CRPC. There are various pathways by which AR can adapt to ADT, such as forming splice variants, amplifying expression and inactivation of corepressors of AR signalling pathways.

Forming many mRNA isoforms via splicing allows a range of proteins, encoded by the same gene, to have different roles within the cell. Aberrant AR mRNA splicing has been linked to the onset of different types of cancer and specifically PCa (Pal et al., 2012). There are many different AR splice variants, but the most prevalent are the isoforms AR-V7 and Arv567es, which lack the LBD but are still able to localise to the nucleus when there are no androgens present (Hu et al., 2009, Sun et al., 2010). PCa patients that express these splice variants have poor prognoses (Hornberg et al., 2011). In particular, AR-V7 has been used as a biomarker for resistant prostate cancer as it has been found in circulating tumour cells of CRPC patients (Steinestel et al., 2015).

Mutations in *AR* have been found in 10-30% of CRPC patients (Wallen et al., 1999). The majority of these mutations occur in the LBD, but many also occur in the NTD (Gottlieb et al., 2012). The most common mutation in CRPC patients is the point mutation T877A which can be used as another biomarker for CRPC. The substitution

of a threonine for an alanine at position 877 in the LBD results in a decrease in AR specificity to DHT. The mutation increases the space in the binding pocket, allowing for other hormones such as oestrogen and progesterone to enter (Risstalpers et al., 1993, Gaddipati et al., 1994).

AR expression is increased in CRPC patients, which allows the tumour cells to be hypersensitive to the low levels of testosterone. AR copy number has been found to be highly elevated in 30% of CRPC patients, resulting in more protein being expressed (Visakorpi et al., 1995).

AR signalling occurs via the non-genomic pathway when androgens are not present. Src expression has been shown to be upregulated in CRPC cells to increase AR signalling (Asim et al., 2011). Src inactivates corepressors which bind to transcription factors or AR itself, thereby restricting the transcriptional activation of AR under normal circumstances. In particular, the activity of the corepressor LCoR is suppressed by Src kinase which is an important step in the development of PCa carcinogenesis *in vivo* (Asim et al., 2011).

1.3.5 The role of AR in differentiation

AR has been found to be essential for differentiation of basal cells to terminally differentiated luminal cells in a range of studies (Berthon et al., 1997, Lee et al., 2012, Ling et al., 2001, Niu et al., 2008, Whitacre et al., 2002, Wu et al., 2007). AR also plays a role in proliferation of the epithelium, however there are conflicting studies as to whether it promotes or inhibits proliferation (Berthon et al., 1997, Simanainen et al., 2007).

The role of AR during differentiation of the prostate epithelia has been investigated using both mouse knock-out (KO) models and cell line models. Mouse models show that when AR is not present, luminal differentiation cannot reach completion. Firstly, Wu *et al.*, showed that in mice that lack AR in the mature prostate (KO of exon 2 which

codes for the DBD) do not form the glandular infoldings and the luminal cells are a lot shorter than in the WT mice. However, it must be noted that luminal cells are still present and the gross structure of the prostate remaining intact, which suggests that differentiation is still able to occur despite AR not being expressed (Wu et al., 2007). Similarly, Simanainen *et al.*, also generated a mouse KO model with an edit to the DBD which showed similar effects to Wu *et al.*, whereby the prostate development was hindered (Simanainen et al., 2007). Lee *et al.* has also used a mouse KO model, as well as cell lines, to look specifically at the role of AR in basal cells. They found that increasing levels of AR in basal cells drives differentiation into luminal cells (Lee et al., 2012).

The majority of research has been done using mouse KO models, and this poses many limitations due to the differences in mouse and human prostate epithelial structure. Whitacre *et al.*, used the rat prostate cell line CA25 transfected with AR, instead of a mouse model, to show that the addition of DHT results in the formation of luminal-like columnar epithelial cells (Whitacre et al., 2002). They also found an increase in the expression of $\alpha 6$ integrin which is a marker for terminal differentiation in mouse keratinocytes. Whitacre et al. took this as another piece of evidence that differentiation was occurring with AR present. However, $\alpha 6$ integrin is a differentiation marker in a different cell type and animal, so it might not symbolise differentiation in the rat prostate. Also, it needs to be considered that the rat prostate is still different to the human prostate and so has not brought research closer to elucidating the role of AR in the human prostate.

Recent research published during the course of this project showed that potentially AR is not required for luminal differentiation (Chua et al., 2018). CARNs are a rare population of luminal progenitor cells that are found in androgen deprived mice. Mice carrying a conditional allele of AR with an inducible NKX3.1 CreERT2 (cre recombinase) drive were used to demonstrate that in the absence of AR luminal markers, CK18 and

CK8 were still expressed and basal markers CK5 and p63 were not expressed. These results contradict the current research in mice models, however this could be due to the use of targeting rare CARN cells.

To assess the role of AR in the human prostate, research by Berger et al. used newly immortalised primary human prostate epithelial cells and tumourigenic prostate epithelial cells. Expression of AR in these human cells resulted in a decrease in p63 expression, a marker for basal cells, as well as small increase in the secretion of PSA, a marker for luminal cells. This hints at the possibility of AR being involved in luminal differentiation, but Berger et al. noted that not all the luminal cell markers are expressed (Berger et al., 2004). Therefore, the role of AR during differentiation of luminal cells in the human prostate is yet to be elucidated

Furthermore, it is unknown to what extent AR determines luminal differentiation and whether other factors are involved. It is known that retinoic acid (RA) and androgens work together to initiate bud development in the embryo urogenital sinus to form the prostate (Bryant et al., 2014). However, using androgen-dependent and independent cell lines, it has been shown that both RA receptor (RAR) and AR are also required for luminal differentiation in the adult prostate (Rivera-Gonzalez et al., 2012, Rane et al., 2014). This is the first evidence of AR playing a minor role in the regulation of prostate specific genes and that RA is also required for development in the mature prostate (Rivera-Gonzalez et al., 2012). Therefore, perhaps RA receptors could also be involved in the differentiation of the prostate epithelium alongside AR.

1.4 Genetic Engineering Technologies Using Programmable Nucleases

The development of programmable nucleases has allowed genome editing to become a powerful tool in research, biotechnology and medicine. Over the last three decades, a range of technologies has been developed: zinc finger nucleases (ZFNs),

transcription-activator-like effector nucleases (TALENs) and clustered regularly interspaced short palindromic repeats/Cas9 (CRISPR/Cas9) (Table 1.3).

Modern genetic engineering technologies involve directing a DNA nuclease using protein or RNA that are designed to recognise specific nucleotide sequences. The nucleases then cleave the DNA to form a double stranded break (DSB). The cell recognises that there is a break in the DNA and it induces two repair mechanisms; non-homologous end joining (NHEJ) and homology-directed repair (HDR). The NHEJ pathway is preferred when a gene KO is required, as it results in small insertions, deletions and possibly a frame shift, causing the gene to no longer function. If two DSBs are created, they will be repaired by NHEJ by removing the DNA flanked by the DSBs. On the other hand, HDR can occur which can be used to insert point mutations or a sequence of DNA. This requires an exogenous donor DNA template, which are either single stranded oligodeoxynucleotides for small insertions or plasmids for a large gene insertion (Hendriks et al., 2016) (Figure 1.8).

Table 1.3: Comparison of different genetic engineering technologies using programmable nucleases (Adapted from Kim and Kim, 2014)

	TALENs	ZFNs	CRISPR/Cas9
Target DNA recognition	Protein-DNA	Protein-DNA	RNA-DNA
Components	TALE-FokI fusion protein	ZF-FokI fusion protein	gRNA and Cas9
Success rate	Low	High	High
Off-target efficiency	Low	High	Low
Time consumption	Long	Long	Short
Cost	High	High	Low

1.4.1 ZFNs

ZFNs were developed in 1994 and were the first genetic engineering technology which utilised the fusion of a DNA nuclease (FokI) with DNA binding proteins (zinc finger proteins) (Choo and Klug, 1994). Zinc finger (ZFs) proteins are each formed of

a single atom of zinc bound to approximately 30 amino acids (Pavletich and Pabo, 1991). The ZFs are bound to FokI via a short linker, and a spacer of five to six bp is required between the binding sites for FokI (Fig 1.7A) (Bibikova et al., 2001). In order for FokI to cleave DNA it must dimerise. Therefore, a pair of ZFNs is required to target a specific DNA site, which greatly increases the specificity of ZFNs. In each ZFN there is usually three to six zinc finger repeats which are able to recognise between nine to 18 bp on the target DNA. Each repeat recognises three nucleotides which greatly reduces the target range of ZFNs (Carroll, 2011).

1.4.2 TALENs

TALENs replaced ZFNs in 2009 (Boch et al., 2009). They are similar to ZFNs due to the use of FokI fused with customisable DNA binding proteins. In the case of TALENs the DNA binding domain is composed of repeats derived from transcription-activator-like effectors (TALEs). TALEs are proteins secreted by *Xanthomonas* bacteria via their type III secretion system to alter the transcription of the host plant they are invading (Boch and Bonas, 2010). The DNA binding domain of TALEs contain 33-34 highly conserved amino acids, each of which recognises a single nucleotide (Figure 1.7B). The 12th and 13th amino acids are referred to as the repeat variable diresidue (RVD) (Moscou and Bogdanove, 2009). The variation of amino acids at these positions allows for greater target DNA specificity. ZFNs and TALENs have similar efficiencies when targeting a specific DNA sequence. However, TALENs are easier to design and have a higher rate of cleavage activity (Kim and Kim, 2014).

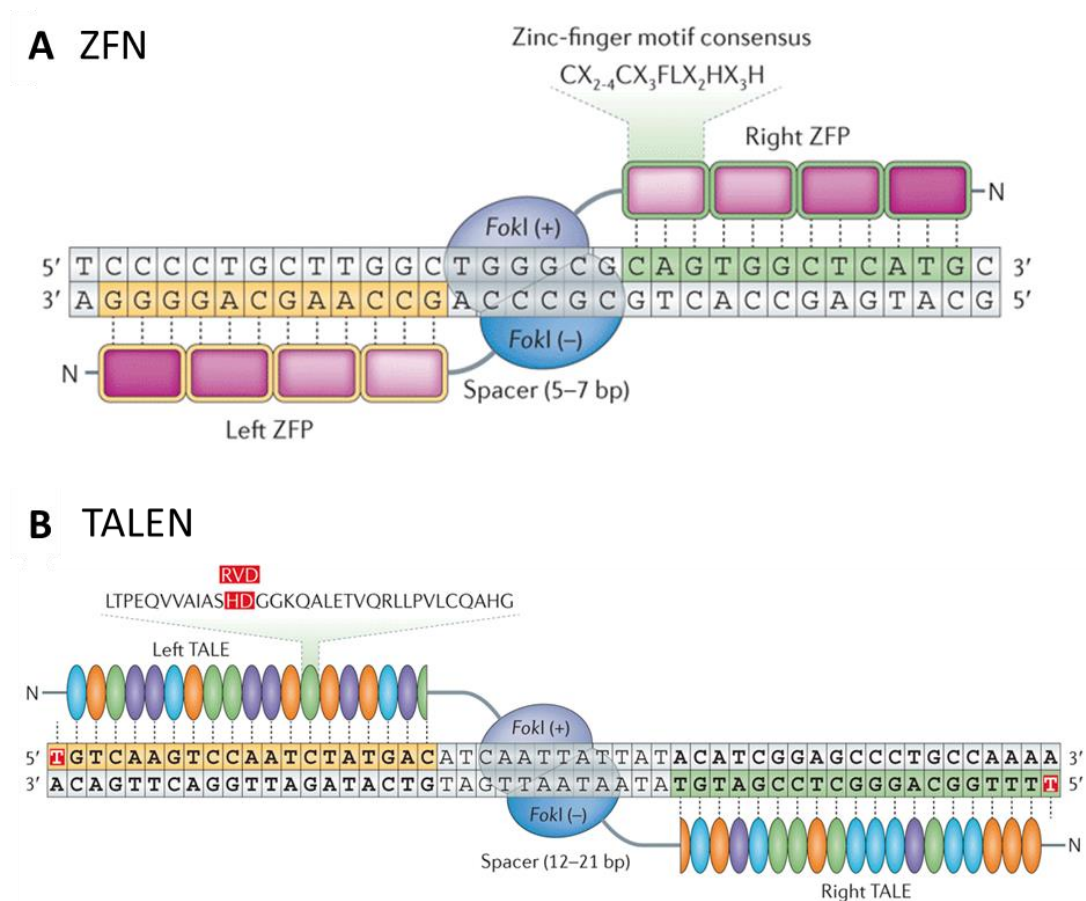


Figure 1.7: ZFN and TALEN programmable nucleases. (A) ZFNs are formed of two FokI nucleases connected to zinc finger proteins via a linker. Each zinc finger repeat recognises a nucleotide triplet. (B) TALENs are formed of two FokI nucleases connected to transcription-like effectors. Each transcription-like effector recognises a single nucleotide via the repeat variable diresidue (Adapted from Kim and Kim, 2014)

1.4.3 CRISPR/Cas9

The CRISPR/Cas9 genetic engineering system has recently become a popular method for modifying specific sites within a gene in a variety of organisms. It is a more efficient, reliable and rapid way of editing genes than ZFNs and TALENs.

CRISPR/Cas9 is derived from a bacterial adaptive immunity system, which was first found in *Streptococcus pyogenes*. The CRISPR locus contains repetitive elements (repeats) that are interspaced with incorporated invading DNA sequences (protospacers). This is used as a 'memory' store of previous infections so if the bacterium is re-infected it can fight the invader. When a reinfection occurs, the CRISPR repeat arrays are transcribed into crRNAs (CRISPR RNA). Each crRNA contains a part of the CRISPR repeat and a protospacer. The crRNAs then hybridizes with tracrRNA (trans-activating RNA) to form a complex with the nuclease Cas9 (crRNA-tracrRNA:Cas9). This complex is guided by the protospacers that recognise protospacer adjacent motifs (PAMs) and the complementary protospacers within the invading DNA. PAMs are found at the 3' end of the protospacer in the invader DNA, but not in the bacterial DNA CRISPR region. This allows the bacteria to distinguish itself from the invader (Mali et al., 2013). Cas9 nuclease is led towards the invading DNA where it can then cleave the DNA to form a DSB to stop an infection from occurring (Sander and Joung, 2014).

This CRISPR/Cas9 system from *S. pyogenes* has been adapted to be able to create specific DSB breaks to allow genes to be edited, knocked-out or introduced within the laboratory. An engineered guide RNA (gRNA) contains crRNA and tracrRNA like sequences (Figure 1.8). It contains a designed 20 bp sequence (like the protospacer in bacterial CRISPR) that targets a sequence flanked by a PAM in the target genome. It also contains a sequence which helps scaffold the gRNA to the Cas9 (Hille and Charpentier, 2016).

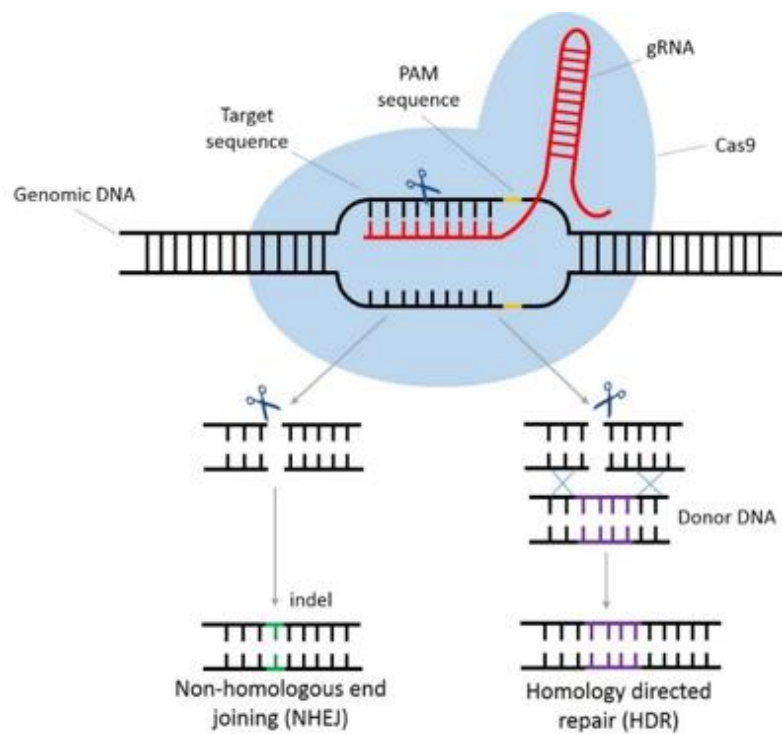


Figure 1.8: CRISPR-Cas9 genetic editing system. The nuclease Cas9 is directed to a specific site within the DNA via a designed gRNA. From here a DSB is formed which is then repaired by the cell via NHEJ or HDR. This results in either indel changes in the DNA causing a gene KO or inserting donor DNA into the host DNA.

1.4.3.1 Applications of CRISPR/Cas9

CRISPR/Cas9 is an incredibly diverse system which not only can be used for gene editing but also for epigenetic modifications, transcriptional control, generating animal models and allowing high throughput genetic screens.

The most simple and effective use for CRISPR/Cas9 is to generate a gene KO that has been previously described. But guiding donor DNA to a desired location within the genome can also use it to create a gene knock-in. CRISPR/Cas9 can also create specific single nucleotide edits.

Editing the epigenome allows changes to gene expression without permanent changes to the DNA sequence. CRISPR/Cas9 has been adapted to edit both DNA methylation and histone modifications. This occurs by fusing Cas9 with methyltransferases (e.g DNMT3A) (Anton and Bultmann, 2017), acetyltransferases (e.g p300) (Hilton et al., 2015) or histone demethylases (e.g LSD1) (Kearns et al., 2015).

The CRISPR/Cas9 system has been adapted to create two modified systems called CRISPRi and CRISPRa which are both able to activate or repress genes without editing their epigenetics. Both systems use an inactive form of Cas9, referred to as "dead" Cas9 (dCas9) (Bikard et al., 2013). dCas9 has no catalytic function but is still able to bind to specific DNA sequences. From here it can block RNA polymerase but also induce the formation of heterochromatin to cause gene silencing. This method of gene regulation is referred to as CRISPRi (Qi et al., 2013). CRISPRa on the other hand involves dCas9 fusing to the transcriptional activation domain Vp64 to induce gene expression (Maeder et al., 2013).

Similar to the use of RNAi, CRISPR/Cas9 can be used to screen for modifications in whole genomes within a single experiment. Cas9 and gRNA libraries can be introduced into cells to generate a range of knock-outs and the phenotypes of interest can be screened. In cancer research, this allows the identification of novel

genes involved in cancer development (Chen et al., 2015, Shi et al., 2015) and drug resistance (Wang et al., 2014).

CRISPR/Cas9 is therefore a very powerful tool that has many applications within genetic and molecular biology. However, the extent of the off-target effects is still unclear. A recent study has demonstrated that off-target effects caused by CRISPR/Cas9 can result in large chromosomal rearrangements (Kosicki et al., 2018).

1.5 Models Used to Study Prostate Cancer

1.5.1 Culture of cell lines in 2D


There are a number of immortalised prostate specific cell lines that allow the study of PCa biology and progression (Table 1.4). Cell lines are a good model of study due to their ease and indefinite culture in 2D. They are also easy to transfect and manipulate, which makes them a suitable candidate for genetic editing. However, many cell lines have been around for decades and therefore no longer represent the patient from which they were harvested (Izadpanah et al., 2008, Kawai et al., 1994, Meissner et al., 2008) (Figure 1.9). This is due to the accumulation of genetic and epigenetic mutations. Therefore, cell lines are a useful model to study for initial research, but to replicate the changes that occur within a patient other models need to be used.

BPH is a chronic disease that occurs later in a man's life and involves the hyperproliferation of prostate cells in the transition zone. It results in the constriction of the descending urethra causing urinary tract infections and discomfort (Briganti *et al*, 2009). Unlike PCa, BPH involves the proliferation of basal cells instead of luminal cells (Dermer, 1978). The BPH-1 cell line is an epithelial cell line derived from the prostate of a 68-yr-old man undergoing transurethral resection of the prostate (TRUP) due to urinary constriction caused by BPH. When cultured in RPMI +5% FCS medium, they remain undifferentiated and do not express AR (Hayward *et al*, 1995). However, when they are triggered to differentiate into luminal cells, they start to express AR

(Pellacani et al., 2014). The BPH-1 cell line has been previously transduced with a lentiviral vector in the Maitland lab by Frame and Pellacani (Frame et al., 2010). The lentiviral vector contains mOrange which is regulated by the luminal prostate specific PSA-probasin promoter. The mOrange can be visualised when the cells differentiate into luminal cells, and in particular when the BPH-1 cells are grown in 3D into spheroids (Pellacani et al., 2014). Non-tumourigenic BPH-1 cells can also initiate tumour growth when recombined with carcinoma associated fibroblasts (CAFs) or being exposed to carcinogenic levels of testosterone and estradiol (Hayward et al., 1995). Therefore, for these reasons BPH-1 cells were chosen as a model for basal prostate differentiation.

P4E6 cells were derived in our lab as a model for early, non-metastatic prostate cancer (Maitland et al., 2001). They express luminal and basal markers such as CK5, CK14 and PSA, but do not express AR when undifferentiated (Lang et al., 2006). This model was chosen to investigate the role of AR during the early development of cancer. Therefore, combined with BPH-1 cells as a model, the importance of AR in the differentiation of basal cells can be investigated in both cancerous and non-cancerous cells.

Table 1. 4: Comparison of available prostate cell lines (Adapted from Oldridge et al., 2012).

Cell Line	Origin	Immortalisation method	Reference	Increasing Malignancy
PNT1a	Normal prostate cells from young male donors	Transfection with the SV40 large T antigen	(Berthon <i>et al</i> , 1995)	
PNT2-C2				
BPH-1	Epithelial cells from 68-yr-old man with benign hyperplasia	Transfection with the SV40 large T antigen	(Hayward <i>et al</i> , 1995)	
P4E6	Well differentiated early Gleason 4 cancer	Transfection with the human papillomavirus-16 E6 gene	(Maitland <i>et al</i> , 2001)	
RC165	Benign tissue collected from African-American PC cancer patient	Telomerase	(Miki <i>et al</i> , 2007)	
Bob	TURP of CRPC tissue	Spontaneous	(Attard <i>et al</i> , 2009)	
Serbob	TURP of CRPC tissue	Spontaneous	(Attard <i>et al</i> , 2009)	
PC346C	Non-metastatic advanced prostate adenocarcinoma	Transfection with a retrovirus	(Marques <i>et al</i> , 2006)	
LNCaP	Metastatic PC cells harvested from the left supraclavicular lymph node	Spontaneous	(Horoszewicz <i>et al</i> , 1983)	
VCaP	Metastatic PC cells harvested from the vertebrae.	Spontaneous	(Korenchuk <i>et al</i> , 2001)	
DU145	Metastatic PC cells from the brain	Spontaneous	(Stone <i>et al</i> , 1978)	
PC3	Grade 4 metastatic PC cells harvested from the bone	Spontaneous	(Kaighn <i>et al</i> , 1979)	

1.5.2 Culture of cell lines in 3D

Recently, the ability to culture cells into 3D spheroids has led to a greater understanding of what occurs *in vivo* without the use of mouse models (Figure 1.9). Unlike normal 2D culture of cell lines, growing cell lines into spheroids in ECM (Matrigel™ Corning) surrounded by stroma, mimics the microenvironment that basal and luminal cells develop within the prostate. This promotes basal cell differentiation, and results in a hollow sphere that mimics an acinus, with a luminal and basal epithelial bilayer surrounding a lumen. This architecture is similar to what is seen in human prostate glands, thereby making spheroids a suitable model for prostate differentiation (Lang et al., 2006, Lang et al., 2001, Lang et al., 2000, Pellacani et al., 2014).

1.5.3 Culture of patient primary cells

Culture of primary cells harvested from patient biopsies allows an invaluable insight into the heterogeneity of PCa and the variation between different patients (Figure 1.9). The primary cell cultures are not immortalised, which avoids any genetic changes that occur during the immortalisation process, but subsequently this means that the cells can only be cultured for a limited time. Patient primary cells are also difficult and expensive to keep in culture.

1.5.4 Mouse models

The mouse model is used for the majority of *in vivo* research into PCa. Cell lines and primary tissue can be transplanted into immunocompromised mice (NOD/SCID or RAG^{-/-} IL2γC^{-/-} mice) to form xenografts (Figure 1.9). This has shed light into the molecular mechanisms of how PCa develops. However, the mouse prostate is significantly divergent from the human prostate. Firstly, mouse prostates tend to atrophy instead of developing cancer or benign hyperplasia. Due to mice having a shorter life span, they are unable to accumulate the same level of mutations than a human would over many years (Sharma and Schreiber-Agus, 1999). The gross

structure of the prostate varies between humans and mice; mice have three lobes to the prostate whereas humans are alobular. Also, humans have a double layer of epithelial cells whereas the murine prostate only has a single layer (Maitland, 2013). Therefore, results derived from mouse models need to be treated with caution.


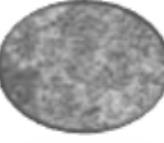


Comparison of Prostate Cancer Models	Cell Lines 	Primary Cultures 	3D Models 	Xenografts 
COST				
TIME				
EFFICIENCY				
CLINICAL RELEVANCE				
HETEROGENEITY				

Figure 1.9: A comparison of different prostate cancer models. Every model has different advantages and disadvantages. Obtained with permission from Fiona Frame.

1.6 Research Aims

There is conflicting evidence as to whether AR is essential for luminal differentiation. Therefore the aim of this was project to investigate whether AR is required for differentiation of basal to luminal secretory cells, and if so to what extent it is required.

Hypothesis: Deletion of the *AR* gene via the CRISPR/Cas9 system still allows the differentiation of a normal luminal phenotype in prostate cancer.

To investigate this hypothesis, I have two clear aims:

1. To KO all of the copies of the *AR* gene in basal BPH-1 and P4E6 cells using CRISPR/Cas9 system
2. To investigate the role AR plays in normal basal to luminal differentiation in order to further understand differentiation of epithelial cells during the development of prostate cancer.

Strategy: Once *AR* was successfully knocked-out in both the basal cell line models, differentiation was induced by growing the cells into 3D spheroids. From here it was investigated whether the cells are able to form spheroids, and if so, to what extent differentiation had occurred. This was then tested by staining for well-known differentiation markers.

Possible outcomes: If AR is essential for differentiation the ARKO spheroids will not successfully form. However, if spheroids do form they will lack a structure consisting of basal and luminal layers. The ARKO clones will also remain basal, indicated by markers such as p63 and CK5. On the other hand, if AR is not essential for differentiation it could still occur. This might be due to other receptors taking over such as RAR, which has been shown to work alongside AR in prostate development. This will be detected by the presence of luminal markers (CK18, NKX3.1, PSA) in ARKO spheroids.

2. Materials and Methods

2.1 Mammalian cell culture

2.1.1 Cell culture of cell lines

All cell lines used in experiments were purchased from the American Type Culture Collection (ATCC, USA) except for the P4E6 cell line which was derived in our laboratory (Maitland et al., 2001) (Table 2.1). BPH-1 cells were gifted from Simon Hayward and BPH-1 PSA-Probasin mOrange (BPH-1 PPmO) cells were generated in our laboratory (Frame et al., 2010). BPH-1 and BPH-1 PPmO cells were cultured in Roswell Park Memorial Institute-1640 (RPMI, Gibco) supplemented with 5% foetal calf serum (FCS, Gibco) and 2 mM L-Glutamine (Invitrogen) (Table 2.1). LNCaP cells were cultured in RPMI with 10% FCS (Table 2.1). VCaP cells were cultured in Dulbecco's Modified Eagle's Medium (DMEM, Gibco) supplemented with 10% FCS and 2 mM L-Glutamine. P4E6 cells were cultured in Keratinocyte Serum-Free Medium (KFSM, Gibco) supplemented with 2% FCS, 50 µg/ml bovine pituitary extract (Invitrogen), 5 ng/ml Epidermal Growth Factor (EGF, Invitrogen) and 2 mM L-Glutamine. All cell lines were cultured in T25, T75 and 10 cm dishes (Sarstedt or Corning) in sterile conditions at 37 °C in 5% CO₂.

2.1.2 Live cell counting using a haemocytometer

Trypan Blue exclusion was used to count the number of viable cells. Briefly, cells grown as a monolayer were trypsinized and 0.4% Trypan Blue Stain (Sigma-Aldrich) was added to a cell suspension at a 1:1 ratio. The number of unstained cells was counted using a haemocytometer (Neubauer) as they were equivalent to live cell number.

Table 2.1: A summary of the human prostate cell lines used.

Cell line	Description	Growth medium	Reference
BPH-1	Human prostate epithelial cells derived from a 68 year-old man with benign hyperplasia and immortalised with SV-40.	RPMI + 5% FCS (R5)	(Hayward et al., 1995)
BPH-1 PPMO	BPH-1 cells with a reporter gene inserted (PSA-Probasin mOrange) which fluoresce when AR is expressed upon differentiation.	RPMI + 5% FCS (R5)	(Frame et al., 2010)
VCaP	Metastatic prostate cancer cells harvested from the vertebrae.	DMEM + 10% FCS (D10)	(Korenchuk et al., 2001)
P4E6	Human prostate epithelial cells derived from a well differentiated early stage cancer and immortalised with HPV16 E6 retrovirus.	KSFM + 2% FCS (K2)	(Maitland et al., 2001)
LNCaP	Metastatic prostate cancer cells harvested from the left supraclavicular lymph node.	RPMI + 10% FCS (R10)	(Horoszewicz et al., 1983)

2.1.3 Cryopreservation of cell cultures

Cultured cells were harvested via trypsinisation and centrifuged at 1200 RPM for 3 min. They were resuspended in freezing medium (10% (v/v) dimethyl sulfoxide (DMS), 20% (v/v) FCS in RPMI) at a concentration of $1-2 \times 10^6$ cells/ml and transferred into 2 ml cryovials (Greiner Bio-One). Before transferring to liquid nitrogen for long term storage, they were stored at $-80\text{ }^{\circ}\text{C}$ for 24 hr.

2.2 Generation and Identification of AR Knock-Out Clones

2.2.1 Minimal lethal dose of puromycin

BPH-1 and P4E6 cells were seeded onto a 6-well plate at a density of 200,000 cells per well. The cells were grown until they were 70-80% confluent. Spent media was aspirated and the cells were washed with PBS. 2 ml of media containing increasing concentrations of the antibiotic puromycin dihydrochloride (0.25 $\mu\text{g/ml}$, 0.5 $\mu\text{g/ml}$,

1.0 µg/ml, 1.5 µg/ml, 2.0 µg/ml) (Sigma-Aldrich) was then added. The puromycin-containing media was changed every two days for a week, after which the cells were then stained with 1% crystal violet (Sigma-Aldrich) and imaged.

2.2.2 CRISPR/Cas9 transduction

The CRISPR/Cas9 lentivirus was designed by Sigma-Aldrich to target exon 1 of the *AR* gene. Before lentiviral infection, 200,000 cells were seeded per well on a 6-well plate. They were infected with the *AR* targeting lentivirus for 12 hr at a 2:1 and 1:1 ratio (lentivirus:cell) as calculated from the transfection units per ml value provided. Controls used included an *EMX1* targeting lentivirus (positive control) and a non-targeting lentivirus (negative control) (Sigma-Aldrich). *EMX1* is a gene involved in brain development and therefore it should not have any effect on the biology of prostate cells when it is knocked out (Chan *et al*, 2001). The transfected cells were then selected using 1.0 µg/ml puromycin in BPH-1 and BPH-1 PPMO cells and 2.0 µg/ml puromycin in P4E6 cells. The transduced cells were grown in puromycin for 1-2 weeks until they reached 80% confluency.

2.2.3 Ring cloning

To generate individual colonies, 1000 cells were seeded onto a 10 cm dish and grown further. A sterile cloning ring was coated in sterile vacuum grease (Beckman Coulter) and then placed over a single colony to make a seal. The colony was subsequently seeded into a well on a 6-well dish via trypsinisation. Cells were then grown in a 10 cm dish until confluent.

2.2.4 Dilution cloning

Cells were seeded onto a 96-well plate with a theoretical 1 cell per well. When confluent, cells were seeded into a well on a 6-well dish. Cells were grown up to a confluent 10 cm dish.

2.2.5 Sanger sequencing

Sanger sequencing for *AR* and *EMX1* genes was performed by the Genomics and Bioinformatics Lab at the University of York using BigDye Terminator v3.1 Cycle Sequencing Kit from Applied Biosystems. Samples were run on an Applied Biosystems 3130xl Genetic Analyser. Sequences were analysed by myself using SeqScanner 2. When edited sequences produced multiple peaks, which is indicative of edits in multiple alleles, CRISP-ID was used to analyse the sequences (Dehairs et al., 2016). CRISP-ID is a web application which allows the identification of indels in up to three different alleles from a single Sanger trace.

2.3 Isolation and Analysis of Genomic DNA

2.3.1 DNA extraction

Genomic DNA (gDNA) was extracted using the Qiagen DNeasy Blood and Tissue Kit (Qiagen) following the manufacturer's protocol from cell pellets. Briefly, up to 5×10^6 were trypsinised and harvested. The cells were pelleted by stopping the trypsin in R10 and centrifuging the cells at 1200 RPM for 3 min. The supernatant was aspirated, and the pellet was resuspended in 200 μ l PBS. 20 μ l of proteinase K, 4 μ l of RNase A and 200 μ l of ATL buffer was added and the lysate was vortexed. The lysate was incubated at 56 °C for 10 min. 200 μ l of 100% ethanol was added to the lysate and it was mixed by vortex. The homogenate was transferred to a DNeasy Mini spin column in a 2 ml collection tube. The column was centrifuged at 8000 RPM for 1 min. The flow-through was discarded. 500 μ l of AW1 buffer was added to the spin column and centrifuged at 8000 RPM for 1 min. The flow-through was discarded. 500 μ l of AW2 buffer was added to the spin column and centrifuged at 13,000 RPM for 3 min. The spin column was transferred to a 1.5 ml microcentrifuge tube and 30 μ l of nuclease-free water (Sigma-Aldrich) was added to the column to elute the gDNA. The column was centrifuged at 8000 RPM for 1 min and discarded. The concentration of the gDNA was determined by the NanoDrop ND-1000 spectrophotometer (ThermoFisher Scientific).

gDNA samples were stored at -20 °C. gDNA was considered to be pure if the ratio between the 260nm and 280nm absorbance readings was ~1.8.

2.3.2 PCR

Polymerase chain reaction (PCR) was carried out on gDNA to amplify the region of *AR* and *EMX1* genes targeted by the CRISPR/Cas9 lentivirus. PCR reagents were obtained from Promega and primers were manufactured by Sigma-Aldrich (Table 2.2). In each PCR reaction, between 100 ng – 200 ng of gDNA was added to a 50 µl reaction (5 µl gDNA and 45 µl master mix) and each reaction was run in a GeneAmp PCR System 9700 thermal cycler (Applied Biosystems).

2.3.2.1 *AR* master mix and PCR programme

Promega 5x flexi buffer (1x), 25 mM MgCl₂ (2.5 mM), 10 mM dNTPs (0.4 mM) (Invitrogen), 10 µM forward primer (0.2 µM), 10 µM reverse primer (0.2 µM), high-performance GoTaq® G2 DNA Polymerase (2.5 U) and 26 µl of nuclease-free water to total 45 µl per sample (Table 2.2). The PCR programme used was as follows:

1 hold: 94 °C, 2:00 min
35 cycles: $\left(\begin{array}{l} 94\text{ °C, 30 sec} \\ 60\text{ °C, 30 sec} \\ 72\text{ °C, 30 sec} \end{array} \right)$
2 holds: 72 °C, 5:00 min

2.3.2.2 *EMX1* master mix and PCR programme

Promega 5x flexi buffer (1x), 25 mM MgCl₂ (2.0 mM), 10 mM dNTPs (0.4 mM) (Invitrogen), 10 µM forward primer (0.2 µM), 10 µM reverse primer (0.2 µM), high-performance GoTaq® G2 DNA Polymerase (2.5 U) and 27.5 µl of nuclease-free water to total 45 µl per sample (Table 2.2). The PCR programme used was as follows:

1 hold: 94 °C, 2:00 min
30 cycles: $\left(\begin{array}{l} 94\text{ °C, 30 sec} \\ 59\text{ °C, 30 sec} \\ 72\text{ °C, 30 sec} \end{array} \right)$
2 holds: 72 °C, 5:00 min

Table 2.2: Primers for PCR

Target	Product length	Primer Sequence
<i>AR</i>	424 bp	Forward: AGCCTGTTGAACTCTTCTG
		Reverse: GTTGCTGTTCCCTCATCCA
<i>EMX1</i>	507 bp	Forward: ATGGGAGCAGCTGGTCAGAG
		Reverse: CAGCCCATTGCTTGTCCCT

2.3.4 PCR Purification

PCR products were purified using the QIAquick PCR purification Kit (QIAGEN). Buffer PB was added to PCR products in a 1:5 ratio (v/v) and transferred to a QIAquick spin column. The samples were then centrifuged at 13,000 RPM for 1 min. The flow-through was discarded and 750 µl of Buffer PE was added to wash the column. The samples were centrifuged at 13,000 RPM for 1 min and the flow-through was discarded. To elute the DNA, the column was transferred to a 1.5 ml microcentrifuge tube and 30 µl of nuclease-free water (Sigma-Aldrich) was added for 1 minute before centrifuging at 13,000 RPM for 1 minute. This step was repeated to total 60 µl of eluted DNA. The concentration was determined using a NanoDrop ND-1000 spectrophotometer and samples were stored at -20 °C.

2.3.5 Gel electrophoresis

PCR products were visualised on a 1% (w/v) agarose (Invitrogen) gel stained with GelRed® 10,000X nucleic acid gel stain (Biotium) with a 100 base pair (bp) DNA ladder (New England Biolabs). The gels were run at 80 V for approximately 70 min and imaged with UV illumination on the Pxi system (Syngene).

2.3.6 Copy number analysis of genomic *AR*

The copy number of *AR* and *DMD* was investigated via qPCR in the cell lines BPH-1, BPH-1 PPMO, P4E6, VCaP as well as female and male DNA. *GAPDH* was used as an endogenous control. In each 15 µl reaction, 20 ng of gDNA was loaded. The 1x master mix consisted of 7.5 µl BioRad SSoFast EvaGreen Supermix, 0.6 µl of 10 nM forward primer, 0.6 µl of 10 nM reverse primer (Table 2.3) and 4.3 µl nuclease-free water.

Reactions were pipetted onto a FrameStar® 96 Well Skirted PCR Plate (4titude) sealed with an optically clear seal (BioRad) and spun at 1100 RPM at 4 °C for 2 min. The qPCR reaction was performed on the BioRad CFX machine with the programme as follows: (98 °C 2:00, 98 °C 0:05, 58 °C 0:05) x44 and a melt curve at 65 °C 0:05, 95 °C 0:50. The $\Delta\Delta C_t$ method was used to analyse the relative expression of *AR* and *DMD* to *GAPDH* and the male control. For example for the BPH-1 cell line, $\Delta C_t = C_{tAR} - C_{tGAPDH}$ and $\Delta\Delta C_t = \Delta C_{tBPH-1} - \Delta C_{tmale}$. Therefore $2^{-\Delta\Delta C_t}$ calculates the copy number of AR and DMD.

Table 2.3: Primers for copy number analysis

Target	Primer Sequence
<i>AR</i>	Forward: TCATTATCAGGTCTATCAACTCTT
	Reverse: GTCATCCCTGCTTCATAACATTC
<i>DMD</i>	Forward: TTGGTTGCCAGTTATGGGCT
	Reverse: CCAGCTGTCATGCAAAACCC
<i>GAPDH</i>	Forward: ATGCTGCATTGCGCCCTCTTA
	Reverse: GCGCCCAATACGACCAAATC

2.4 Isolation and Analysis of Protein Expression

2.4.1 Protein extraction

Harvested cells were resuspended in CytoBuster™ protein extraction reagent (Novagen) with cComplete™ Mini EDTA-free Protease Inhibitor Cocktail (Roche). The lysates were incubated at room temperature for 5 min and then centrifuged at 16,000 g for 4 min at 4 °C. The supernatant was collected and stored at -80 °C.

2.4.2 Bicinchoninic acid assay (BCA) for protein concentration determination

The protein lysate concentration was quantified using the BCA protein assay kit (Thermo Scientific) according to the manufacturer's instructions. BSA standards and samples were pipetted in triplicate into a 96 well plate. Working reagent was added to each well and the plate was incubated at 37 °C for 30 min. The absorbance was read on a POLARstar OPTIMA microplate reader (BMG labtech) at 562 nm. A standard

curve of known protein concentrations was generated to determine the concentration of the unknown samples.

2.4.3 SDS-PAGE gel electrophoresis

Protein lysate (20 µg) was added to 4x Laemmli Sample Buffer (Bio-Rad) and heated to 100 °C for 4 min in a QBD2 heating block (Grant). Samples were loaded onto 10% Tris-SDS acrylamide gels along with Precision Plus Protein™ Kaleidoscope™ Prestained Protein Standards (Biorad). The gels were run at 80 V for 2 hr in SDS running buffer (3.5 mM SDS, 0.19 M Glycine, 25 mM Tris).

2.4.4 Western blotting

Table 2.4: Primary and secondary antibodies for AR and GAPDH western blots

	Antibody	Product Size (KDa)	Working dilution	Species Isotype	Manufacturer	Cat. No.
Primary Antibodies	Anti-AR	110	1:750	Rabbit polyclonal	Santa Cruz	sc-815
	Anti-GAPDH	37	1:10000	Rabbit polyclonal	abcam	ab9485
Secondary Antibody	Anti-Rabbit IgG, HRP-linked Antibody	N/A	1:10000	Goat	Cell Signalling Technology	7074

The resolved proteins were transferred onto Immobilon-P membrane (Millipore) pre-treated with methanol in transfer buffer (48 mM Tris, 39 mM Glycine, 10% (v/v) Methanol) at 100 V for 1.5 hr. Immediately after, membranes were blocked in 5% non-fat milk in 0.1% Tris-buffered saline-tween (TBST) (150 mM NaCl, 50 mM Tris/HCl, pH 7.5, 0.1% (v/v) Tween) for 1 hr at room temperature. The membranes were then

incubated with primary antibodies diluted in 1% non-fat milk at 4 °C overnight (Table 2.4). Membranes were washed three times for 5 min each in TBST and then incubated in the secondary antibody, diluted in 1% non-fat milk for 1 hr at room temperature. Membranes were washed again three times in TBST. Chemiluminescent detection was performed using the BM Chemiluminescence Blotting Substrate (POD) system (Roche). The proteins were visualised using ECL hyperfilm (Amersham) and processed using the Kodak GBX developer and fixer solutions (SLS).

2.5 *In vitro* Differentiation of Prostate Epithelial Cells

2.5.1 Development of an epithelial bilayer

BPH-1 and BPH-1 PPmO cells were seeded at 100% confluency (4×10^5) onto a 12 well plate in triplicate. They were grown in non-differentiating media (R5) and differentiating media (D5 with 10 nM DHT). After two weeks, the expression of mOrange was analysed using flow cytometry on a Cytoflex S (Beckman Coulter). mOrange fluorescence excitation wavelength is 548 nm and the emission wavelength is 562 nm, therefore a 561 nm laser was used. Debris was excluded using FS Area/ SS Area. Doublets were excluded using FS Area/FS Width. mOrange positive cells were gated on ECD Area/ PE Area.

2.5.2 3D co-Culture of prostate spheroids

BPH-1 PPmO and P4E6 cells were grown into 3D spheroids under conditions previously optimised in our lab. The stromal cells used in this study were obtained from the CRU bio-bank of primary cultures. The cells were harvested from human prostate tissue obtained, with patient consent and full ethical approval and were from patients undergoing radical prostatectomy and channel transurethral resection (TURP) for prostate cancer (ethics number: 07/H1304/121). Stromal cells were seeded at a density of 2×10^5 in 6 well plates, in DMEM with 10% FCS (D10) and 10 nM DHT (Sigma-Aldrich) and were grown until 70-80% confluent. To set up the co-culture, 2 ml of Matrigel™ (Corning) was added to 0.4 μ M inserts (Falcon) at a ratio of 1:1 with

2 ml of K2 medium. This Matrigel™ plug was incubated at 37 °C for 30 min. 1.5×10^5 of BPH-1 PPMO and P4E6 cells were resuspended in 50% Matrigel™:K2 media supplemented with 10 nM DHT, 10 nM β -estradiol and 2 mM CaCl_2 (Sigma-Aldrich) and seeded on to the Matrigel™ plug. The Matrigel™ was allowed to set for 30 min at 37 °C and 1 ml of the supplemented K2 media was subsequently added to the insert. To maintain the spheroids, 500 μl of spent epithelial media was aspirated and replaced with 500 μl of fresh media on alternate days. The stromal cells were fed on those days with 2 ml of stromal media. The spheroids and stromal cells were grown for up to 14 days.

2.5.2.1 Quantification of mOrange Expression

Spheroids were visualised on a Leica DMIL LED fluorescent microscope. The total number of spheroids and the number of spheroids expressing mOrange were counted in four random fields of view. The percentage of mOrange spheroids was calculated.

2.6 Detection of AR Expression

2.6.1 Spheroid cell recovery

Spheroids were harvested from Matrigel™ to form a pellet using Cell Recovery Solution (Corning). Initially the spent media was collected and transferred to an ice-cold 15 ml falcon tube. 2 ml of Cell Recovery Solution was added to and a cell lifter was used to break up the Matrigel™. The mixture was transferred to the 15 ml falcon tube. A further 4 ml of Cell Recovery Solution was added and the remaining Matrigel™ was transferred to the 15 ml falcon tube. The falcon tube was then mixed for 1 hr in ice on a rocker. The falcon tube was centrifuged for 5 min at 300 g at 2 °C. The supernatant was aspirated, and the pellet was washed by resuspending it in 1 ml of ice-cold PBS. The mixture was centrifuged for 5 min at 300 g at 2 °C. This step was repeated, and the final pellet was stored at -20 °C.

2.6.2 RNA extraction

RNA was extracted from cell and spheroid pellets using an RNeasy Mini Kit (Qiagen) as per the manufacturer's instructions. Spheroid pellets were collected as described in section 2.6.1. Cell pellets were harvested via trypsinisation. The trypsin-EDTA was stopped with R10 and the cells were centrifuged at 1200 RPM for 3 min. The supernatant was aspirated, and the pellet was lysed with 350 μ l of Buffer RLT with 1:100 (v/v) β -mercaptoethanol (β -Me) and vortexed for 20 seconds. To homogenise the samples, the lysate was transferred to QIAshredder spin column (Qiagen) and centrifuged at 13,000 RPM for 2 min. Then 350 μ l of 70% ethanol was added and the homogenate was transferred to a RNeasy Mini spin column. The mixture was centrifuged at 10,000 RPM for 1 min. The flow-through was discarded and the column was washed with 700 μ l of RW1 Buffer. The mixture was centrifuged at 10,000 RPM for 1 min. The flow-through was discarded and the column was washed with 500 μ l of RPE Buffer. The mixture was centrifuged at 10,000 RPM for 1 min. The flow-through was discarded and the column was washed again with 500 μ l of RPE Buffer. The mixture was centrifuged at 10,000 RPM for 2 min and the flow-through was discarded. The column was dried by centrifuging at 10,000 RPM for 1 min in a new collection tube. Each column was then placed in a 1.5 ml microcentrifuge tube and 30 μ l of RNase free water was added to elute the RNA. The microcentrifuge was left for 1 minute before centrifuging at 10,000 RPM for 1 min. This step was repeated again to result in a final elution of 60 μ l. RNA quality and concentration was then determined using NanoDrop ND-1000 spectrophotometer. The RNA samples were stored at -20 $^{\circ}$ C.

2.6.3 cDNA synthesis

All RNA samples were reverse transcribed into complementary DNA (cDNA). Two master mixes were made (Invitrogen) according to Table 2.5. In a PCR tube the appropriate volume of RNA was added, 2 μ l of master mix 1 and then the mixture was made up to 13 μ l with nuclease-free water (Sigma-Aldrich). The mixture was incubated

at 65 °C for 5 min. The tubes were put on ice for 2 min and then 7 µl of master mix 2 was added. The tubes were then incubated at 23 °C for 10 min, 55 °C for 10 min and 80 °C for 10 min. This was conducted using a GeneAmp PCR System 9700 (Applied Biosystems). The PCR product was then purified as described in section 2.3.4 and the concentration was determined using NanoDrop ND-1000 spectrophotometer.

Table 2.5: cDNA synthesis master mixes

	Component	Volume
Master Mix 1	50 µM random primers	1 µl
	10 mM dNTP mix	1 µl
	RNA (up to 5 ug)	up to 11 µl
	Nuclease-free water	to 13 µl
Master Mix 2	5x SSIV Buffer	4 µl
	100 mM DTT	1 µl
	RNase OUT™	1 µl
	Superscript® IV reverse transcriptase (200 U/µl)	1 µl

2.6.4 Quantitative reverse transcriptase (qRT-PCR) detection of *AR* mRNA

Quantitative reverse transcriptase PCR (qRT-PCR) was performed using a CFX96 Real-Time PCR Detection System (Bio-Rad). SYBR Green chemistry was used with 5 µl SsoFast EvaGreen Supermix (Bio-Rad), 0.9 µl 10 nM forward primer, 0.9 µl 10 nM reverse primer and 1.2 µl Sigma water (Table 2.6). 2 µl cDNA (5 µg/ml) was added on the bench top to total 10 µl per reaction. Reactions were pipetted onto a FrameStar® 96 Well Skirted PCR Plate (4titude) sealed with an optically clear seal (BioRad) and spun at 1100 RPM at 4 °C for 2 min. The qPCR reaction was performed on the BioRad CFX machine with the programme as follows: (95 °C 2:00, 95 °C 0:10, 60 °C 0:05) x39

and a melt curve at 65 °C 0:05, 95 °C 0:50. The standard curve method was used to determine the fold difference in expression between the calibrator sample and unknown samples. The results were analysed using the Bio-Rad CFX Manager 2.

Table 2.6: Primers for qRT-PCR

Target	Primer Sequence
AR	Forward: CTCATGCCCCCTTTCAGATGTC
	Reverse: GAAAAAAAAAAGCCCAGCAAATAGAAT
RPLPO	Forward: GCACTGGAAGTCCAACTACTTC
	Reverse: TGAGGTCCTCCTTGGTGAACAC

2.7 Paraffin-embedding and Sectioning of Prostate Spheroids

2.7.1 Collection and preparation of spheroids

The media and Matrigel™ containing spheroids was transferred to a 15 ml falcon tube using a Pasteur pipette. 1 ml of PBS was added to the remaining Matrigel™ and transferred to the falcon tube using a Pasteur pipette. The Matrigel™ was spun at 1500 RPM for 5 min. The supernatant was aspirated, and the pellet was washed 5 times with PBS. The pellet was resuspended in 225 µl of citrate-plasma and 5.6 µl of 1 M calcium chloride. Following this, 22.5 µl of thrombin is added and the mixture is stirred gently with a pipette until coagulation. The coagulated pellet was moved to a histocassette which is made up of a layer of filter paper, a sponge layer with a hole for the pellet and a layer of filter paper on top. The histocassette was left in 4% formaldehyde for 4 hr and then stored in 70% ethanol until paraffin embedding.

2.7.2 Paraffin-embedding spheroids

When the spheroids are ready for paraffin embedding they were transferred in the histocassette to fresh 70% ethanol for 10 min. This was followed by 100% ethanol 3 x 10 min, propan-2-ol 2 x 10 min and xylene 4 x 10 min. The histocassettes were blotted on blue roll and then placed into melted paraffin pots 4 x 15 min. The paraffin was

kept at 60 °C and melted the night before. The spheroid pellet was then removed from the histocassette and placed into a metal mould filled with molten paraffin. The lid of the histocassette was placed on top containing the label, and then left to harden on the cold plate for up to 20 min. The samples were removed from the mould and stored at room temperature before sectioning.

2.7.3 Sectioning spheroids

SuperFrost Plus Slides (ThermoFisher Scientific) used for sectioned spheroids were initially coated in 3-Aminopropyltriethoxysilane (APES) before use. They were submerged in a 2% APES bath for 3 min followed by washes in acetone and then distilled water. They were left to dry overnight on a slide dryer.

The paraffin-embedded spheroids were sectioned (5 µm thick) using a Leica RM2235 microtome. A water bath was used to flatten the paraffin sections onto APES coated slides. They were left to dry overnight on a slide dryer.

2.8 Immunohistochemistry of spheroids

On a slide dryer, the paraffin-embedded spheroid and cell pellet sections were baked at 45 °C for 20 min. Paraffin was removed and the sections were rehydrated by immersing the slides in the following baths: xylene 2 x 10 min, xylene 2 x 1 min, 100% ethanol 3 x 1 min and 70% ethanol 1 x 1 min. The slides were then washed under running tap water for 5 min. Heat-induced epitope retrieval (HIER) was conducted overnight using the 2100 Antigen Retriever (Aptum Biologics) with the slides immersed in sodium citrate buffer (pH 6).

The slides were washed with PBS 3 x 5 min at medium speed on an orbital shaker the following day. Using a PAP pen (Dako), a circle was drawn around each section to form a hydrophobic barrier. The sections were then blocked in 10% (v/v) FCS in PBS for 1 hr at room temperature in a dark and moist box. The block was removed with a

PBS wash and the sections were incubated in primary antibody (Table 2.7) diluted in 10% (v/v) FCS in PBS overnight at 4 °C in the box.

The next day the slides were washed with PBS 3 x 5 min. Endogenous peroxidases were removed by treating the sections with 3% (v/v) hydrogen peroxidase in PBS for 30 min. The hydrogen peroxidase was washed off with PBS. The slides were then incubated with the secondary biotinylated antibody (Table 2.7) diluted in 10% (v/v) FCS in PBS for 30 min at room temperature. The slides were washed again with PBS 3 x 5 min to remove the secondary antibody. The sections were then incubated with the tertiary antibody (Table 2.7) (streptavidin-HRP) diluted in 10% (v/v) FCS for 30 min at room temperature. The tertiary antibody was removed by washing with PBS for 2 x 5 min. The sections were incubated in diaminobenzidine (ImmPACT DAB peroxidase substrate, Vector Laboratories) for 90 sec. The slides were rinsed in distilled water and then running water for 5 min. The sections were subsequently counterstained with haematoxylin for 3 sec and then rinsed with running water for 5 min. Finally, the sections were dehydrated by immersion in the following baths: 70% ethanol 1 x 1 min, 100% ethanol 3 x 1 min and xylene 2 x 1 minute. A coverslip was mounted onto each slide using DPX (Sigma-Aldrich).

Table 2.7: Antibodies used for IHC

	Antibody	Working Dilution	Species	Manufacturer	Cat. No.
Primary	CK5	1:500	Rabbit monoclonal	Abcam	Ab52635
	p63	1:500	Mouse monoclonal	Dako	M7317
	CK18	1:800	Mouse monoclonal	Sigma-Aldrich	C8541
	NKX3.1	1:500	Rabbit monoclonal	Cell Signalling	D6D2Z
	AR	1:100	Mouse monoclonal	Santa-Cruz	441
Secondary	Goat anti-rabbit biotinylated	1:500	Goat polyclonal	Dako	E0432
	Rabbit anti-mouse biotinylated	1:200	Rabbit polyclonal	Dako	E0354
Tertiary	Streptavidin-HRP	1:100	N/A	Dako	P0397

2.9 Cell Viability Assay

BPH-1 PPmO and P4E6 spheroids were set up in triplicate as described in section 2.5.2 on a 0.4 μm insert (Millicell) in a 24 well plate (Corning) and left to grow for 8 days. The day before the CellTiter-Glo[®] 3D cell viability assay (Promega) was conducted, the working reagent was moved from $-20\text{ }^{\circ}\text{C}$ to $4\text{ }^{\circ}\text{C}$ and left overnight to thaw. The next day, the working reagent was placed at room temperature along with the plate of spheroids for 30 min. ATP (Sigma-Aldrich) was diluted in water to produce standards at $50\text{ }\mu\text{M}$, $10\text{ }\mu\text{M}$, $2\text{ }\mu\text{M}$, $0.4\text{ }\mu\text{M}$, $0.08\text{ }\mu\text{M}$, which were plated in triplicate at $100\text{ }\mu\text{l}$ onto an opaque bottom 96 well plate (Nunc). $100\text{ }\mu\text{l}$ of the working reagent was added to each well of spheroids and ATP standards. The plates were mixed on an orbital shaker for 5 min at maximum speed. $200\text{ }\mu\text{l}$ of the media and working reagent mix from the

spheroids was then plated onto the 96 well plate. Luminescence was recorded on a POLARstar OPTIMA microplate reader (BMG labtech). A standard curve of known ATP concentrations was generated to determine the concentration in the spheroids to determine their viability.

2.10 Statistical Analyses

All statistical tests were carried out using Graph Pad Prism 7 software (San Diego, USA). Results were displayed as a mean of three technical replicates with associated standard deviation. Statistical significance was represented on graphs as * $p = 0.01$ to 0.05 , ** $p = 0.001$ to 0.01 , *** $p = 0.0001$ to 0.001 , **** $p < 0.0001$.

3. Results

3.1 Generation of *AR* Knock-Out in Basal Prostate Cells

3.1.1 Basal cell lines contain one or more copies of *AR*

Prior to the CRISPR/Cas9 experiments, the number of *AR* copies within BPH-1, BPH-1 PPMO and P4E6 cell lines needed to be determined. The original karyotype of the BPH-1 cell line suggested there would be two copies of *AR* due to the presence of two X chromosomes (Hayward et al., 1995). However the number of copies of *AR* is unknown in BPH-1 PPMO cells.

Copy number analysis was conducted via qPCR of gDNA from different cell lines. Copy number was normalised to *GAPDH* and then to male cells. *DMD* was used to distinguish between ploidy and amplification of *AR* because *DMD* is not near *AR* on the X chromosome and therefore it is unlikely that it will be amplified. Hence, *DMD* is used as a proxy for the number of X chromosomes. Female and male gDNA were used as controls for two X chromosomes and one X chromosome respectively. VCaP cells were used as a positive control as their *AR* copy number has been previously determined (Li et al., 2012). The analysis showed that P4E6 cells have one X chromosome and one copy of *AR* (Figure 3.1). BPH-1 cells have two X chromosomes and two copies of *AR*. BPH-1 PPMO cells have three X chromosomes and three copies of *AR*. The comparison of *AR* copy number to *DMD* copy number is not significantly different for any cell lines except for VCaP (paired t-test, $p=0.0441$).

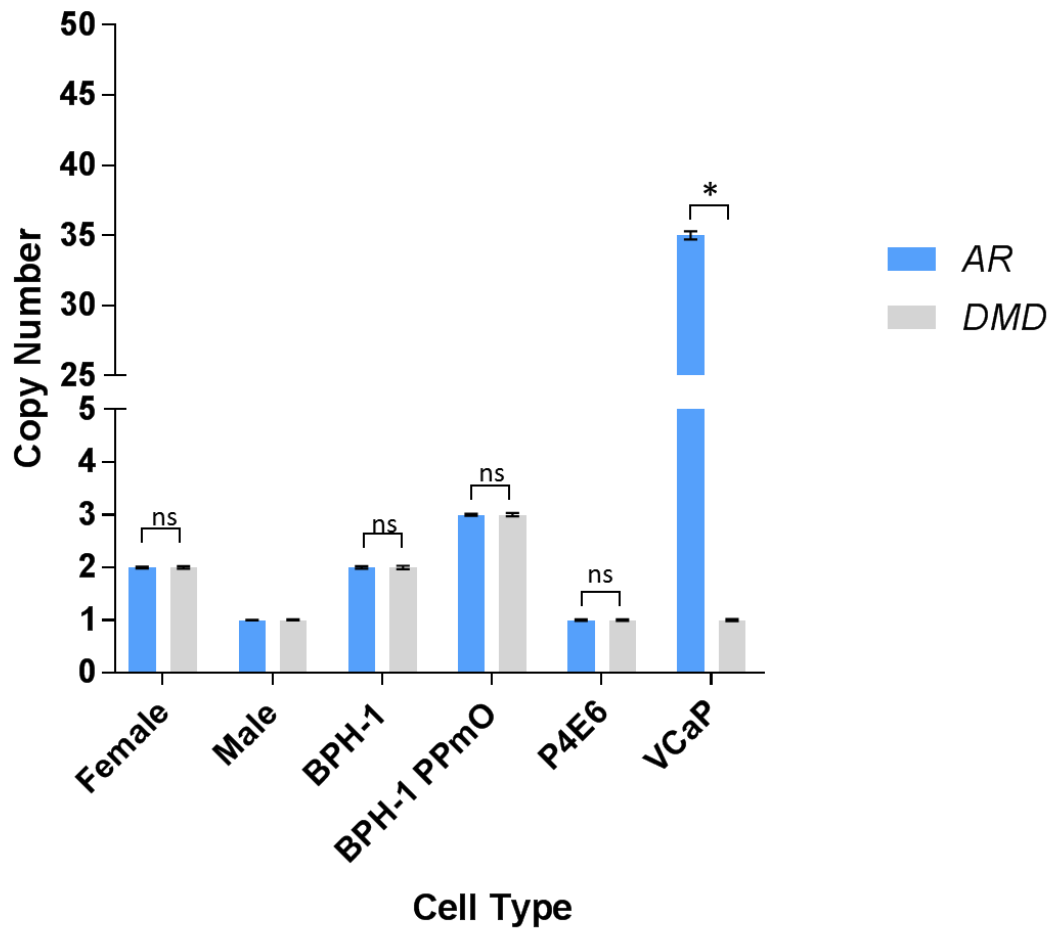


Figure 3.1: AR and DMD copy number varies in different prostate cell lines. qPCR was used to analyse the copy number of AR and DMD in the gDNA of different prostate cell lines. Male and female gDNA were used as controls. Paired t-test, * = $p \leq 0.05$, $n=3$. Error bars represent standard deviation calculated from the coefficient of variation.

3.1.2 Determination of minimal lethal dose of puromycin

The CRISPR/Cas9 lentivirus cassette contained the resistance gene for the antibiotic puromycin. Initially the minimal lethal dose (MLD) of puromycin was determined for both BPH-1 and BPH-1 PPmO cells. This was defined as the minimum concentration required to kill all the cells. Following 7 days of exposure to increasing concentrations of puromycin (0.25 µg/ml to 2.0 µg/ml) cells were stained with 1% crystal violet in order to visualise the remaining cells. It was concluded that the MLD of puromycin for BPH-1 and BPH-1 PPmO cells was 1.0 µg/ml (Figure 3.2). Previous work done in our lab showed that the MLD for P4E6 cells was 2.0 µg/ml (unpublished).

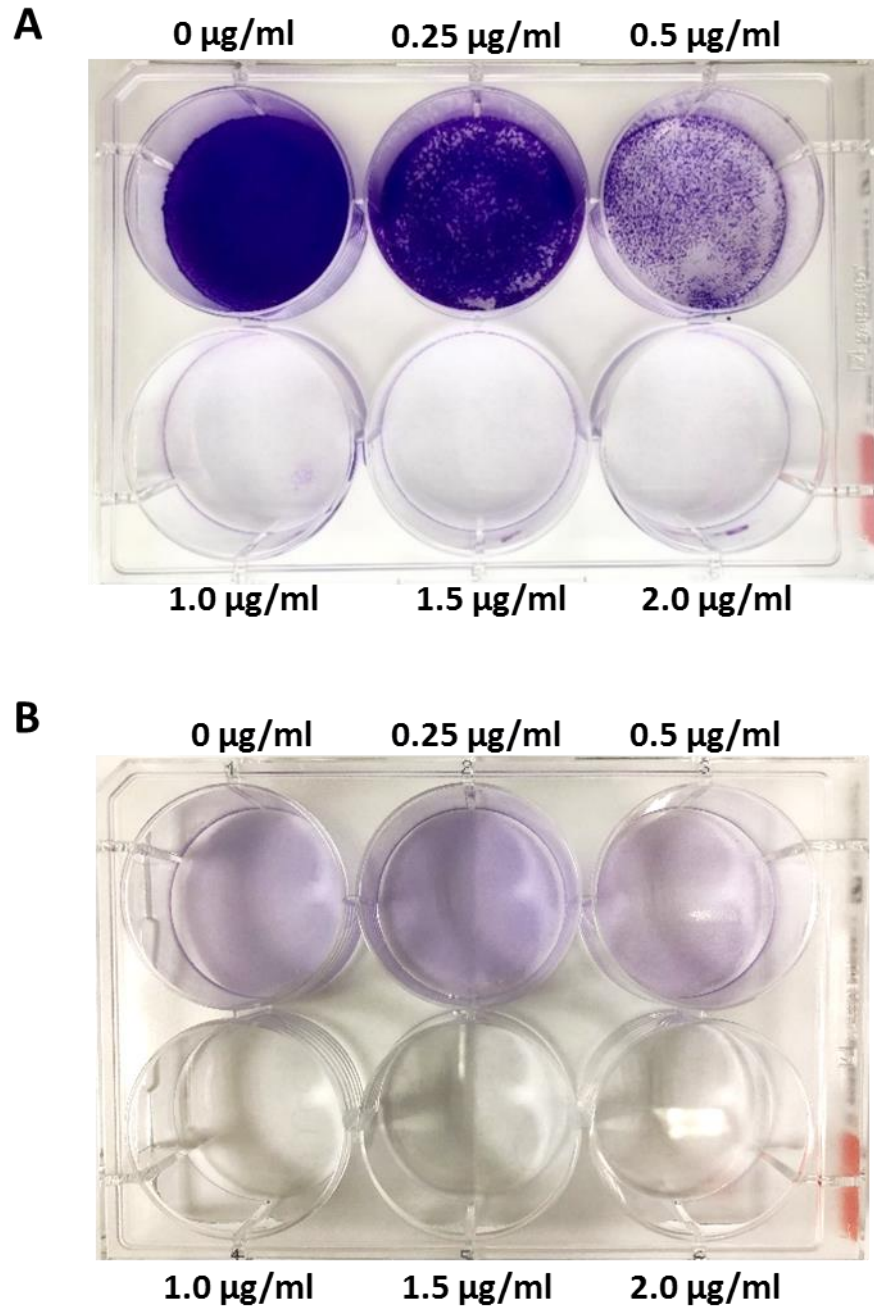


Figure 3.2: Minimum lethal dose of puromycin for BPH-1 and BPH-1 PPmO cells. Puromycin was added to BPH-1 (A) and BPH-1 PPmO (B) cells for 7 days in concentrations ranging from 0 $\mu\text{g/ml}$ to 2.0 $\mu\text{g/ml}$. The cells were stained with 1% crystal violet.

3.1.3 PCR Optimisation of *AR* primers

In order to determine if the CRISPR/Cas9 had successfully edited *AR*, primers were designed to flank the gRNA target sequence and the subsequent PCR products were sequenced. This required optimisation of PCR conditions to produce a single product suitable for sequencing. Initially a range of concentration from 1 mM to 2.5 mM of MgCl₂ was used. VCaP gDNA was used as a positive control and the primers were tested on BPH-1 gDNA. It was determined that the optimal concentration of MgCl₂ was 2.0 mM due to this being the minimum concentration for bands to appear (Figure 3.3).

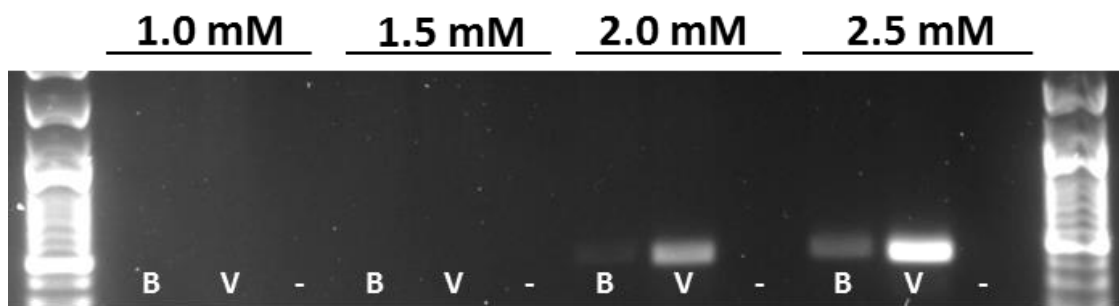


Figure 3.3: Optimisation of PCR conditions for AR primers. Electrophoresis gel showing bands detecting AR at 424 bp. MgCl₂ concentrations where varied from 1.0 mM to 2.5 mM. B: BPH-1 gDNA. V: VCaP gDNA. - : water

3.1.4 CRISPR/Cas9 successfully produced AR KO clones in basal prostate cell lines

The BPH-1, BPH-1 PPmO and P4E6 cell lines were incubated with the CRISPR/Cas9 lentivirus targeting exon 1 of the *AR* gene for 12 hours (Figure 3.4). The transduced cells were selected using puromycin for 2 weeks. Between 18 – 22 individual clones were isolated using ring and dilution cloning. A PCR, with primers flanking the gRNA target sequence in exon 1 of *AR*, was then conducted and the products were sequenced (Figure 3.5C). The sequences were analysed for multiple alleles using CRISP-ID (Dehairs et al., 2016). Nucleotide and protein sequences were aligned to the WT using the Needleman-Wunsch algorithm. Homozygous edits were defined as the same sequence modifications occurring in all alleles of *AR* on the X chromosome. Heterozygous edits were defined as multiple alleles having modifications and hence different amino acid sequences being produced, but no WT sequence was identified. Non-edited clones were defined when the sequence was purely WT. Partially edited clones were defined when there were some modifications, but a WT sequence was still identified (Figure 3.5A). CRISPR/Cas9 editing was successful in all three cell lines: BPH-1, BPH-1 PPmO and P4E6 (Table 3.1). All successful ARKO clones were viable and proliferated in standard cell culture.

Table 3.1: Summary of AR CRISPR/Cas9 clones

	BPH-1	BPH-1 PPmO	P4E6
Homozygous edited clones	0	0	7
Heterozygous edited clones	7	6	6
Non-edited clones and partially edited clones	11	14	9
Total number of clones	18	20	22
Percentage of clones edited	39%	30%	59%

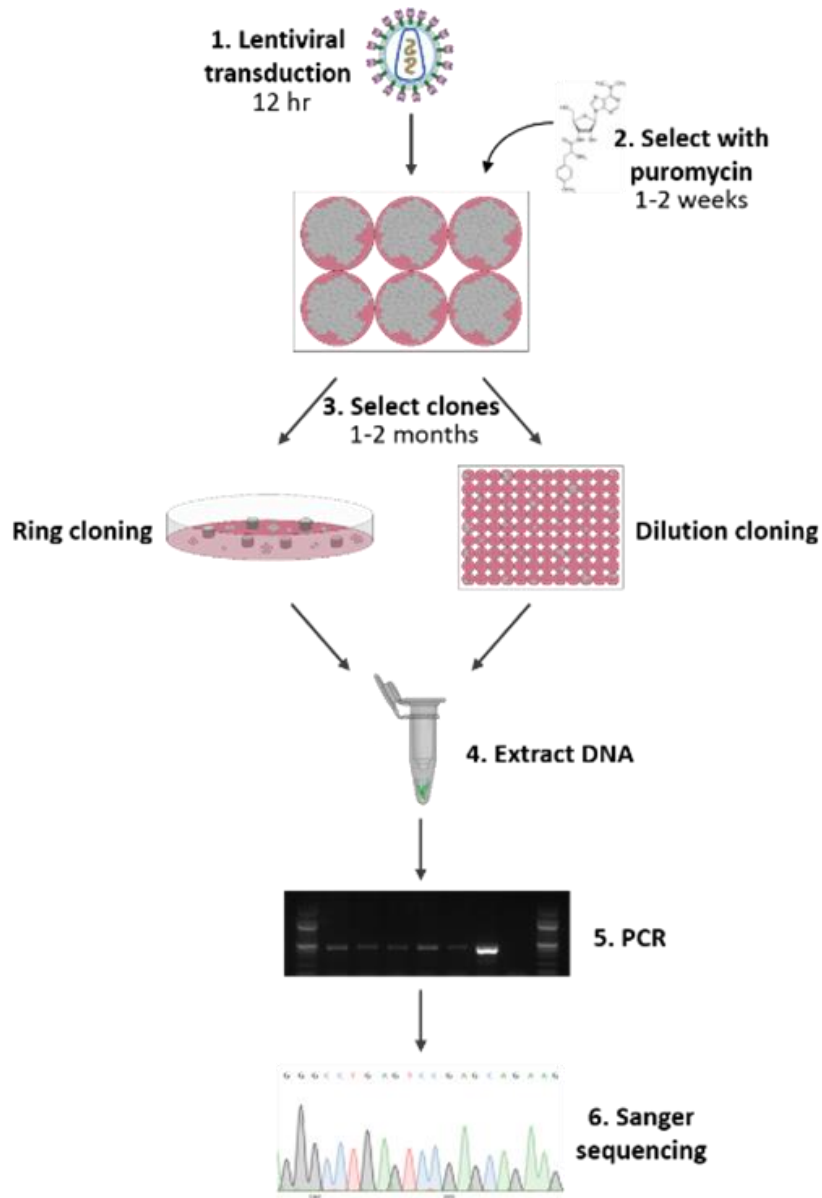
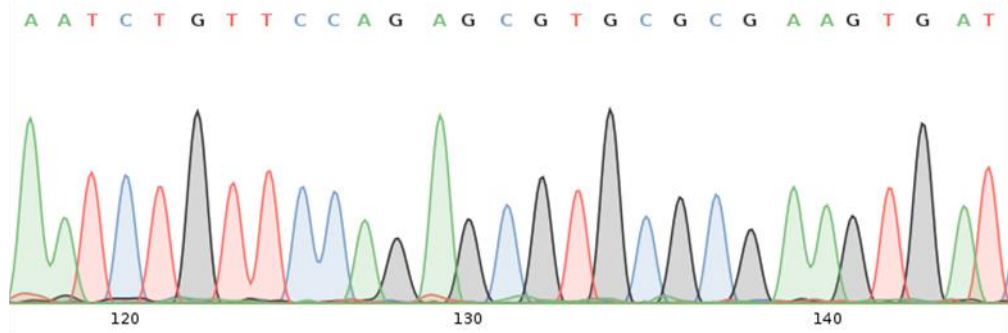


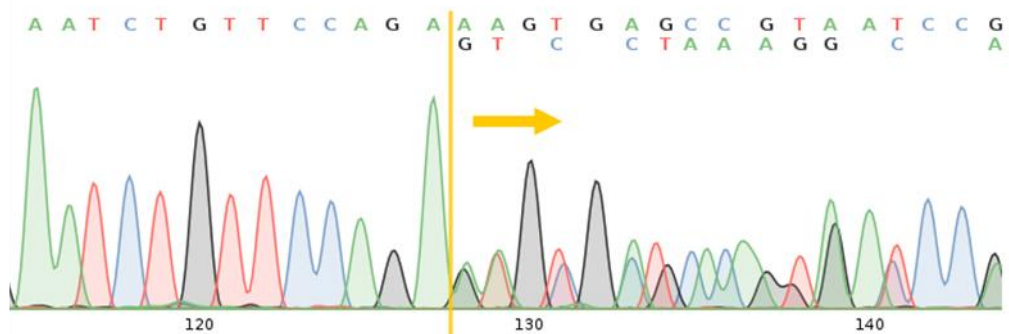
Figure 3.4 A work flow of the CRISPR/Cas9 experimental set up. Cells transduced with CRISPR/Cas9 lentivirus were selected using puromycin. Single cell clones were generated using ring cloning or dilution cloning. DNA was extracted and the PCR product for the target gene was sequenced.

The positive control which was initially used was a lentivirus which targeted *EMX1*. The *EMX1* gene encodes a transcription factor which helps control brain development (Chan et al., 2001). This was a lentivirus positive control recommended by Sigma-Aldrich for CRISPR/Cas9 experiments that should have no impact on *AR* expression. However, qRT-PCR showed that *AR* expression was knocked down in these clones (data not shown). Multidimensional scaling of other *EMX1* KO clones in the lab conducted by Leanne Archer showed that there was a large variation in total gene expression between multiple clones. Therefore, the *EMX1* KO clones were not a suitable positive control. Instead clones which were treated with the *AR* targeted lentivirus but did not have any genetic edits were used as the positive control. Hereafter these clones will be referred to as the lentivirus control.

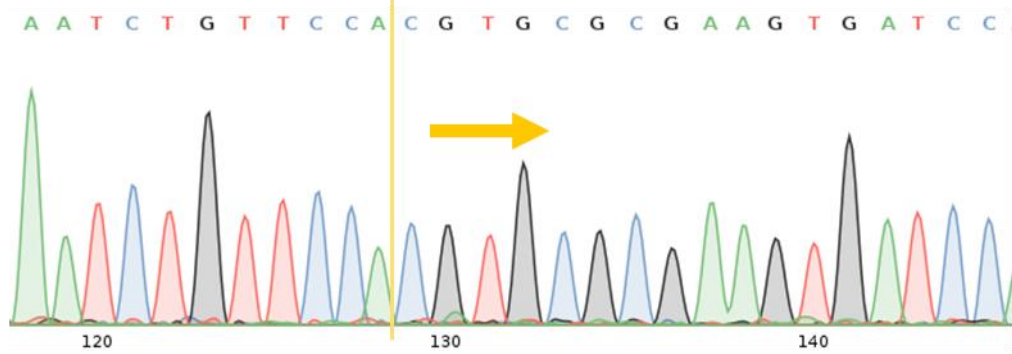
A Non-edited clone



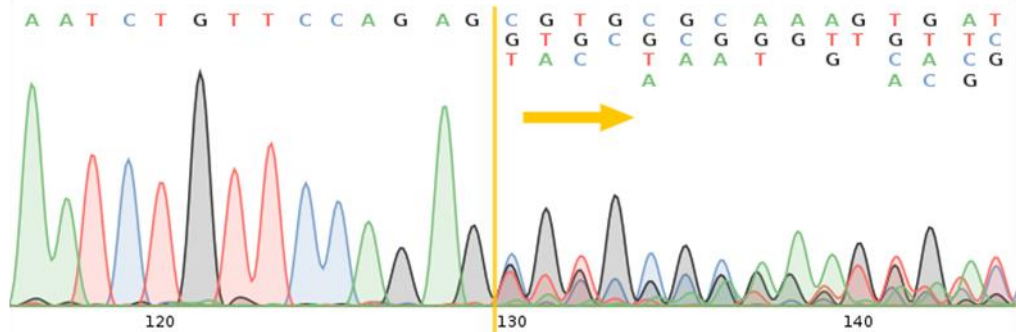
Partially edited clone



Homozygous edited clone



Heterozygous edited clone



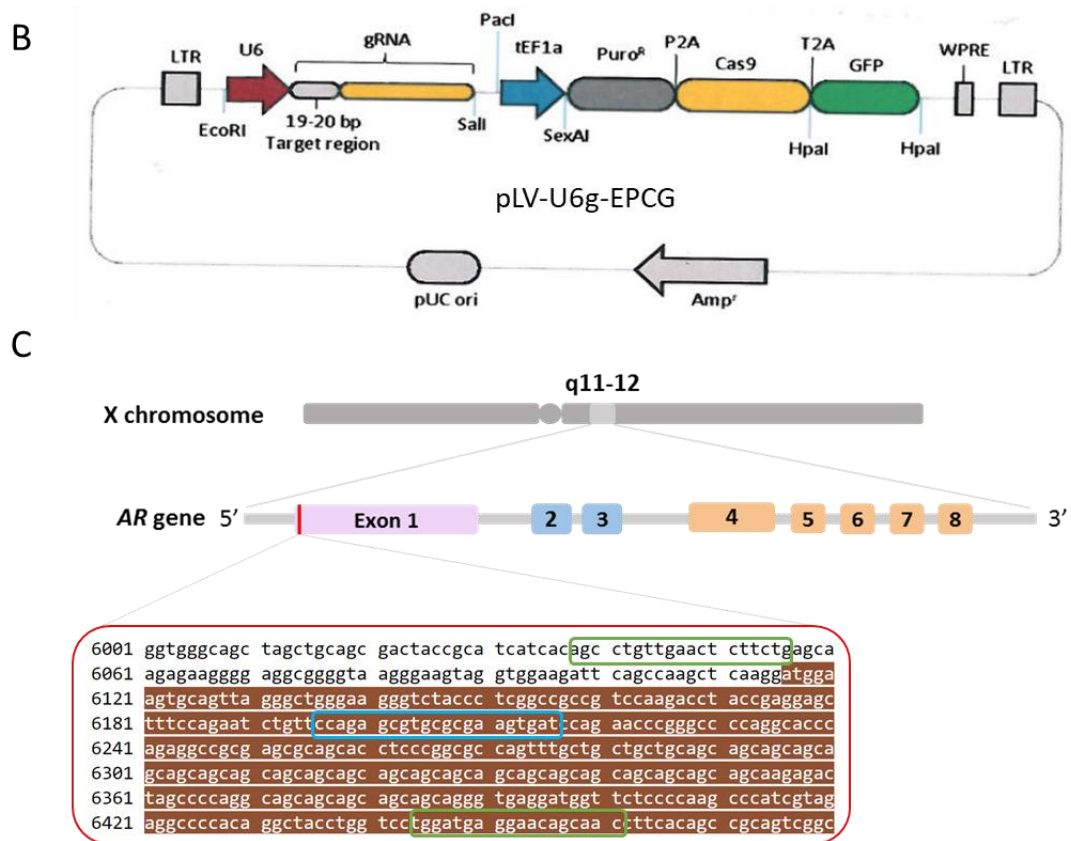
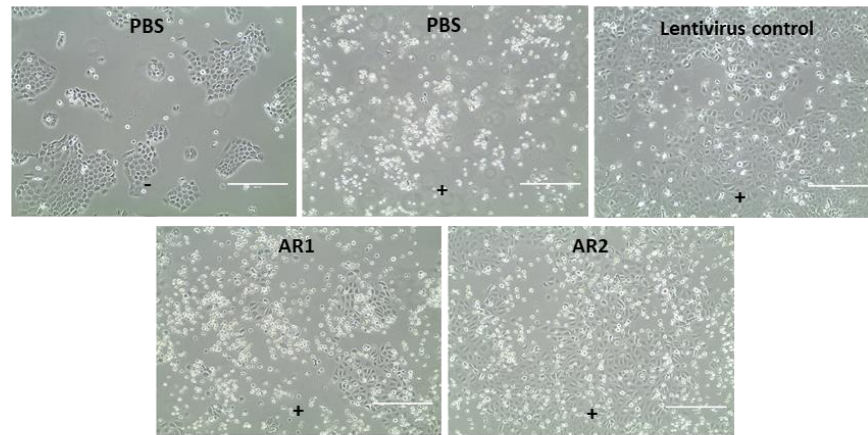


Figure 3.5 The use of CRISPR/Cas9 to KO AR in prostate cell lines. (A) Sanger sequences showing examples of a non-edited clone, a partially edited clone, a homozygous edited clone and a heterozygous edited clone. The yellow arrows show where the first change in the genetic sequence occurs. (B) CRISPR/Cas9 lentivirus vector map designed by Sigma-Aldrich. (C) The CRISPR/Cas9 gRNA (blue) targets the beginning of exon 1 (brown) and with the primers designed to span the gRNA target (green).

Initial AR CRISPR/Cas9 experiments were conducted on BPH-1 cells to test the effectiveness of the lentivirus and to optimise the method of cloning (Figure 3.6). Two dosages were tested; AR1 (1 lentivirus to 1 cell) and AR2 (2 lentiviruses to 1 cell). Both dosages resulted in the *AR* targeting lentivirus successfully transducing to produce puromycin resistant cells (Figure 3.6A). The CRISPR/Cas9 was 39% effective, with seven of the clones possessing heterozygous edits (Table 1 and Figure 3.6B). There were no homozygous edits generated. The selected clones were formed from a mixture of ring and dilution cloning (Figure 3.4). Clones generated in further CRISPR/Cas9 experiments were selected using dilution cloning. This is due to ring cloning having a higher risk of infection and the difficulty of isolating a single colony.

A



B WT

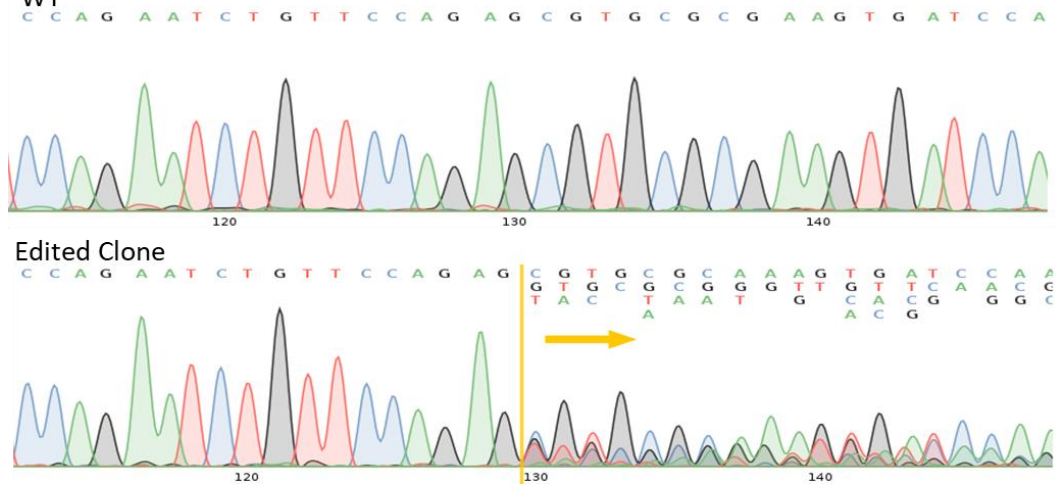
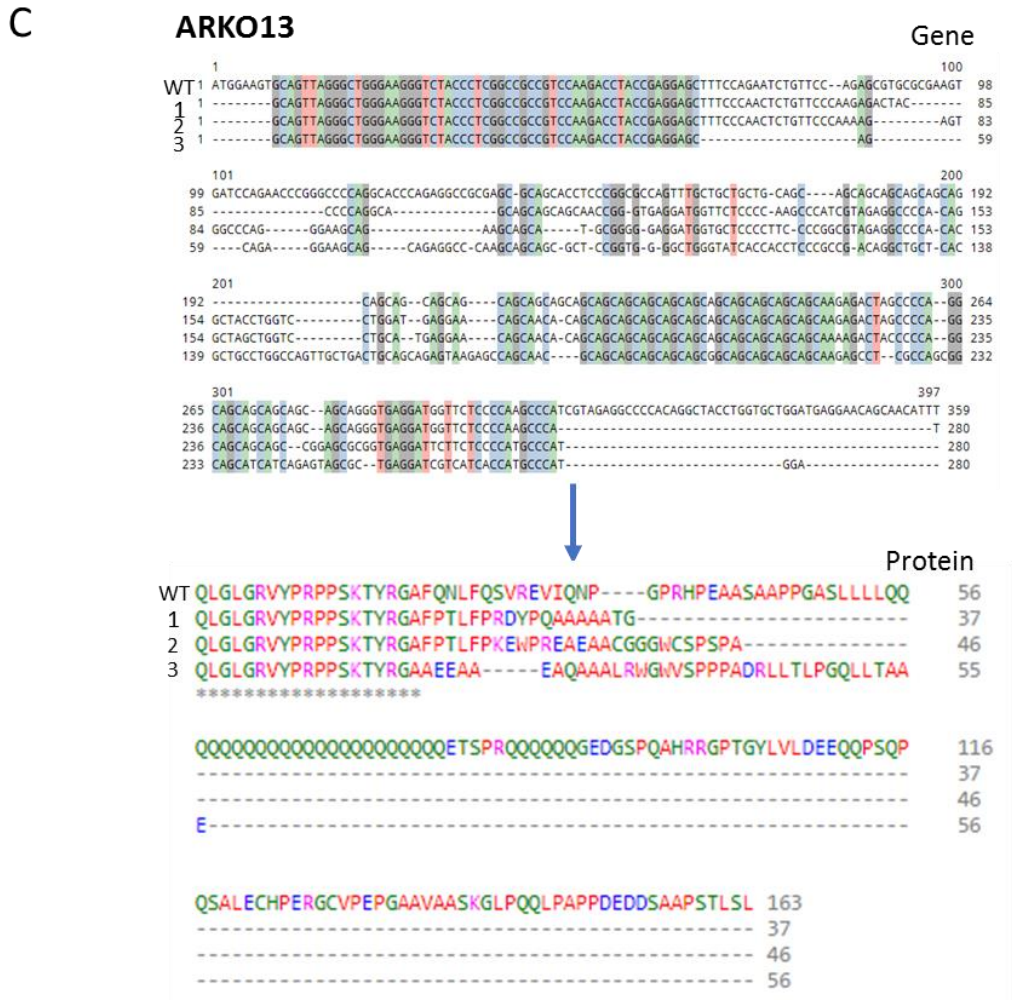
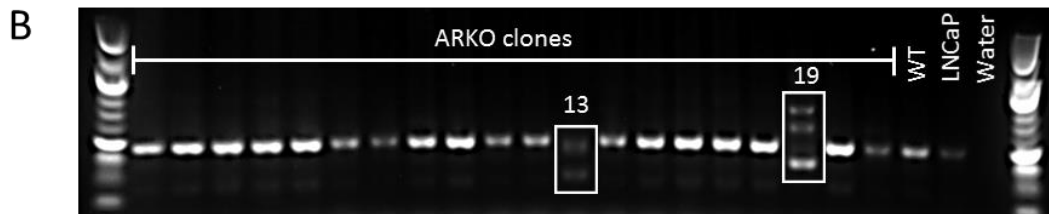
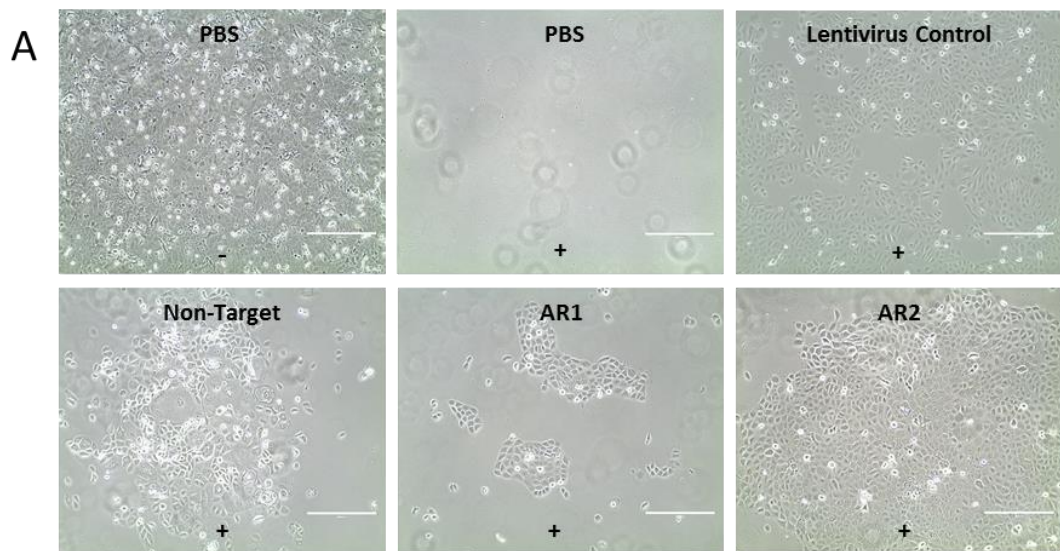


Figure 3.6: BPH-1 cell line AR CRISPR/Cas9 experiment. (A) Images of the cells that were treated with puromycin (+) and those that were not treated with puromycin (-). AR1: AR CRISPR/Cas9 lentivirus 1:1 dosage (lentivirus:cell). AR2: AR CRISPR/Cas9 lentivirus 2:1 dosage. PBS: no CRISPR/Cas9 lentivirus. (B) An example of an edited clone sequence in comparison to the WT sequence. Yellow arrow represents the start of the edited sequence.

CRISPR/Cas9 was then conducted on BPH-1 PPMO cells. These were a more elegant model to monitor differentiation in comparison to BPH-1 cells, due to the presence of the PSA-Probasin promoter which fluoresces mOrange when AR is expressed in luminal cells. Lentivirus transduction was successful and puromycin resistant cells were produced. There were more puromycin resistant cells at the AR2 dosage than the AR1 dosage of the *AR* targeting CRISPR/Cas9 lentivirus (Figure 3.7A). Therefore, the AR2 dosage was used for subsequent CRISPR/Cas9 experiments.

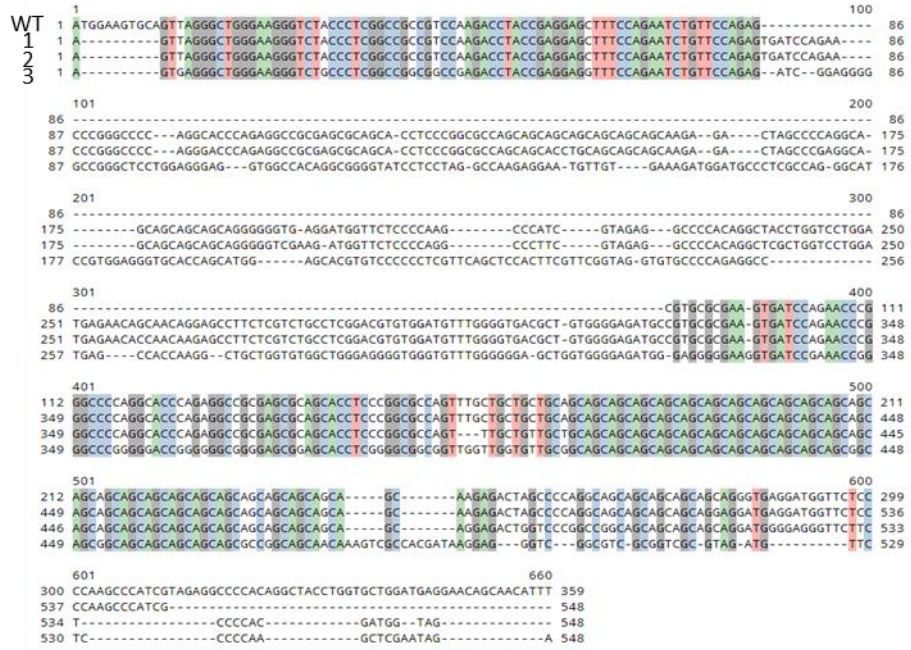
Despite BPH-1 PPMO having three copies of AR, six clones were successfully edited to give a heterozygous KO (Table 1 and Figure 3.7C). In particular, clones 19 and 13 had the largest changes to the *AR* gene, as seen by multiple bands on the electrophoresis gel (Figure 3.7B). CRISP-ID identified three different alleles from both clone 13 and clone 19 (Figure 3.7C). *AR*^{-/-} KO clone 13 (ARKO13) had a range of 7-15 bp deletions, hence producing smaller PCR products (Figure 3.7B). Whereas *AR*^{-/-} KO clone 19 (ARKO19) had large insertions, hence producing the larger PCR products (Figure 3.7B). All of the amino acid sequences generated from ARKO19 and ARKO13 had early stop codons and did not produce the PolyQ motif due to frame shifts disrupting the CAG repeat (Figure 3.7C).



D

ARKO19

Gene



Protein

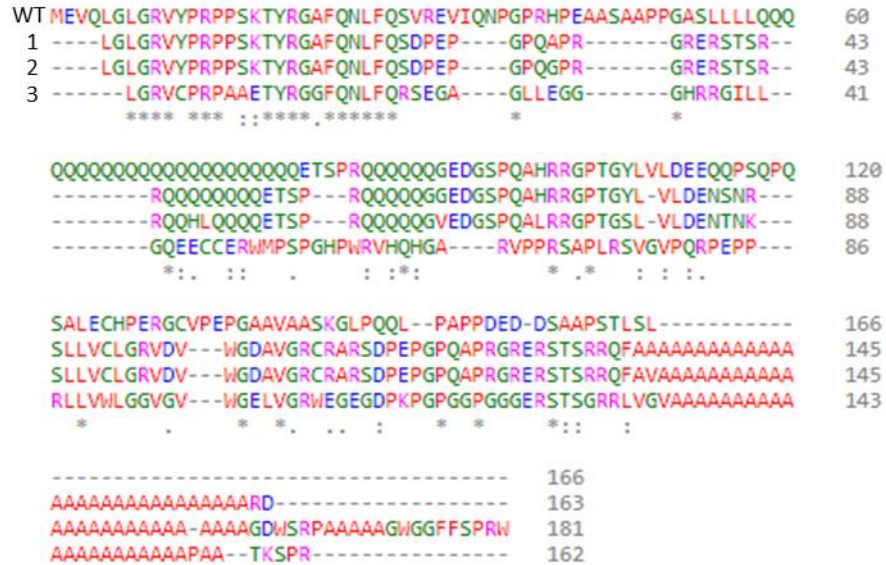


Figure 3.7: BPH-1 PPMo cell line AR CRISPR/Cas9 experiment. (A) Images of the cells that were treated with puromycin (+) and those that were not treated with puromycin (-). AR1: AR CRISPR/Cas9 lentivirus 1:1 dosage (lentivirus:cell). AR2: AR CRISPR/Cas9 lentivirus 2:1 dosage. PBS: no CRISPR/Cas9 lentivirus. (B) Electrophoresis gel detecting AR in 20 ARKO clones producing multiple bands. (C and D) The base sequence changes (top) and amino acid changes (bottom) of the heterozygous clones ARKO13 (C) and ARKO19 (D) using CRISP-ID and multisequence alignment.

P4E6 cells were then targeted by CRISPR/Cas9 to investigate the role of AR in early stage PCa. Similarly to the previous CRISPR/Cas9 experiments, the P4E6 cells transduced with the lentiviruses were puromycin resistant (Figure 3.8A). Due to P4E6 only having a single copy of *AR*, seven homozygous clones were produced (Table 3.1). *AR*⁻ KO clone 22 (ARKO22) and *AR*⁻ KO clone 15 (ARKO15) both had small insertions (1 bp and 4 bp respectively) which resulted in frame shifts, causing early stop codons in the amino acid sequences (Figure 3.8B and C). In particular ARKO22 is predicted to produce a product that is 22 amino acids long instead of 920 amino acids in the WT form (Figure 3.8C).

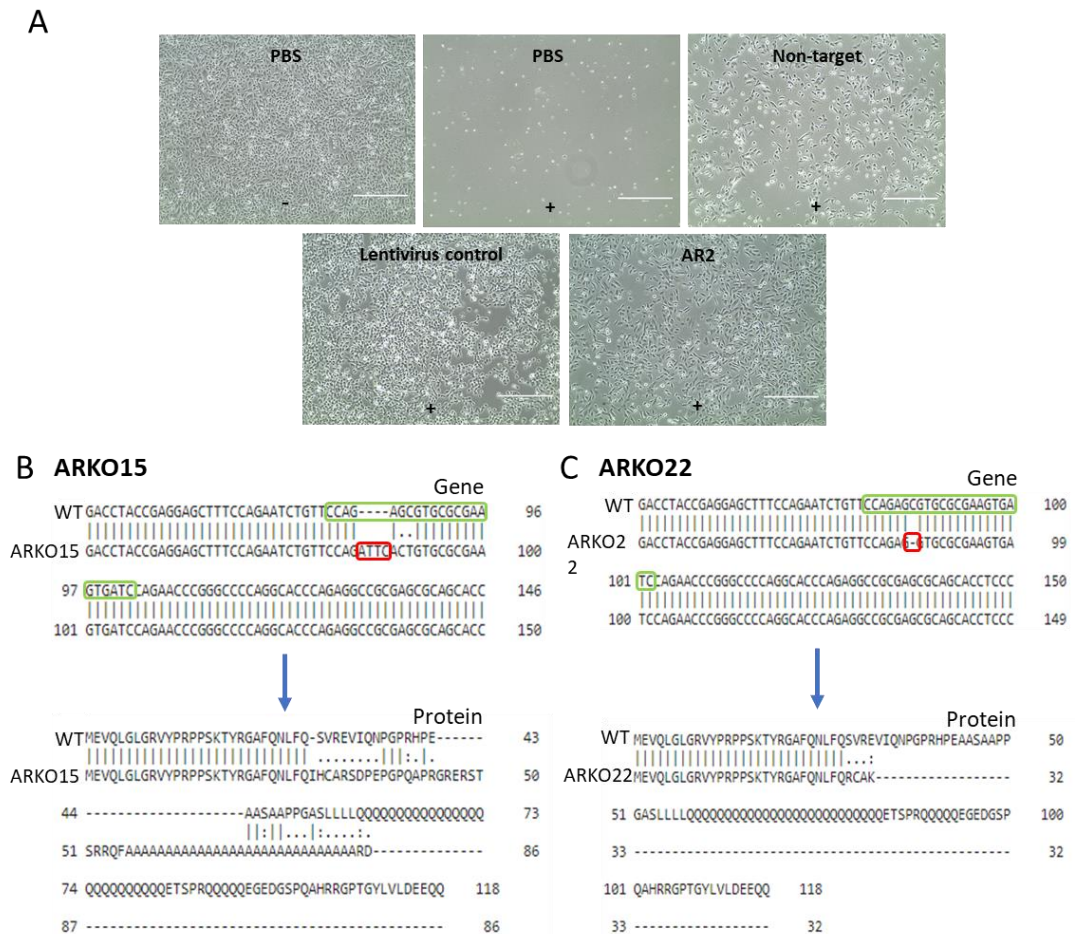


Figure 3.8: P4E6 cell line AR CRISPR/Cas9 experiment (A) Images of the cells that were treated with puromycin (+) and those that were not treated with puromycin (-). AR2: AR CRISPR/Cas9 lentivirus 2:1 dosage. PBS: no CRISPR/Cas9 lentivirus. (B and C) The base sequence changes (top) and amino acid changes (bottom) of the homozygous clone ARKO15 (B) and ARKO22 (C) using multisequence alignment. Green box: gRNA sequence. Red boxes: sequence changes.

3.2 Inducing Differentiation of Basal Cells into Luminal Cells

3.2.1 Basal cell lines do not express AR

A western blot was carried out to confirm whether BPH-1, BPH-1 PPMO and P4E6 basal cells express AR protein when cultured in 2D in their normal growth media. GAPDH was used as a loading control and LNCaP cell lysate was used as a positive control for AR. BPH-1, BPH-1 PPMO and P4E6 cells do not express detectable AR protein (Figure 3.9). Therefore, they must be induced to differentiate into luminal cells to induce the expression of AR.

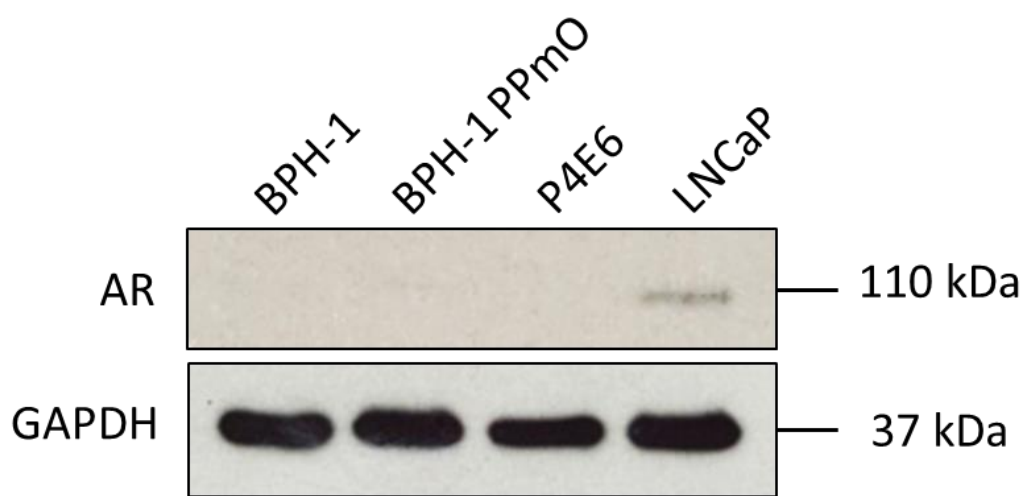


Figure 3.9: Basal cell lines do not express AR protein when undifferentiated. A western blot probed for AR and GAPDH in different prostate cell lines.

3.2.2 Growth in DHT for 24 hr is insufficient to induce full length AR expression

Initially to induce differentiation VCaP, BPH-1 WT and BPH-1 ARKO clones were incubated with DHT for 24 hr while in 2D culture. The DHT activates the AR genomic signalling pathway and hence differentiation. A western blot was carried out to determine if AR expression was induced (Figure 3.10). VCaP cells over express AR and there was no difference in the levels of expression when VCaP cells were grown in DHT. There was no full length AR expression seen for BPH-1 WT cells or BPH-1 ARKO clones 1 and 2 (ARKO1 and ARKO2), both with and without DHT. These results demonstrate that either growth in DHT is not sufficient to push basal BPH-1 cells into differentiation and hence expression of full length AR or the sensitivity of the western blot is not enough to detect rare cells that might have differentiated.

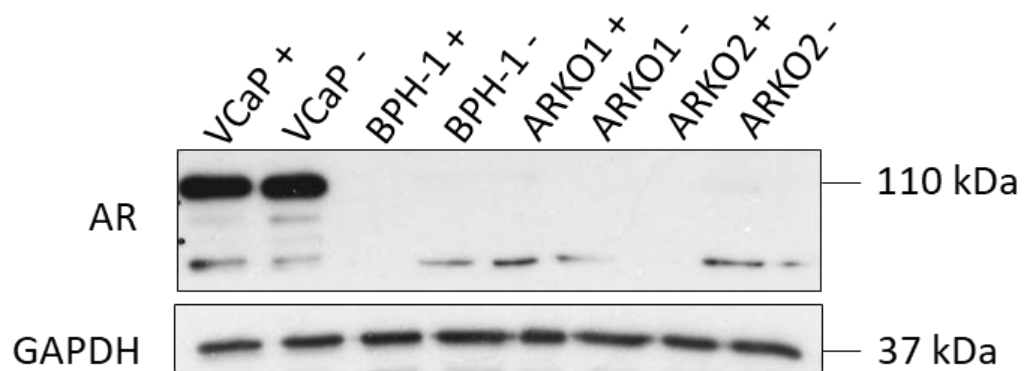


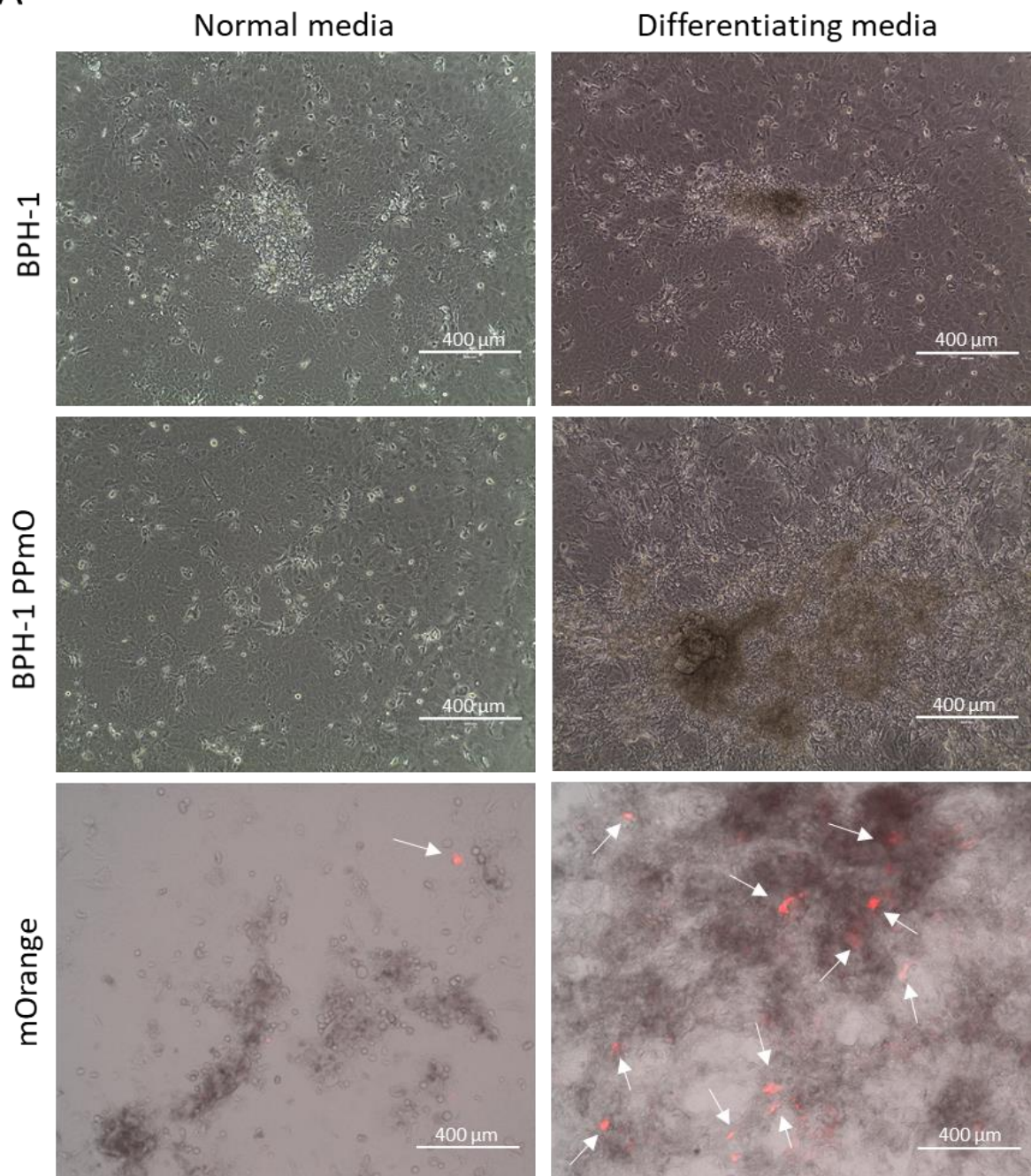
Figure 3.10: Addition of DHT to induce differentiation in BPH-1 cells. A western blot probed for AR and GAPDH in cells treated with 10 nM DHT (+) for 24 hr or grown in normal media (-). VCaP was used as a positive control. ARKO1 and ARKO2 are BPH-1 AR KO clones created by CRISPR/Cas9. BPH-1 has not been treated with CRISPR/Cas9.

3.2.3 Culturing cell lines into a bilayer is insufficient to induce differentiation

Previously in our lab, primary epithelial cells were induced to differentiate by allowing them to proliferate to become overconfluent. This resulted in two layers of adherent cells which mimicked the prostate epithelial bilayer (Frame et al., 2010, Swift et al., 2010). This method of differentiation has not been used with cell lines, and therefore it was tested with BPH-1 and BPH-1 PPmO cells.

WT BPH-1 and BPH-1 PPmO cells were left to grow for 2 weeks in differentiating media (DMEM + 5% FCS with 10 nM DHT) and normal growth media (RPMI + 5% FCS). When the cells were grown in differentiating media, a larger number of cells formed two-layers, mimicking an epithelial bilayer (Figure 3.11A). mOrange fluorescence from BPH-1 PPmO cells can be used as a proxy for PSA expression (a luminal cell marker) and hence late stages of differentiation. There appeared to be more mOrange fluorescence when more BPH-1 PPmO formed a bilayer in differentiating media than when grown in normal media (Figure 3.11A). Flow cytometry was carried out to quantify the number of differentiated bilayer cells (cells fluorescing mOrange) in comparison to monolayer cells in both media conditions. There was no difference between BPH-1 PPmO bilayer cells grown in normal media than in differentiating media (6.56% and 6.85% respectively) (Figure 3.11B). There was half the number of cells expressing mOrange in bilayer than there was in monolayer (12.84% compared to 6.56-6.85%) (Figure 3.11B). Therefore this method does not produce a large number of differentiated cells and other methods were investigated.

A



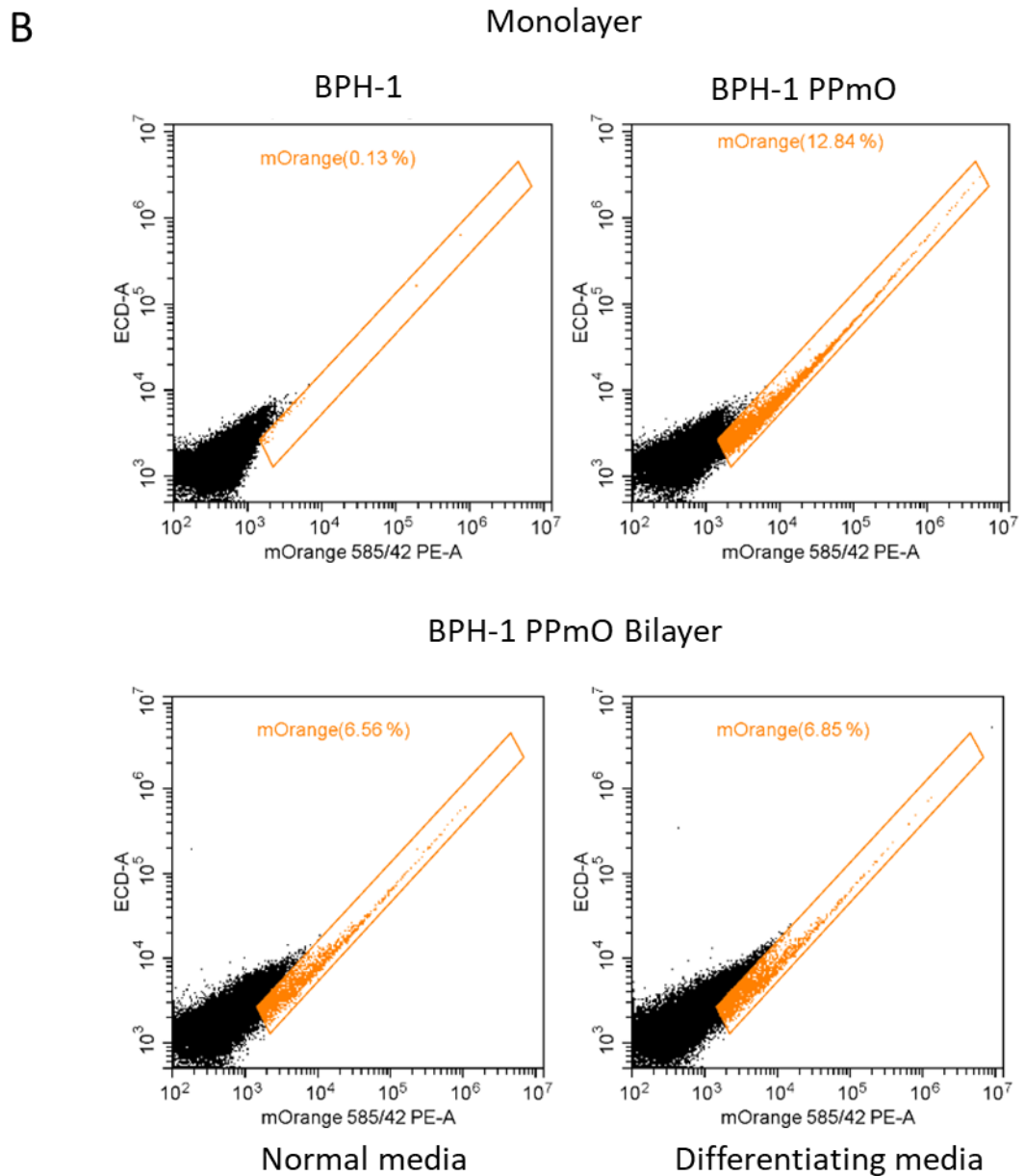


Figure 3.11: Growing cells into a bilayer does not push cells into differentiation. (A) Images of BPH-1 cells, BPH-1 PPmO cells and BPH-1 PPmO cells fluorescing mOrange in normal (R5) and differentiating media (D5 and 10nM DHT) for two weeks. (B) Flow cytometry analysis of mOrange fluorescence of BPH-1 and BPH-1 PPmO cells grown into a monolayer in normal media (top) and BPH-1 PPmO cells grown into a bilayer in normal and differentiating media (bottom). Scale bar = 400 μ m

3.2.4 Co-culturing basal cells with stroma to form 3D spheroids induces differentiation and *AR* expression

Previously in our lab, prostate basal cell lines have been induced to differentiate by growing them into 3D spheroids in co-culture with stroma (Lang *et al*, 2001a). The spheroids have an acini-like structure with a central lumen surrounded by a basal and luminal layer (Figure 3.12C). This mimics the structure of prostate glands found in human tissue (Figure 3.12B). The epithelial cells are embedded in Matrigel™ above a Matrigel™ plug within an insert. The insert sits above a layer of stromal cells, which release growth factors (Figure 3.12A).

Initially BPH-1 PpmO and P4E6 WT cells were grown in 4% Matrigel™ above a 50% Matrigel™ plug. The majority of the cells grew in a monolayer and was therefore not sufficient to induce 3D spheroids (Figure 3.12D). Therefore, the assay was optimised by growing the cells in 50% Matrigel™ above a 50% Matrigel™ plug which allowed no monolayer growth (Figure 3.12E). It was found that growing the spheroids for 7-10 days was the optimum length of time to allow structure to develop. If the spheroids were grown for 14 days it resulted in cell death and low-quality RNA (not shown).

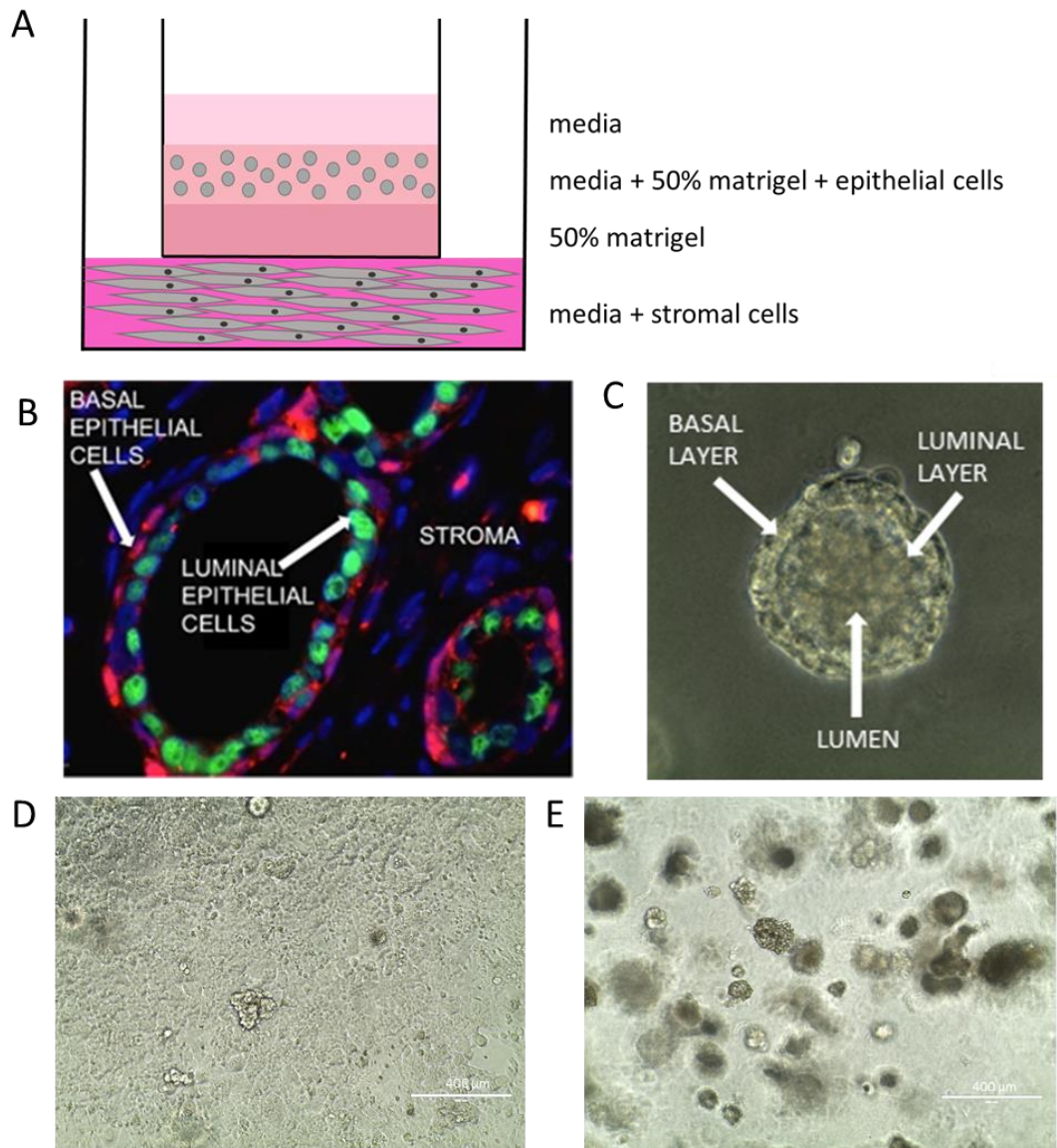


Figure 3.12: Optimisation of prostate spheroids in co-culture with stroma (A) Co-culture experimental set up for growing prostate spheroids. (B) Prostate glands contain an inner luminal layer (NKX3.1 marker, green) and an outer basal layer (p63 marker, red), surrounded by stroma (image from Dr Frame). (C) Representative image of prostate spheroids from this project (P4E6 spheroid). (D) Spheroids embedded in 4% Matrigel™. (E) Spheroids embedded in 50% Matrigel™. Scale bar = 400 μm.

3.2.4.1 The effects of calcium on differentiation and *AR* expression

The presence of calcium has been shown to help initiate differentiation in keratinocytes (Pillai et al., 1990). Therefore, the effects of growing BPH-1 PPMO and P4E6 spheroids in calcium was investigated. There were no apparent morphological differences when both P4E6 and BPH-1 PPMO spheroids were grown in calcium after 7 days (Figure 3.13A). BPH-1 PPMO spheroids underwent differentiation with and without calcium, indicated by the fluorescence of mOrange. mOrange fluorescence was predominantly seen in the centre of the spheroid, where the luminal cells would be present. mOrange fluorescence was also seen scattered throughout the spheroid but at very specific locations, demonstrating that differentiation is occurring in individual cells rather than the spheroid as a whole (Figure 3.13A). This is reminiscent of the formation of a bilayer *in vivo*. The quantification of mOrange fluorescence from BPH-1 PPMO cells (by counting the number of cells by fluorescence microscopy) showed that at day 4 there were significantly more differentiated spheroids when grown in the presence of calcium (19.9% with calcium, 12.4% without calcium, $p=0.0478$, unpaired t-test). However, by day 7 the presence of calcium made no difference to the number of differentiated spheroids (23.2% with calcium, 23.8% without calcium, $p=0.6324$, unpaired t-test) (Figure 3.13B).

Subsequently the role of calcium on *AR* expression in spheroids was investigated using qRT-PCR. The primers were located in exon 9 and relative expression of *AR* mRNA was calculated by comparing to the mRNA levels of the endogenous control *RPLPO* in each sample. The fold difference was then calculated by comparing the relative expression of *AR* in each sample to PC3, which was the calibrator sample. This is referred to as the $\Delta\Delta C_t$ method. LNCaP RNA was used as a positive control and PC3 RNA was used as a negative control. There was no *AR* expression when P4E6 and BPH-1 PPMO cells were grown in monolayer (Figure 3.13C and D). This agrees with the absence of *AR* protein determined by the western blot (Figure 3.9). There is a statistically significant increase of *AR* expression in P4E6 spheroids and BPH-1 PPMO

spheroids when grown without calcium in comparison to monolayer cells (One way ANOVA with a Dunnett's multiple comparisons test, $p=0.0488$ and $p=0.0421$ respectively) (Figure 3.13C and D). However there is no statistically significant difference in *AR* expression in P4E6 spheroids and BPH-1 PPMO spheroids when grown with calcium in comparison to monolayer cells (One way ANOVA with a Dunnett's multiple comparisons test, $p=0.3540$ and $p=0.8604$ respectively) (Figure 3.13C and D). Hence, in further experiments both P4E6 and BPH-1 PPMO spheroids were not grown in calcium. Detection of *AR* expression confirmed the utility of this model to study differentiation.

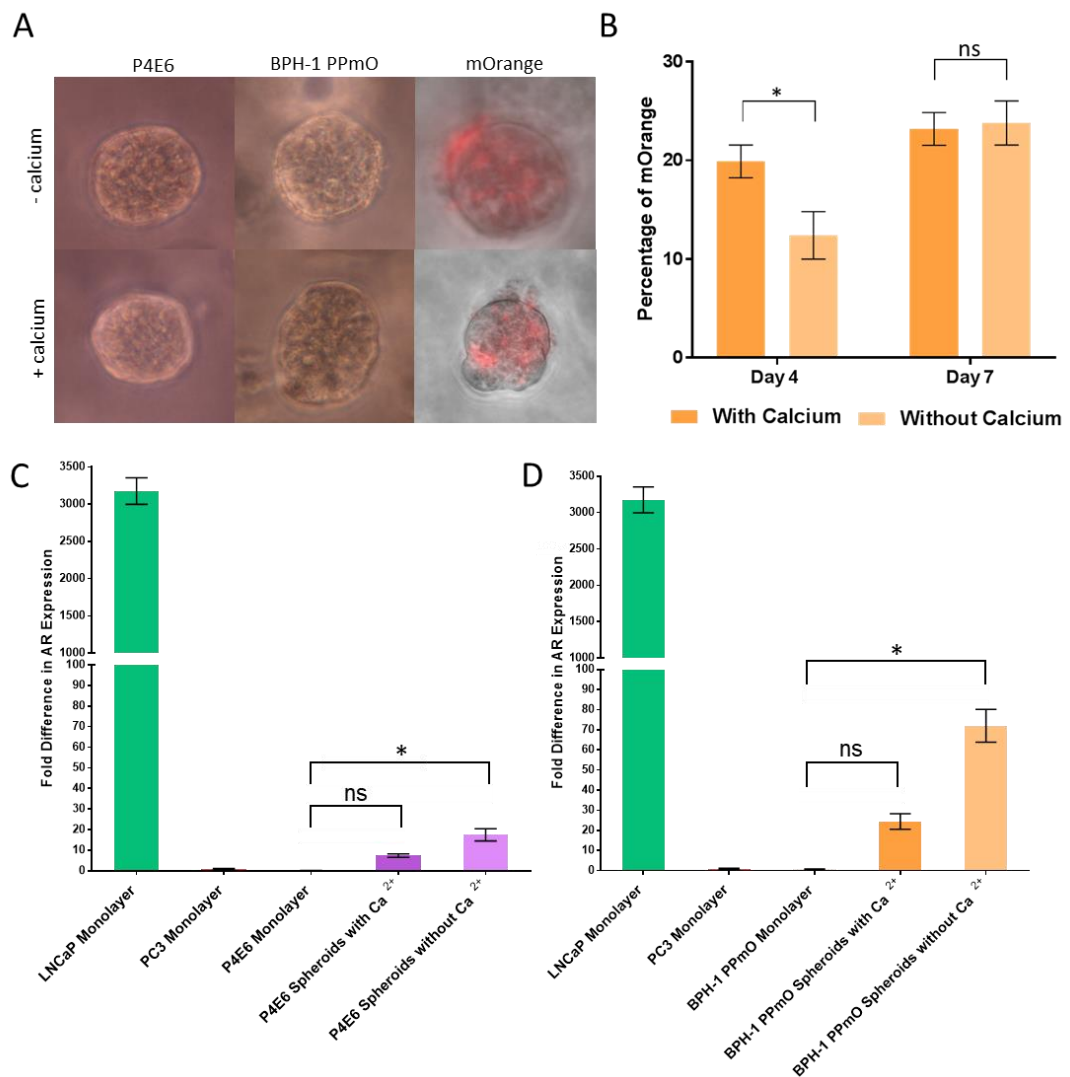


Figure 3.13: Growing cells into spheroids induces the expression of AR without the presence of calcium. (A) Representative images of P4E6 and BPH-1 PPmO spheroids, with and without calcium, to induce differentiation. (B) Percentage of mOrange expressing spheroids grown with and without calcium after 7 days. Two tailed unpaired t-test, * = $p \leq 0.05$ and ns = $p > 0.05$. Error bars represent standard error of the mean. (C and D) Fold difference in AR expression between monolayer cells to spheroids grown for 7 days with and without calcium using qRT-PCR. AR expression is relative to the endogenous control RPLPO and normalised to PC3, the calibrator sample. One way ANOVA with a Dunnett's multiple comparisons test, * = $p \leq 0.05$ and ns = $p > 0.05$. Error bars represent standard deviation calculated from the coefficient of variation.

3.2.4.2 *AR* expression is reduced in ARKO clones

Once the method to form differentiated spheroids had been optimised in WT cells, the process was then repeated with ARKO clones. This was to confirm whether *AR* had been successfully knocked-out by CRISPR/Cas9. Subsequently, the extent of differentiation could then be investigated.

ARKO clones were grown to form spheroids in the absence of calcium. This demonstrates that AR KO does not affect spheroid formation and are able to retain the same yield as WT spheroids. They were then collected and their RNA was extracted. qRT-PCR was then performed and the $\Delta\Delta C_t$ method was used, to measure spheroid induced *AR* expression in comparison to WT spheroids. The primers were found in exon 9. Monolayer LNCaP and PC3 RNA were used as the positive and negative controls respectively. Whilst there was a decrease in *AR* expression in BPH-1 PPMO ARKO clones (ARKO13 and ARKO19) it was not statistically significant (One way ANOVA with a Dunnett's multiple comparisons test, $p=0.0575$ and $p=0.1070$ respectively) (Figure 3.14A). This is likely due to the large variance in the data. There was a statistically significant decrease in *AR* expression in the P4E6 clone ARKO15 but not in the P4E6 clone ARKO22 (One way ANOVA with a Dunnett's multiple comparisons test, $p=0.0114$ and $p=0.8744$ respectively) (Figure 3.14B).

When calculating the relative expression of *AR* to *RPLPO* it became clear how important it is to choose an appropriate endogenous control. Three endogenous controls were tested due to large variation between the WT and ARKO clones. The BPH-1 PPMO cell line had the largest variation between monolayer cells and spheroids, as well as between WT spheroids and ARKO spheroids (see appendix 1.2). However the qRT-PCR results still showed an overall reduction in *AR* expression in ARKO clones which agrees with the nucleotide and protein sequence changes created by the CRISPR/Cas9.

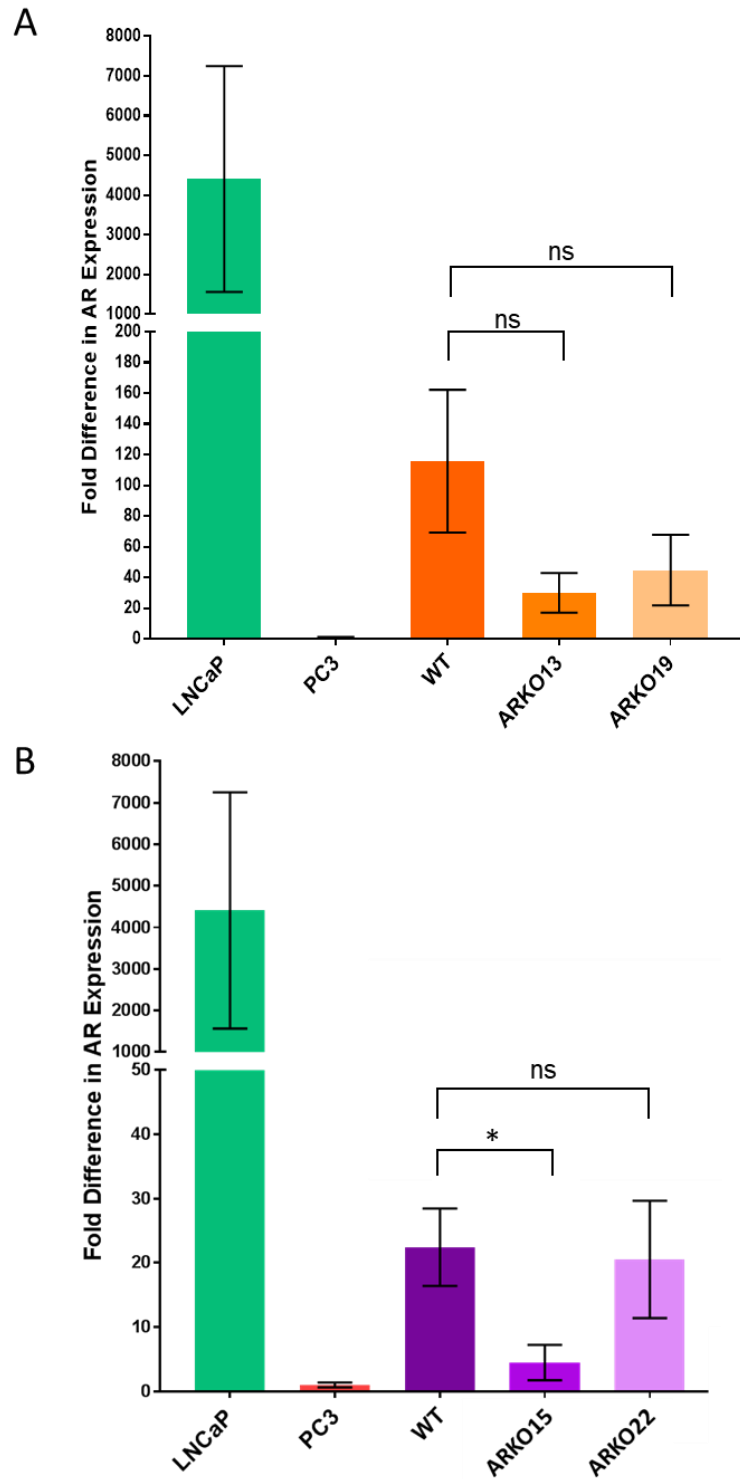


Figure 3.14: AR expression is reduced in CRISPR/Cas9 AR KO clones. qRT-PCR was used to determine AR expression in BPH-1 PPMO WT and ARKO clone spheroids (ARKO13 and ARKO19) (A) and P4E6 WT and ARKO clone spheroids (ARKO15 and ARKO22) (B). AR expression is relative to the endogenous control RPLPO and normalised to PC3, the calibrator sample. One way ANOVA with a Dunnett's multiple comparisons test. , * = $p \leq 0.05$ and ns = $p > 0.05$. Error bars represent standard deviation calculated from the coefficient of variation.

3.3 Characterising Differentiated ARKO Clone Spheroids

3.3.1 Cell viability assay optimisation

In order to verify whether knocking out the *AR* gene disrupts the cell viability and if there were any differences between clones, the CellTiter-Glo[®] assay (Promega) was used with WT BPH-1 PPmO and P4E6 spheroids in co-culture. The assay works by using ATP released from viable cells to convert luciferin to oxyluciferin. This then releases a luminescent signal which then can be detected and quantified. The assay has an upper limit of detecting 10 μM before the sensitivity and reliability of the results diminish. Therefore, preliminary experiments were performed to determine the number of cells seeded in co-culture that produces less than 10 μM of ATP. A standard curve of 50 μM – 16 nM ATP was generated and using the equation of the line ($y = 3524.2x + 9358.9$) the concentration of ATP released was calculated from the average luminescence. This was performed for WT BPH-1 PPmO and P4E6 spheroids in triplicate, at three different cell densities: 5,000, 10,000 and 15,000.

All cell densities in both cell lines produced over 10 μM ATP i.e. the detection limit of the assay (Figure 3.15). BPH-1 PPmO cells produced a relatively constant amount of ATP despite the difference in cell seeding densities. 5,000 BPH-1 PPmO cells produced the highest amount of ATP at 18.1 μM compared to 15,000 cells at 12.4 μM and 10,000 cells at 14.1 μM ATP. 10,000 P4E6 cells produced the most ATP at 27.8 μM and 15,000 P4E6 produced 16.9 μM . 5,000 P4E6 cells produced the least amount of ATP at 11.9 μM . This assay requires further optimisation in order to determine a cell density at which to seed BPH-1 PPmO and P4E6 cells to ensure they produce less than 10 μM ATP (Figure 3.15).

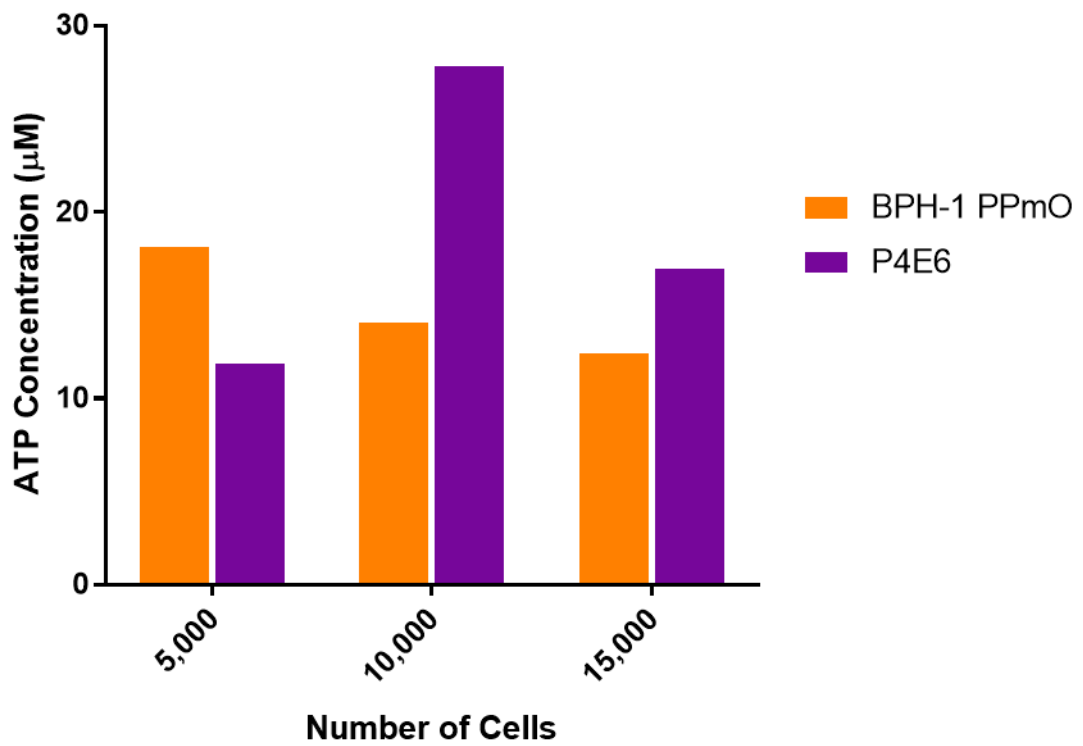


Figure 3.15: Optimisation of the CellTiter-Glo[®] assay. WT BPH-1 PPmO and P4E6 cells were seeded at different densities in co-culture with stroma to form spheroids. CellTiter-Glo[®] reagent was added after 1 week to test for cell viability and ATP concentration was measured.

3.3.2 Spheroid morphology and structure varies between cell lines

The effect of ARKO on the structure and morphology of spheroids was investigated. After growing spheroids for 7 days they were imaged (Figure 3.16). Overall BPH-1 PPmO spheroids were irregular in shape, more prone to form aggregates and less smooth than P4E6 spheroids. Aggregates were defined as when spheroids lacked distinct structure and had to have merged with many other cells. ARKO13 and ARKO19 had to be smaller than the BPH-1 PPmO WT and lentivirus control (Table 3.2 and Figure 3.16). Conversely ARKO15 and ARKO22 were larger than the P4E6 WT and lentivirus control (Table 3.2 and Figure 3.16). All types of spheroids had heterogeneous morphology within and between experiments.

Table 3.2: Summary of spheroid morphology in BPH-1 PPmO and P4E6 WT and ARKO clones.

	Cell type	Size in comparison to WT	Shape	Smooth	Aggregates
BPH-1 PPmO	WT	/	Irregular	No	Yes
	Lentivirus control	Similar	Irregular	No	Yes
	ARKO13	Smaller	Irregular	No	Yes
	ARKO19	Smaller	Irregular	No	Yes
P4E6	WT	/	Spherical	Yes	No
	control	Similar	Spherical	Yes	No
	ARKO15	Larger	Spherical	Yes	No
	ARKO22	Larger	Spherical	Yes	No

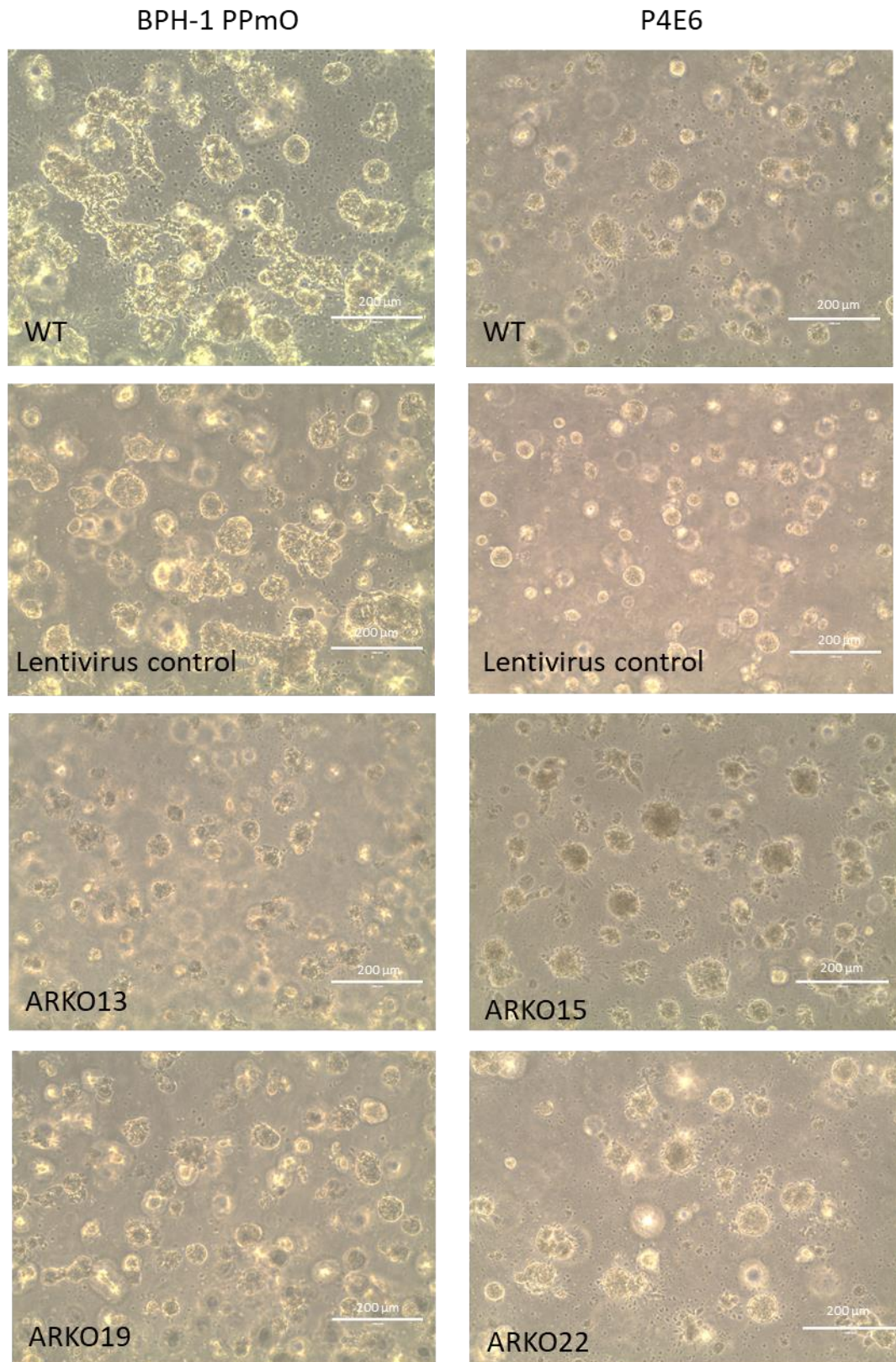


Figure 3.16: Spheroid morphology is heterogeneous between cell lines and differs in ARKO clones. Representative images of BPH-1 PpmO and P4E6 WT, lentivirus control and ARKO clone spheroids after 7 days. Scale bar = 200µm.

3.3.3 Optimisation of AR and NKX3.1 IHC antibodies

Prior to investigating the extent of differentiation in WT and ARKO spheroids, the antibodies for AR and NKX3.1 were optimised for IHC. Spheroids were then embedded in paraffin and sliced onto slides. The NKX3.1 antibody was provided by Cell Signalling (D6D2Z) and was tested with range of dilutions (1:500, 1:250 and 1:100) on patient derived BPH tissue. All concentrations resulted in a positive signal in the nucleus of luminal cells and hence the lowest dilution 1:500 was used in further experiments (Figure 3.16B). It is important to note that the antibody is specific to the columnar luminal cells that line the lumen (black arrow Figure 3.17B) and there is no signal seen in the thin basal layer underneath the luminal cells (blue arrow Figure 3.17B).

A variety of AR antibodies were tested (N20, C19 and 441 all provided by Santa-Cruz) with a range of dilutions (1:1000, 1:800, 1:500 and 1:200) on LNCaP cells as well as WT BPH-1 PPMO and P4E6 spheroids embedded in paraffin (Figure 3.17A). Both N20 and C19 antibodies stained the background of WT BPH-1 PPMO and P4E6 spheroids as well as the spheroids themselves but was gave a positive stain in LNCaP embedded cells. LNCaP cells stained with the N20 antibody had the strongest positive signal. The 441 antibody did not stain the background or the spheroids but there is a signal seen in the LNCaP cells (black arrow Figure 3.17A). The 441 antibody was used in further experiments due to the lack of non-specific binding to the background of embedded spheroids. However none of the antibodies tested were optimal therefore more specific AR antibodies need to be investigated.

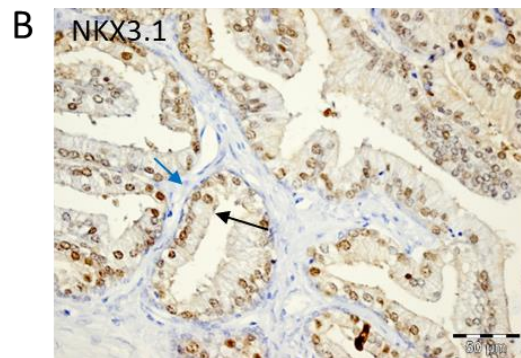
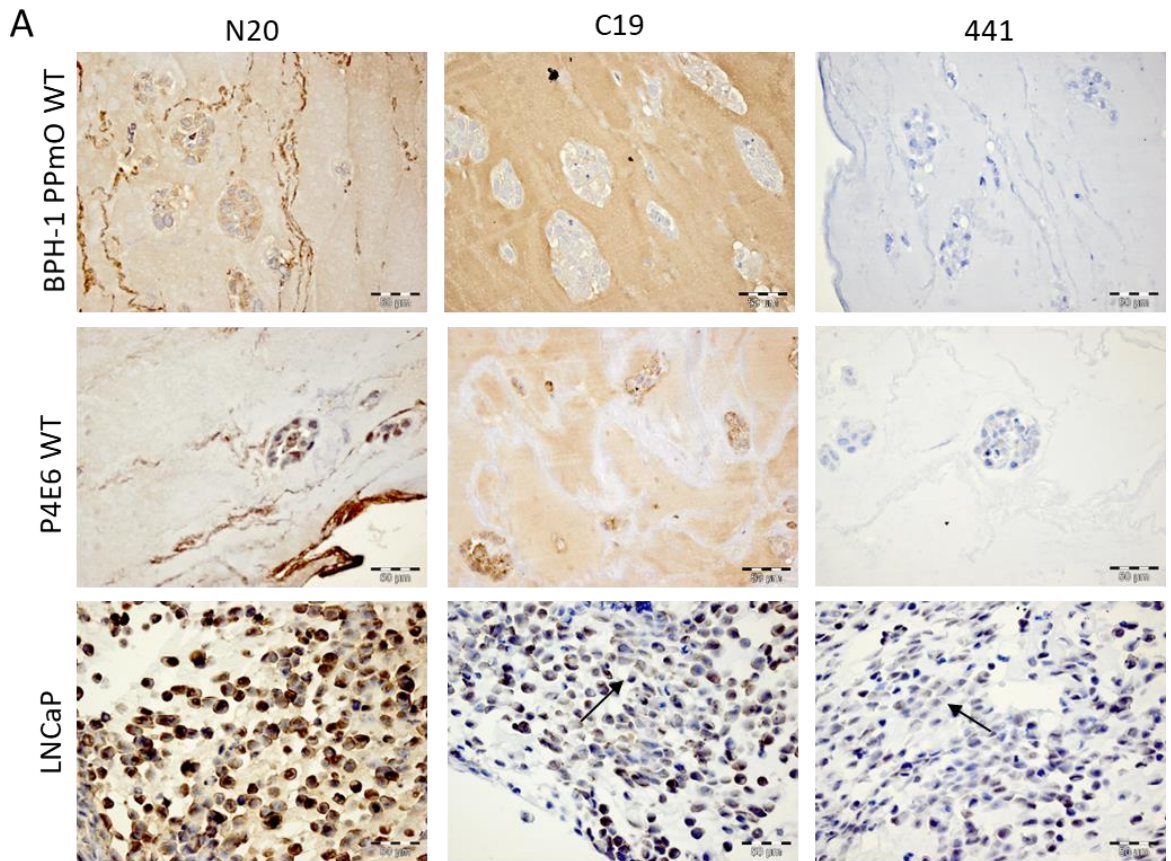


Figure 3.17: Optimisation of AR and NKX3.1 antibodies for IHC. (A) Three different AR antibodies (N20, C19 and 441) were tested at 1:200 dilution on paraffin embedded BPH-1 PPmO WT spheroids, P4E6 WT spheroids and LNCaP cells. Black arrows indicate positive AR expression in LNCaP cells. (B) NKX3.1 antibody tested at 1:500 dilution on BPH tissue. Black arrow indicates positive AR expression in luminal cells. Blue arrow indicates negative AR expression in basal cells. Scale bar = 50 µm.

3.3.4 BPH-1 PpmO and P4E6 spheroids display heterogeneous expression of differentiation markers

Despite confirming with qRT-PCR and the detection of mOrange that spheroids are able to induce differentiation of basal cells, this needed to be confirmed on the protein level. The spheroids were collected and embedded in paraffin as described previously. IHC was then conducted to test the presence and location of basal markers (CK5 and p63) and luminal markers (CK18, AR, NKX3.1). The antibodies for CK5, p63 and CK18 were previously optimised in our lab. The expression levels of the differentiation markers are summarised in Table 3. Highest levels of expression are denoted +++, medium levels of expression are denoted ++, low levels of expression are denoted + and no expression is denoted -.

All of the spheroids had low levels of expression for the early luminal marker CK18 (Figure 3.19). None of the spheroids expressed the advanced differentiation markers NKX3.1 and AR (Figures 3.21 and 3.22). P4E6 lentivirus control spheroids did not express any basal markers (CK5 and P63) (Figures 3.18 and 3.19). They were also significantly smaller than when they were growing in Matrigel™ before embedding (Figure 3.16). P4E6 ARKO clones only expressed one of the basal markers (ARKO22 expressed CK5 and ARKO15 expressed p63) and not both (Figures 3.18 and 3.19). All BPH-1 PpmO spheroids had high levels of expression both basal markers (Figures 3.18 and 3.19).

Table 3.3: Expression levels of different differentiation markers in prostate spheroids

	Cell type	CK5	p63	CK18	NKX3.1	AR
BPH-1 PPmO	WT	+++	++	++	-	-
	Lentivirus control	+++	+++	+	-	-
	ARKO13	++	+++	-	-	-
	ARKO19	+++	+++	+	-	-
P4E6	WT	+++	+++	+	-	-
	Lentivirus control	-	-	+	-	-
	ARKO15	-	++	-	-	-
	ARKO22	++	-	+	-	-

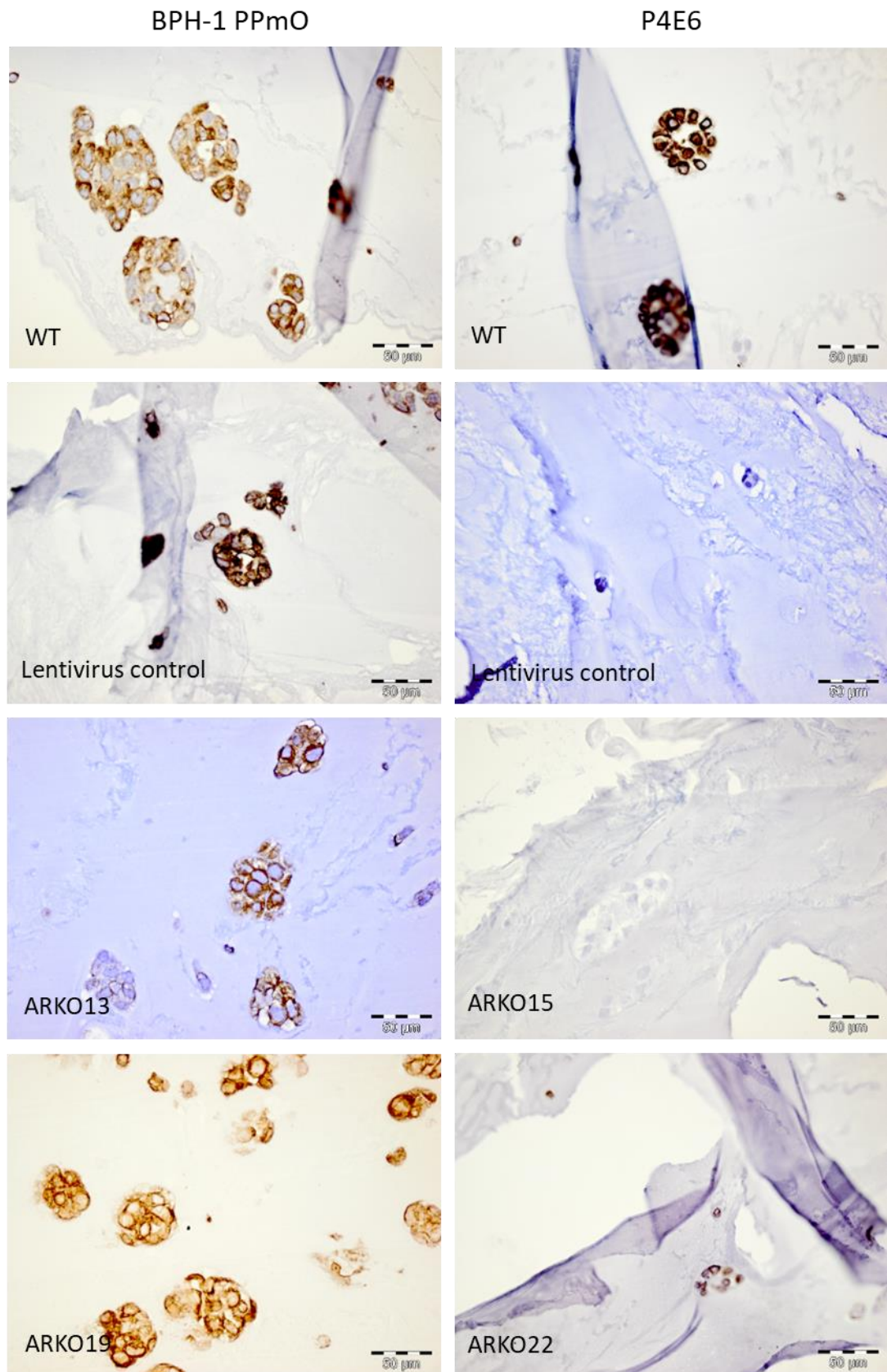


Figure 3.18: Expression of CK5 in spheroids. IHC for CK5 expression in WT, lentivirus control and ARKO clones of BPH-1 PPmO and P4E6 spheroids. Scale bar = 50 μ m.

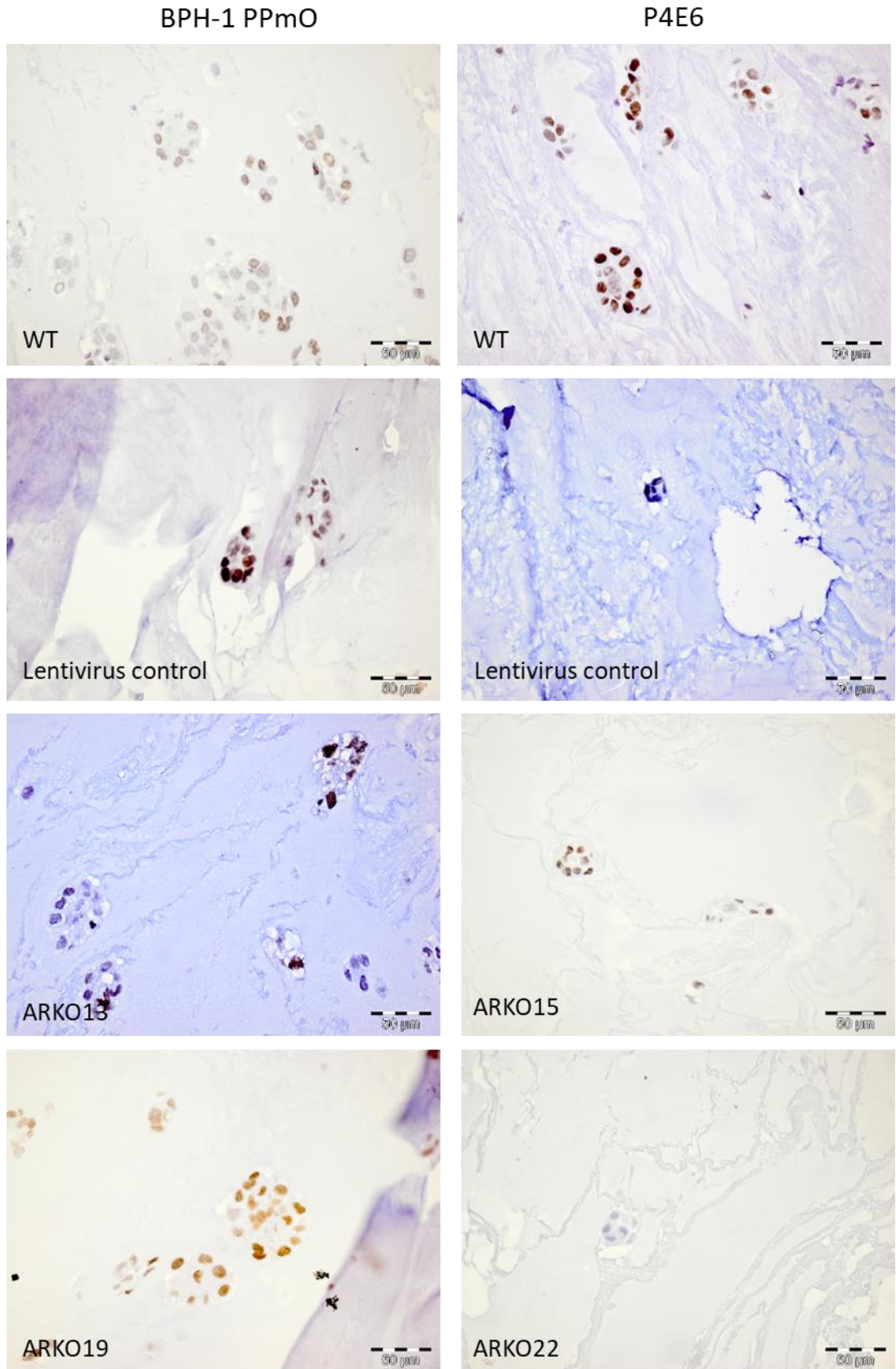


Figure 3.19: Expression of p63 in spheroids. IHC for p63 expression in WT, lentivirus control and ARKO clones of BPH-1 PpmO and P4E6 spheroids. Scale bar = 50 μ m.

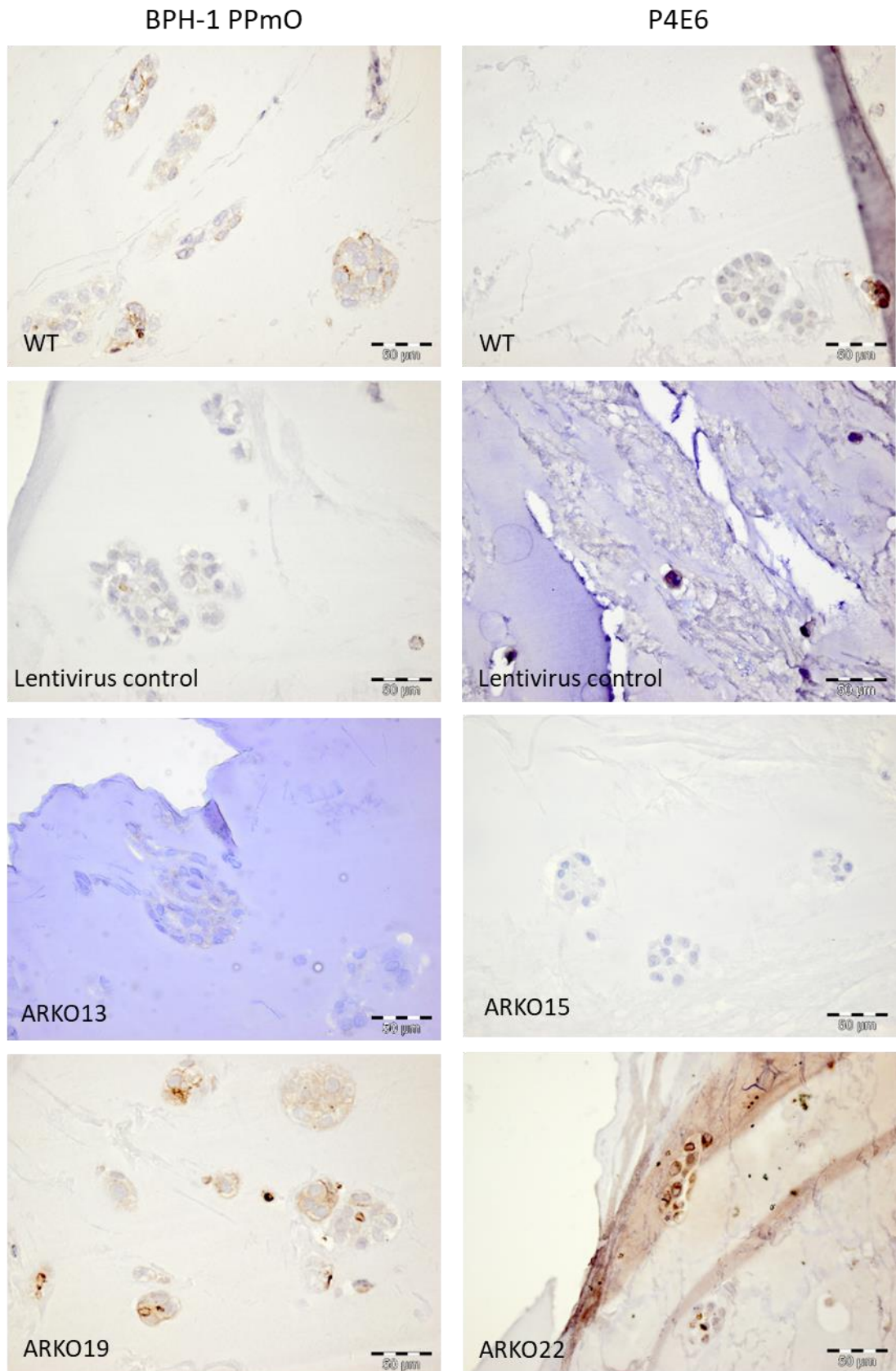


Figure 3.20: Expression of CK18 in spheroids. IHC for CK18 expression in WT, lentivirus control and ARKO clones of BPH-1 PpmO and P4E6 spheroids. Scale bar = 50 µm.

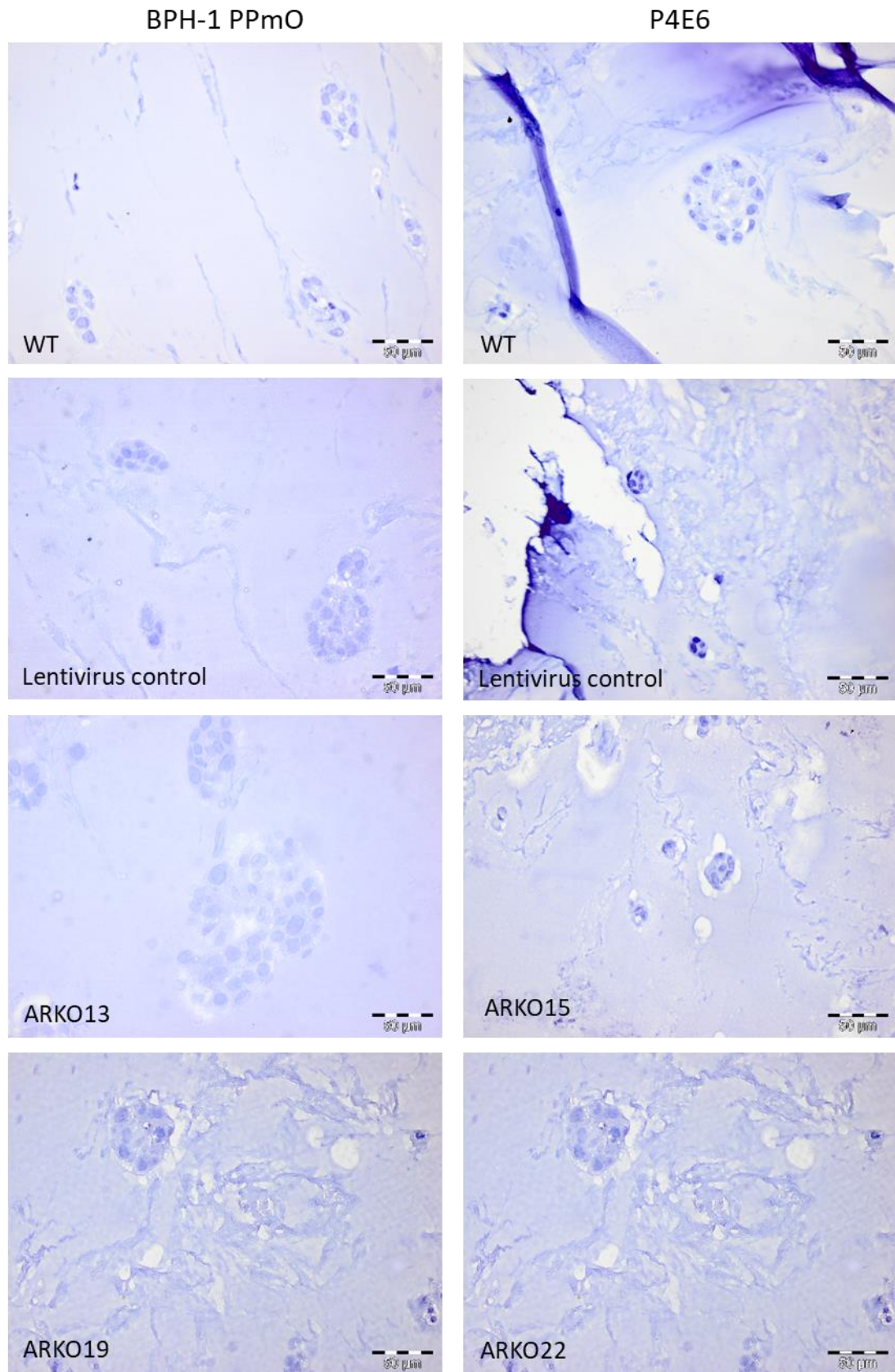


Figure 3.21: Expression of NKX3.1 in spheroids. IHC for NKX3.1 expression in WT, lentivirus control and ARKO clones of BPH-1 PPmO and P4E6 spheroids. Scale bar = 50 μ m.

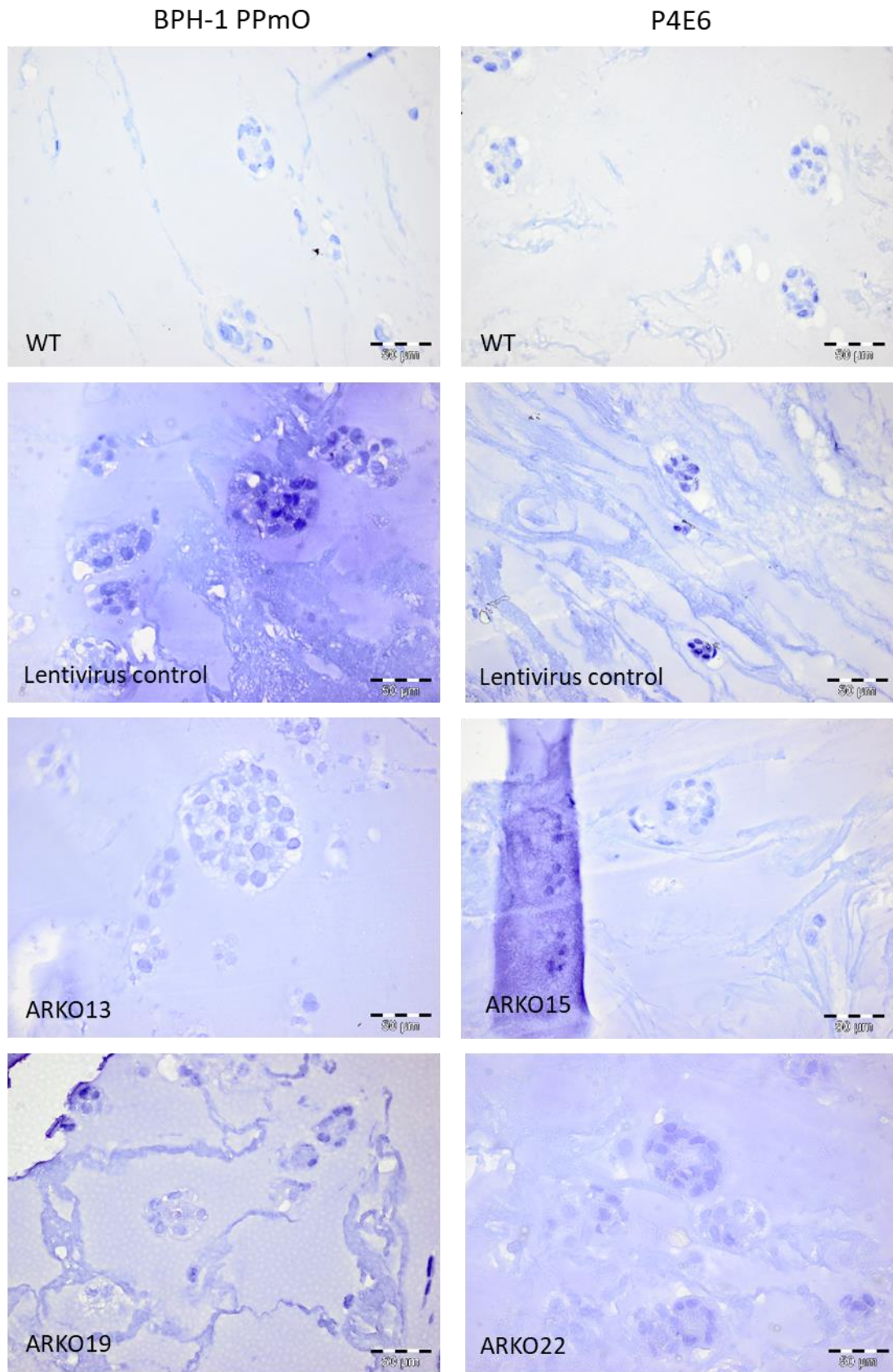


Figure 3.22: Expression of AR in spheroids. IHC for AR expression in WT, lentivirus control and ARKO clones of BPH-1 PPmO and P4E6 spheroids. Scale bar = 50 μ m.

3.3.5 AR is potentially required for differentiation

mOrange fluorescence is used as a proxy for PSA expression, which only occurs in differentiated luminal cells due to the presence of AR. mOrange fluorescence of BPH-1 PPMO spheroids was quantified after 7 days of growth. Four random fields of view were chosen and each spheroid in every plane of view was categorised into either negative, dim or bright mOrange fluorescence (Figure 3.23A). Over half of spheroids do not express mOrange and hence do not differentiate in WT, control or ARKO conditions (Figure 3.23B). This indicates the difficulty of inducing differentiation in basal cell lines in 3D culture. Bright mOrange fluorescence was only seen in WT and lentivirus control spheroids (1.8% and 1.5% respectively). Dim mOrange fluorescence was seen in ARKO clones (ARKO13 and ARKO19) as well as WT and lentivirus control (Figure 3.23B). This is potentially due to the PSA-Probasin-mOrange promoter being leaky. Only bright mOrange represents differentiation and hence it could be suggested that AR might be for differentiation based upon this result.

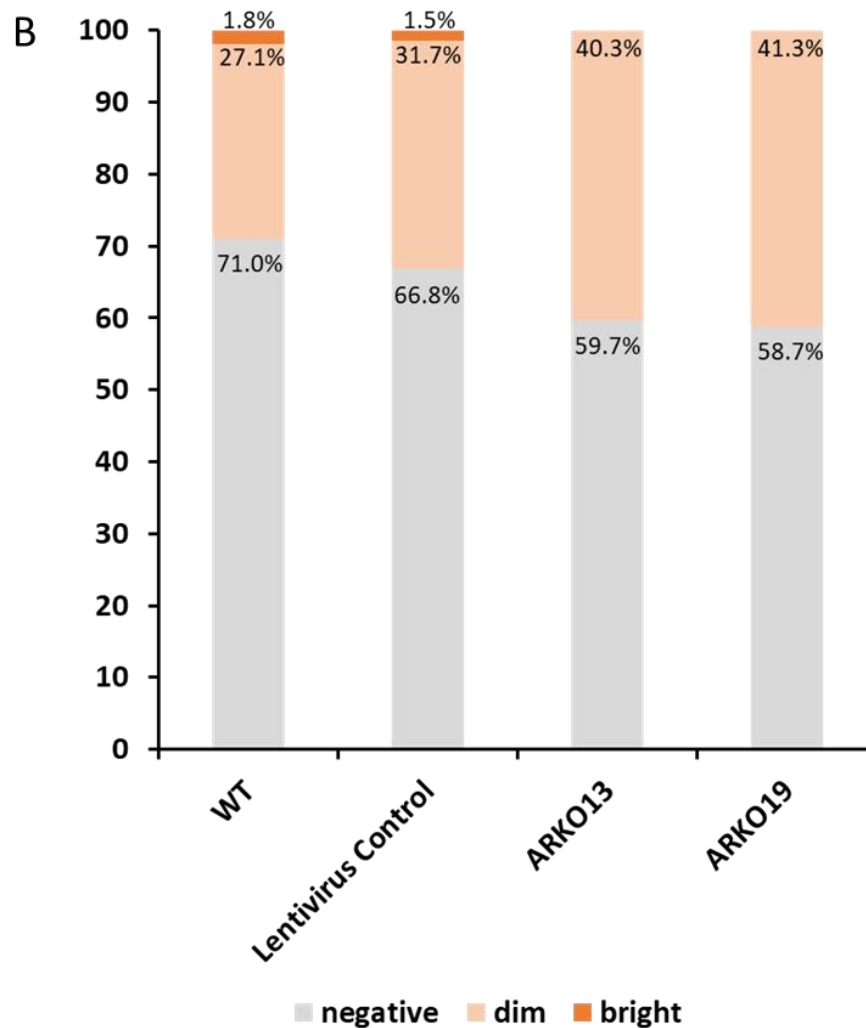
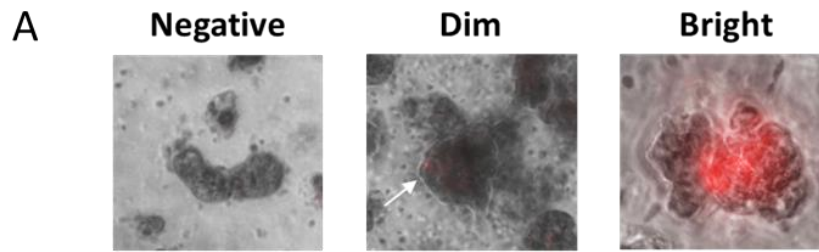


Figure 3.23: AR is potentially required for differentiation in BPH-1 PpmO cells. The mOrange fluorescence of the BPH-1 PpmO spheroids in four random fields of view were counted in WT, lentivirus control and ARKO clones after 7 days. Each spheroid was categorised as either negative, dim or bright mOrange expression. (A) Representative images of negative, dim and bright mOrange fluorescence in BPH-1 PpmO spheroids. (B) mOrange fluorescence quantified in WT, lentivirus control and ARKO clones. Number of spheroids assessed ranged between 218-433, N= 3.

4. Discussion

AR is vital for the development of the prostate as well as the proliferation and differentiation of prostate basal cells. Hence it is widely considered to be a master regulator. The research into how AR regulates differentiation of basal to luminal cells in both a normal and cancerous setting within the prostate is extensive. However, the majority of this research has been conducted on mouse prostate models or mouse and rat cell lines, which differ greatly from the human prostate (Lee et al., 2012, Simanainen et al., 2007, Whitacre et al., 2002, Wu et al., 2007). Therefore, the aim of this project was to explore the utility of the CRISPR/Cas9 system in order to create a permanent ARKO model in human basal cell lines. The role of AR in differentiation could then be investigated by culturing the ARKO cells in 3D to mimic differentiation of basal cells *in vivo*.

4.1 CRISPR/Cas9 is a successful tool to generate gene KO models

Prior to this project, CRISPR/Cas9 had never been used to KO *AR* in human prostate cell lines. Therefore the initial strategy was to test the efficiency of the CRISPR/Cas9 lentivirus and optimise the work flow to generate single celled CRISPR/Cas9 edited clones. The work flow was initially optimised using BPH-1 cells because they are easily manipulated. Once it had been determined that the CRISPR/Cas9 was successful, the experiments were repeated on the differentiation models BPH-1 PPMO and P4E6 cells.

The CRISPR/Cas9 lentivirus successfully transduced all three cell lines and genetic edits were detected in 30-59% of clones. CRISPR/Cas9 was most efficient in P4E6 cell lines, despite the cell line being notoriously difficult to transduce. This is possibly due to P4E6 cells being the third cell line to undergo CRISPR/Cas9 KO of *AR*, and therefore the techniques and protocols had been optimised. In order to have the option to choose clones with the greatest genetic and amino acid changes, approximately 20 clones were selected during dilution cloning. The online CRISP-ID tool enabled the

analysis of heterozygous KO clones in cell lines which had more than one copy of *AR* (Dehairs et al., 2016). However, it was limited to only producing three allele sequences, therefore next generation sequencing (NGS) could be used to have a more in depth view into the precise base changes in each copy.

During the course of the project Wei et al. (2018) published a study in which they aimed to KO *AR* using CRISPR/Cas9 in LNCaP cells to investigate the role of *AR* on proliferation. They concluded that when *AR* is not present, proliferation decreases due to an increase in apoptosis. Since they lacked validation to prove *AR* was knocked-out at the gene or protein level, these results must be interpreted with caution. They also did not produce single cell clones from their mixed population treated with CRISPR/Cas9 (Wei et al., 2018). Given only 30% of BPH-1 PPMO clones in this project were edited, the overriding phenotype within a mixed population would be BPH-1 PPMO cells with genetically intact *AR*. Therefore it is vital to select single cell clones and characterise each one before conducting functional assays, which Wei et al. (2018) failed to do.

One of the largest limitations of CRISPR/Cas9 is the occurrence of off-target effects. A recent study by Kosicki et al. (2018) has demonstrated that CRISPR/Cas9 can cause larger and more detrimental chromosomal changes than expected. They discovered that chromosomal translocations can occur, as well as inversions and deletions, ranging from 11 bp to 2.5 Kb. It also became apparent that there was a large range in the size of deletions at the target site, with over 20% of clones bearing deletions greater than 250 bp (Kosicki et al., 2018). In comparison, the clones in this project had deletions ranging from 1 bp to 58 bp. However, clone ARKO19 had an insertion of approximately 286 bp across the multiple alleles. It would therefore be useful in the future to sequence further afield from the target gRNA site to assess if the chosen clones in this project had any other genetic abnormalities. However, this project was focused on knocking-out the *AR* gene which is over 186 Kb long. Therefore, it is

unlikely that large chromosomal rearrangements in the *AR* gene sequence would have a substantial effect on other genes.

To conclude, CRISPR/Cas9 was a relatively simple and easy to use tool which enabled the creation of multiple *AR* gene KO models. The generation of a sufficient number of single cell clones was laborious, but essential to produce clones with a homogenous phenotype. CRISPR/Cas9 was efficient in producing genetic edits in a range of cell lines, but it was most successful in P4E6 cells. However, the largest limitation of CRISPR/Cas9 is the presence off-target genetic edits and their unknown effects. Whole genome sequencing is the only way to elucidate the effects which would be costly and time consuming, but essential. However, the production of multiple clones can partially control for off-target effects.

4.1.1 Therapeutic relevance of CRISPR/Cas9

CRISPR/Cas9 has become a powerful genetic engineering tool to aid cancer research. Since its first use in 2013, it has rapidly spread across the scientific community, and has been adapted for a range of applications. It has now been used to investigate all ten hallmarks of cancer as described by Hanahan and Weinberg (Hanahan and Weinberg, 2011, Moses et al., 2018). In the near future, CRISPR technology could be used in the clinic. Recently CRISPR/Cas9 has been used to modify chimeric antigen receptor (CAR) T-cells which are designed to target and destroy cancer cells (Schumann et al., 2015). Phase I clinical trials are currently being conducted in USA and China (Weidong, 2018). CRISPR/Cas9 has also been used to induce gene knock-outs in both mouse and cell line models to help investigate PCa (Kawamura et al., 2015, Takao et al., 2018, Ye et al., 2017). In particular, Ye *et al.* (2017) discovered that blocking GPRC6A by CRISPR/Cas9 suppressed prostate carcinogenesis in a xenograft model (Ye et al., 2017). Combined with my project demonstrating the efficiency of CRISPR/Cas9 in prostate human cell lines, it could be the start of discovering a novel gene therapy to treat PCa and CRPC using CRISPR/Cas9.

4.2 The role of AR in the prostate epithelium

4.2.1 AR may be required for differentiation

In order to measure basal to luminal cell differentiation, an existing model was used in this study. The induction of mOrange in the BPH-1 model system used is regulated by the PSA-Probasin promoter. PSA is a luminal marker and is regulated by AR, therefore the rationale is that AR must be present in order for mOrange expression to be induced (Kim and Coetzee, 2004). However, only 2% of WT and lentivirus control BPH-1 PPMO spheroids expressed bright mOrange. This is a small percentage of cells, and so in some ways the readout is not optimal. The lack of AR detected in sectioned WT spheroids via IHC is therefore likely due to both a combination of an ineffective antibody and the largest proportion of spheroids not expressing AR. Once a suitable antibody has been optimised, in the future it would be necessary to section the entire paraffin block to search for the 2% of differentiated spheroids. Nevertheless no ARKO clone had any spheroids that were positive for very bright mOrange, and so the implication is that less differentiation occurred in these clones compared to the WT.

Both WT and ARKO BPH-1 PPMO spheroids display dim mOrange fluorescence after seven days in culture. This could be indicative of differentiation, but the complete lack of bright mOrange expression in ARKO clones could suggest dim mOrange fluorescence occurs due to a leaky promoter. This is defined as low level transcription occurring during the inactive state (in the absence of a stimulus) of the promoter (Huang et al., 2015, McCutcheon et al., 2018). This phenomenon is seen classically with the *lac* operon, whereby there is a low level of expression of *lac* promoter control genes even when lactose is not present (Jacob and Monod, 1961). Previous research done in our lab also supports this idea, as Pellacani et al (2014) noted that 50% of spheroids had detectable levels of mOrange, but AR was only found in a rare subpopulation of cells (Pellacani et al., 2014). This is a limitation to the BPH-1 PPMO

model, and perhaps detection of differentiation markers via IHC is a more reliable indicator for the occurrence of differentiation.

The qRT-PCR results demonstrated that AR expression was reduced in BPH-1 PPMO ARKO clones in comparison to WT and control spheroids, which was encouraging. However, some AR expression was still detected in ARKO clones, which contradicts the absence of mOrange fluorescence. This could possibly be due to not all three copies of AR in BPH-1 PPMO ARKO clones being inactive. Also, it is likely that mRNA is still produced by ARKO spheroids which can be detected by the qRT-PCR, but the full AR protein would not be formed. Therefore to validate the KO of AR, further protein analysis will need to be done in the future. Also again, the low amount of AR expression pushes the sensitivity of the qRT-PCR method. The limitation of using the $\Delta\Delta\text{Ct}$ method for small changes in gene expression is that it requires a stable endogenous control for comparison. Three different endogenous controls were tested (Appendix 1.1), but expression varied up to 4.81 Ct values between conditions (Appendix 1.2). Primer efficiencies were also over 110%, and according to MIQE guidelines this could be due to primer-dimers or nonspecific amplicons. This could also explain why clone ARKO22 did not show a reduction in AR expression, despite amino acid sequence alignment predicting it has the shortest amino acid sequence of AR after CRISPR/Cas9 causing a frame shift mutation. Therefore selection of an endogenous control specific to the experimental conditions is important. The $\Delta\Delta\text{Ct}$ method might not be sufficiently sensitive enough to detect the low level of AR mRNA expression. Alternatively, absolute levels of AR mRNA could be determined by creating a standard curve of known copies of AR plasmid DNA. This method for qRT-PCR does not require an endogenous control and would be more sensitive to expression levels.

The formation of prostate spheroids enables researchers to replicate what occurs *in vivo* without the use of mouse models (Adcock et al., 2015). In our lab they have been

used as a method to induce differentiation (Maitland et al., 2001, Pellacani et al., 2014). However this is extremely difficult to achieve due to the challenge of growing luminal cells in culture (Chua et al., 2014). There is a large range of 3D structures described by different authors which makes comparisons extremely difficult (Bello-DeOcampo et al., 2001, Brinkmann et al., 1995, Kogan et al., 2006, Lang et al., 2006, Miki et al., 2007, Webber et al., 1997). During the project we also identified variation in spheroid structure between experiments (not shown). Perhaps a different method of forming the spheroids would result in greater differentiation rates and more consistent phenotypes. For example, a therapeutic screening study of 3D tumour spheroid models found that the pellet culture method used with rabbit bone marrow derived mesenchymal progenitor cells produced the highest amount of spherical spheroids in comparison to other methods (magnetic levitation, hanging drop method and rotating wall vessels) (Johnstone et al., 1998, Zanoni et al., 2016).

Previous work on keratinocytes demonstrated a "calcium switch" induced differentiation. In particular, low calcium (0.03-0.1 mM) prevented the keratinocytes from differentiating, whereas growth in high calcium (0.1-1.4 mM) resulted in the formation of differentiated suprabasal epidermal cells (Boukamp et al., 1988, Hennings et al., 1980, Pillai et al., 1990). Therefore, to test if the same effect occurs in prostate cell lines, BPH-1 PPMO and P4E6 WT spheroids were grown in high calcium (2 mM) for 7 days. A particularly high concentration of calcium was chosen to induce the rate of differentiation as greatly as possible. Initially calcium increased the rate of differentiation but by day 7 there was no difference in the number of mOrange fluorescing spheroids grown with and without calcium. AR expression was also significantly greater when the spheroids were grown without calcium. Perhaps the level of calcium was too high and had an inhibitory effect on terminal luminal differentiation in both BPH-1 and P4E6 cells. Work by Tyson et al. (2007) demonstrated that different prostate cell lines form acini in a range of different

calcium concentrations (Tyson et al., 2007). Therefore, the effect of calcium on differentiation is cell line specific and it can also be found to inhibit lumen formation. The required calcium concentration for optimum differentiation needs to be further investigated. Also the timing at which calcium is added to the media needs to be investigated as it could also have an effect on the rate and extent of differentiation. It is likely that this will vary between the BPH-1 PPMO spheroids and P4E6 spheroids.

In summary, IHC and qRT-PCR are not sufficiently sensitive enough methods to allow the detection of the rare population of differentiated spheroids. Flow cytometry would be the next best candidate to help detect the 1-2% of spheroids which differentiate and express AR. A combination of an AR antibody and detection of mOrange would help count the number of differentiated BPH-1 PPMO cells. This method would also enable counting of differentiated P4E6 cells which was not possible in this study. However, a method to disaggregate spheroids to avoid doublets would need to be optimised. Also, as discussed in section 4.2.2, terminally differentiated luminal cells also undergo apoptosis, and therefore it is imperative that the media is collected in order to detect these cells.

4.2.2 Terminally differentiated luminal cells undergo apoptosis

Previously, the induction of an epithelial bilayer by allowing cells to grow to be over confluent was only attempted in primary cell cultures (Frame et al., 2010, Swift et al., 2010). Here, this method for inducing differentiation was attempted with BPH-1 and BPH-1 PPMO cells, using mOrange as an indicator for luminal differentiation. Initially it appeared via fluorescence imaging that BPH-1 PPMO cells which formed a bilayer had differentiated into luminal cells. However, when this was quantified by flow cytometry there was half the number of mOrange expressing cells when grown in a bilayer than when grown at 80% confluent monolayer. This discrepancy could be due to the terminally differentiated luminal cells undergoing apoptosis and being aspirated during cell collection for flow cytometry (Chen et al., 2016, Pellacani et al.,

2014). This has been previously identified by Pellacani et al. (2014) whereby 80% of the spheroids contained cells undergoing apoptosis within the centre of spheroid, highlighting the instability of differentiated cells (Pellacani et al., 2014). Also, viability dye was not used, which would have been used to gate out dead cells. It has also been observed in our lab that BPH-1 cells are able to undergo spontaneous differentiation during monolayer cell culture. This could explain the presence of differentiated luminal cells while in normal monolayer culture. However, relying on spontaneous differentiation was insufficient for detection of AR via western blot or qRT-PCR and hence the basal cells were differentiated using 3D culture.

4.2.3 AR is not required for basal cell survival

The ability to grow ARKO clones in normal cell culture as well in 3D spheroids, indicates that AR is not essential for basal cell survival. This phenomenon has been discovered in other studies. Xie et al (2017) conditionally deleted *AR* in mouse basal cells, and Caspase 3 staining showed there was no change in apoptosis in the absence of AR (Xie et al., 2017). Lamb et al (2010) also agrees and concluded that differentiated secretory luminal cells required cell-cell adhesion via e-cadherin for survival rather than androgen activity or keratin growth factor (KGF) released from the stroma (Lamb et al., 2010).

In an attempt to confirm that ARKO does not affect cell viability, the CellTiter-Glo[®] 3D cell viability assay was performed. The assay was initially attempted to be optimised for the number of seeded cells required to produce ATP below the detection limit. The number of cells that produced the maximum concentration of ATP differed between cell lines. This is likely due to the difference in structure, size and shape between P4E6 and BPH-1 PPmO spheroids affecting the uptake of the CellTiter-Glo[®] reagent. ATP detected from BPH-1 PPmO spheroids decreased when the number of cells seeded increased. This is likely due to BPH-1 PPmO spheroids forming larger aggregates and hence making it more difficult for the CellTiter-Glo[®] reagent to

penetrate. Mixing the reagent and cells more vigorously and for longer would improve this assay. In the future, sections of WT and ARKO clones could be stained for Caspase 3 to measure the rate of apoptosis in the absence of AR. Alternatively, colorimetric viability assays could be performed such as the MTS or MTT assays (abcam). Differentiation of basal cells could also result in a change in cellular metabolism. Therefore detection of ATP could be misleading for cell viability and instead the spheroids could be disaggregated and the number of cells could be directly counted using a haemocytometer or an automated cell counter.

4.2.4 Identification of AR splice variants

Alternative splicing of AR results in several AR splice variants (ARVs). The majority of ARVs lack the LBD, and hence this allows the development of CRPC in PCa cells treated with ADT. Initial differentiation experiments involved incubating BPH-1 WT and BPH-1 ARKO cells in DHT for 24 hr. The presence of AR protein was then detected via a western blot. Full length AR was detectable at 110 kDa only in the positive control, VCaP cells (Figure 3.10). However, there are multiple bands seen at lower molecular weights which could be different ARVs. VCaP cells have over 35 copies of AR, resulting in high AR expression which is not representative of normal physiological levels (Figure 3.1). Therefore, detection of low levels of AR from WT BPH-1 and P4E6 cells could be missed. To rectify this, VCaP protein lysate could be diluted down to match the levels of AR expression in BPH-1 and P4E6 cells (approximately 1 in 35). Alternatively, patient BPH-1 tissue lysate could be used as the positive control.

The WT BPH-1 and two ARKO clones produced a single band on western blotting at approximately 65 kDa. In general, the band was only seen when DHT was not present and therefore DHT could be suppressing the presence of the ARV. The epitope for the antibody used on the western blot is to the LBD, which rules out the majority of the ARVs. However, a likely candidate for the band is the ARV, AR45 which has been found to be 67kDa in mouse muscle (Ma et al., 2015). Conversely, it has been found in heart

extracts cells to be 45 kDa (Ahrens-Fath et al., 2005). This splice variant is not very well characterised and it has never been detected in BPH-1 cells. To confirm the presence of AR45 and other ARVs, qRT-PCR specific to different ARVs could be performed. Another candidate for the lower band is the presence of Albumin (a common contaminant) at 68 kDa, which would indicate the western blot protocol requires optimisation. Alternatively, the band could be due to non-specific binding and a more specific AR antibody is required.

4.3 Immortalisation of cell lines results in genomic instability

AR is located on the X chromosome and hence healthy human males only possess one copy. However, in CRPC patients *AR* can be amplified as a mode of resistance to ADT (Visakorpi et al., 1995). Therefore, the presence of *AR* amplification and number of X chromosomes (and hence number of copies of *AR*) was investigated in BPH-1, BPH-1 PPMO and P4E6 cell lines. The malignant and androgen-independent cell line VCaP was used as a control as it has been previously characterised that VCaP cells have undergone *AR* amplification (Li et al., 2012, Taurozzi, 2016). The original karyotype of BPH-1 cells produced by Hayward et al. shows that BPH-1 cells had two X chromosomes and hence it was predicted they would have two copies of *AR* (Hayward et al., 1995). This was confirmed by the copy number analysis conducted during this project. The inflation of the number of X chromosomes is likely caused by genetic instability during the immortalisation process. BPH-1 cells are immortalised by the common method of transfection with the SV40 virus large T antigen (LT). However, LT is well known to induce genomic instability resulting in chromosomal structural abnormalities and the generation of aneuploidy in cell lines (Ray et al., 1990, Stewart, 1991, Woods et al., 1994). BPH-1 PPMO cells on the other hand contained three X chromosomes and copies of *AR*. Perhaps subsequent transduction of BPH-1 with a lentivirus containing the reporter gene PSA-Probasin mOrange could have

resulted in further genomic instability. This is an important observation, and one that suggests that such genetically manipulated models may have unforeseen changes. For example, the C4-2 cell line is a metastatic derivative of the LNCaP cell line. However genome and exome sequencing has shown 2056 specific mutations to the C4-2 cell line, which provides evidence for the significant genetic changes which can occur between two related cell lines.

P4E6 cells on the other hand only contained one X chromosome and a single copy of *AR*, which agrees with the results produced by Taurozzi (2016). The lack of X chromosome amplification could be due to the difference in immortalisation methods between P4E6 cells and BPH-1 cells. P4E6 cells were immortalised by HPV16 E6 retrovirus, which has been demonstrated in keratinocytes to upregulate telomerase hTERT gene transcription and activity, as well as degrading the tumour suppressor p53 (Klingelutz et al., 1996, Maitland et al., 2001, Scheffner et al., 1990). The ability to maintain the length of the telomeres will aid the genomic stability. SV40 LT on the other hand does not maintain telomere length but blocks retinoblastoma protein, which results in excessive cell growth (DeCaprio et al., 1988). These two factors combined probably results in the large amount of genomic instability caused by the LT protein. Also, BPH-1 were at a higher passage than P4E6, which could also be a contributing factor to their greater genomic instability and aneuploidy.

4.4 Future work and concluding remarks

The generation of an ARKO model was successful in human basal cell lines using CRISPR/Cas9. This is the first time that several ARKO clones have been generated in human basal cell lines within the field. However, as demonstrated by the copy number analysis, the immortalisation of cell lines results in genomic instability. Hence, to create a better model for the role of AR in the human prostate, CRISPR/Cas9 KO of *AR* could be conducted on human primary cells in the future (Figure 4.1B).

From the results of this project it can be inferred that AR is required for differentiation. However, differentiated spheroids were rare and the PSA-Probasin mOrange promoter is suspected to be leaky. To optimise the differentiation of spheroids, RA could be added to the differentiation media as it has been found previously to be important in the development of the prostate alongside androgens (Figure 4.1A) (Bryant et al., 2014). To further induce differentiation, the next step would be to engraft P4E6 and BPH-1 PPmO WT and ARKO clones into mice with stromal fibroblasts (Figure 4.1C). Hayward et al. (2001) has also demonstrated that BPH-1 cells can initiate tumour growth when recombined with CAFs (Hayward et al., 2001). It would then also be possible to investigate the role of AR in tumorigenesis by engrafting BPH-1 PPmO ARKO clones along with CAFs into mice.

Overall, the extensive characterisation of CRISPR/Cas9 generated ARKO clones will allow further investigation into the role of AR during the development of PCa. This could help further elucidate the mechanisms by which CRPC occurs in order to design more effective treatments.

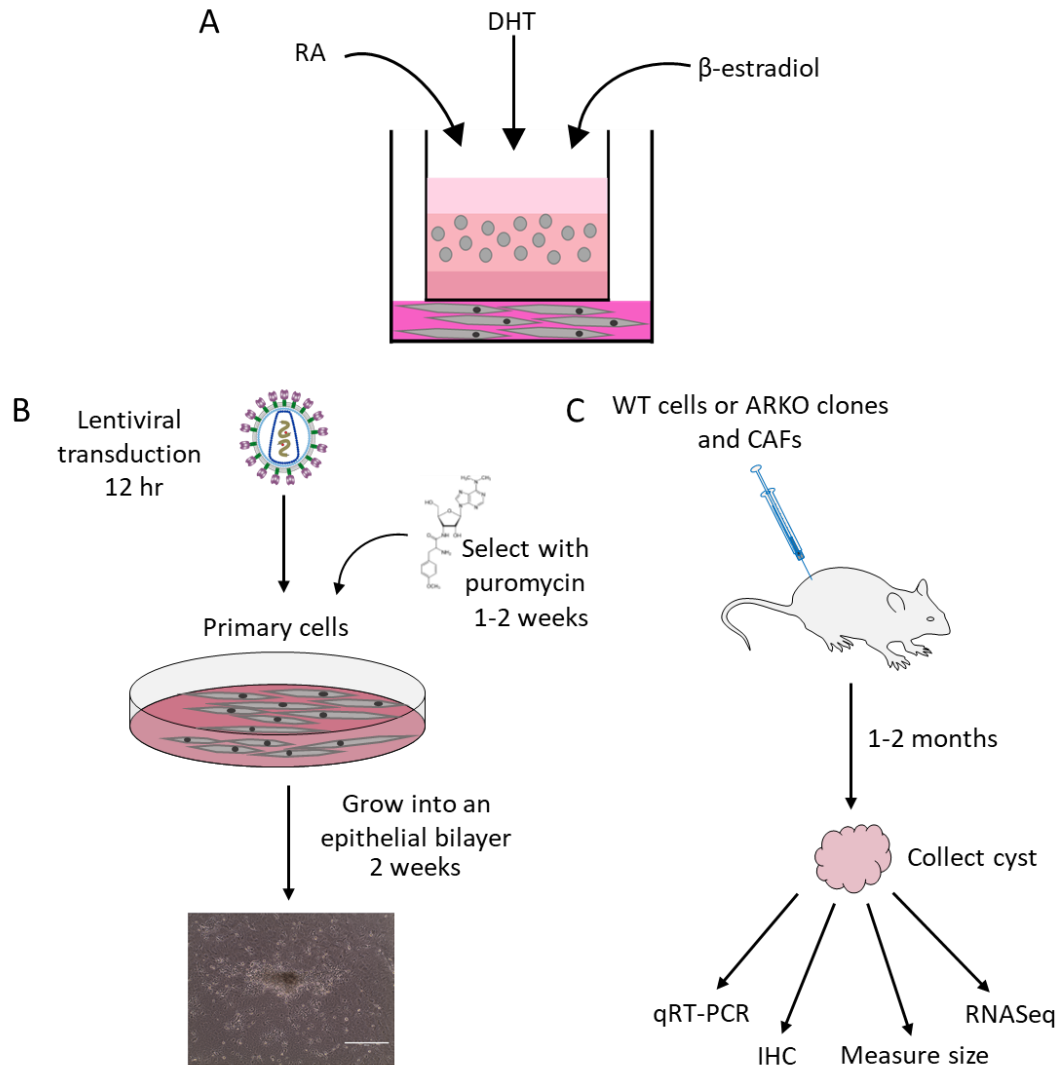


Figure 4.1: Proposed future experiments to determine the role of AR during epithelial differentiation. (A) Addition of RA along with the existing differentiating factors (DHT and β -estradiol) during the growth of WT and ARKO spheroids. (B) KO AR in basal primary cells using CRISPR/Cas9 and select with puromycin. The heterogeneous population of cells would be left to become over confluent to investigate if a differentiated epithelial bilayer would form. (C) Implant WT and ARKO clones into mice and extract the differentiated cyst after 1-2 months. Analyses the cyst for differentiation markers via IHC and qRT-PCR, and total gene expression changes via RNASeq.

Appendix

Appendix 1.1 qRT-PCR Ct values generated from different endogenous controls

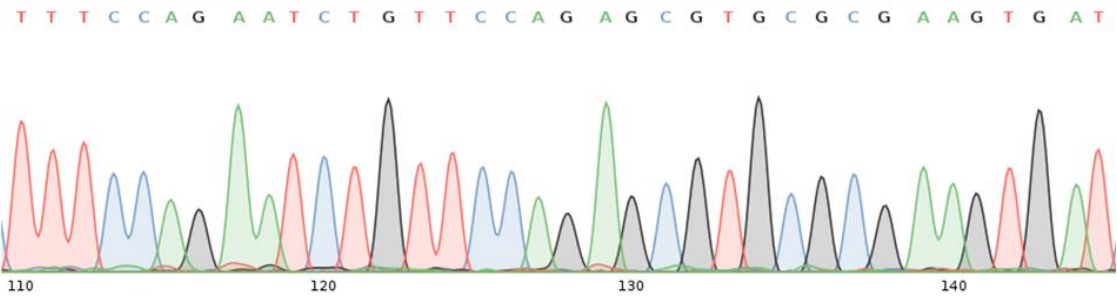
	Cell Type	RPLPO	HPRT	RSP27A
BPH-1 PPMO	Monolayer WT	19.55	22.94	22.03
	WT Spheroid +Ca	22.63	25.67	24.7
	WT Spheroids –Ca	24.36	27.12	26.29
	ARKO13 Spheroid	21.39	23.97	23.54
	ARKO19 Spheroid	22.06	24.88	24.07
P4E6	Monolayer WT	21.41	25.65	23.42
	WT Spheroid +Ca	22.33	26.13	24.12
	WT Spheroids –Ca	21.76	25.52	23.15
	ARKO15 Spheroid	21.08	25.84	23.19
	ARKO22 Spheroid	21.81	28.16	23.74

Appendix 1.2 Range of Ct values generated from different endogenous controls

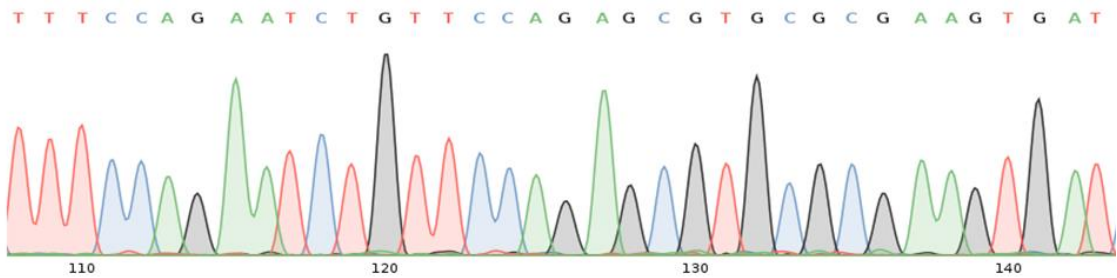
	RPLPO	HPRT	RSP27A
BPH-1 PPMO	4.81	4.18	4.26
P4E6	1.25	2.64	0.97

Appendix 2.1 Sequences of BPH-1 clones targeted with AR CRISPR/Cas9 lentivirus. Yellow arrow indicates the start of the edit site.

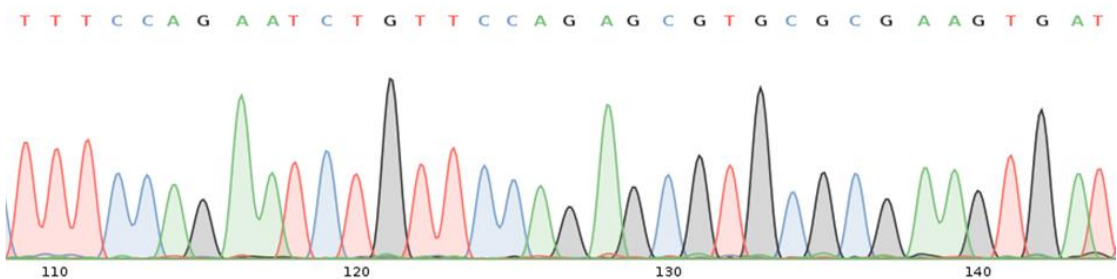
WT



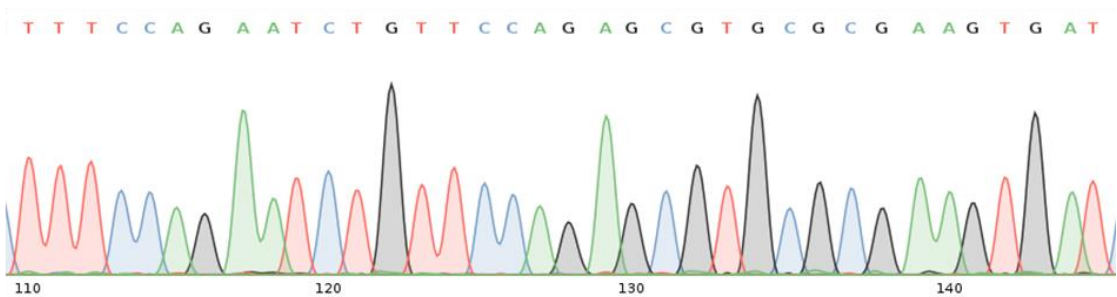
Clone 1.1



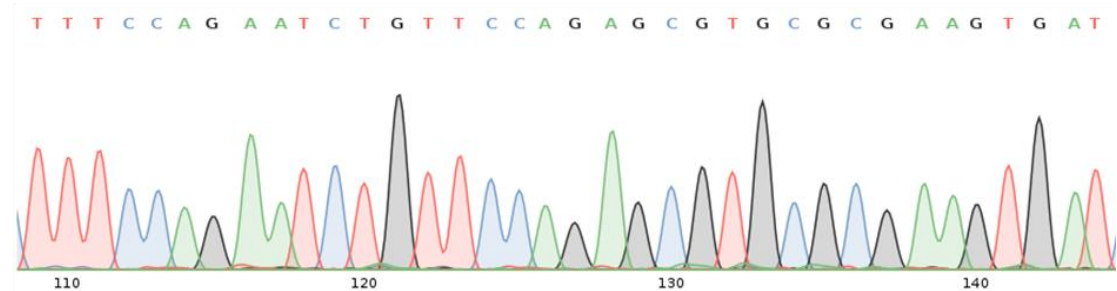
Clone 1.2



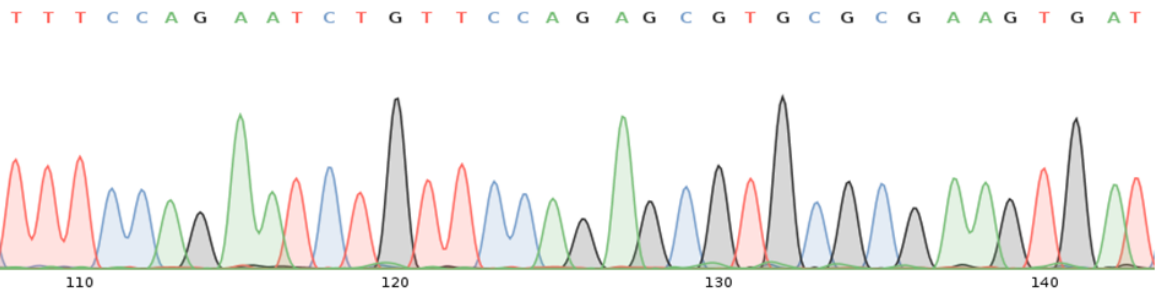
Clone 1.C12



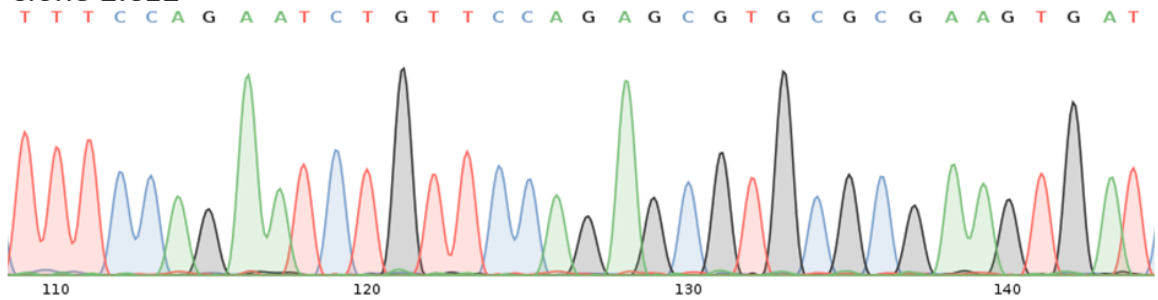
Clone 2.H9



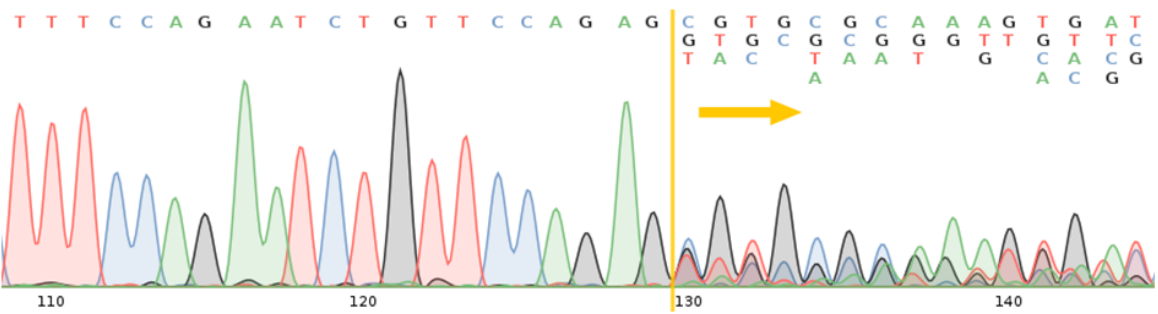
Clone 2.4



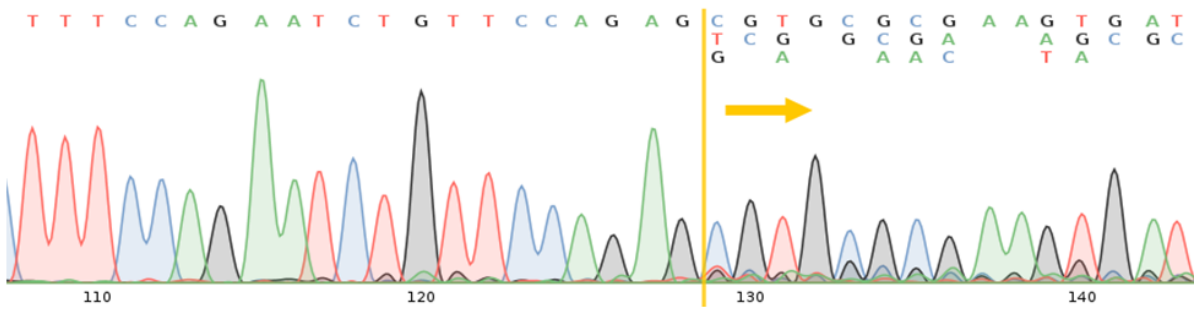
Clone 2.C12



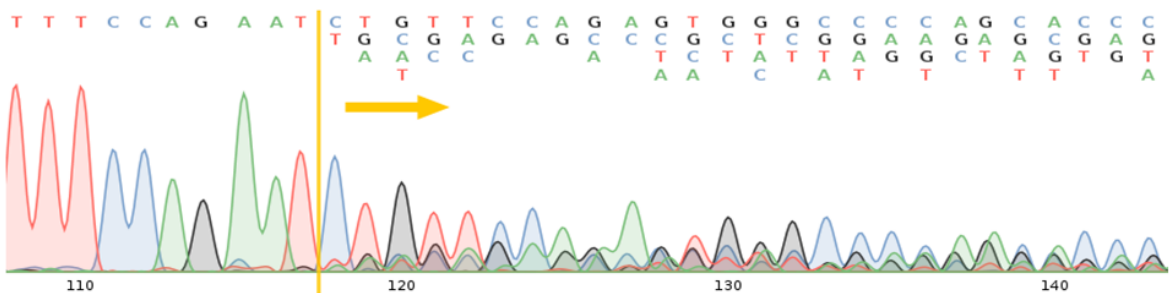
Clone 2.D2



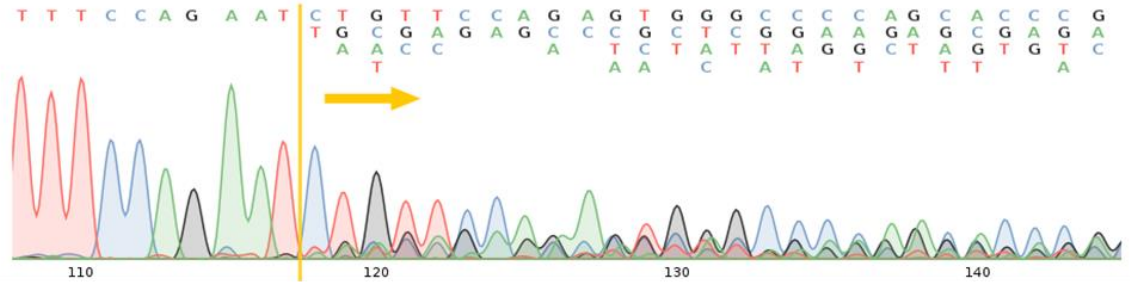
Clone 2.C9



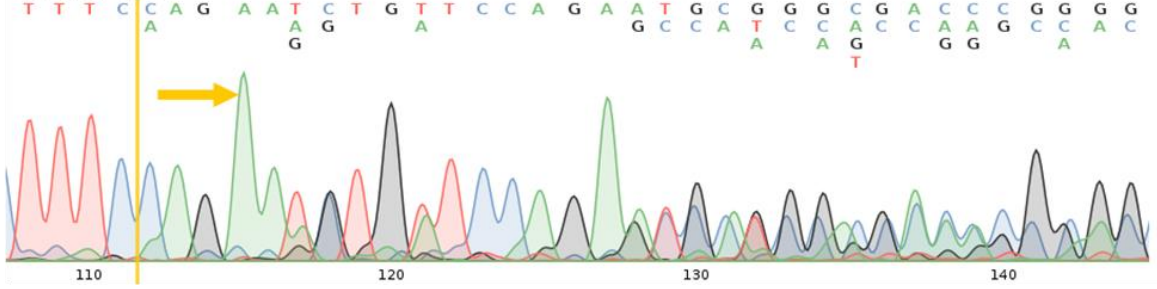
Clone 1.5



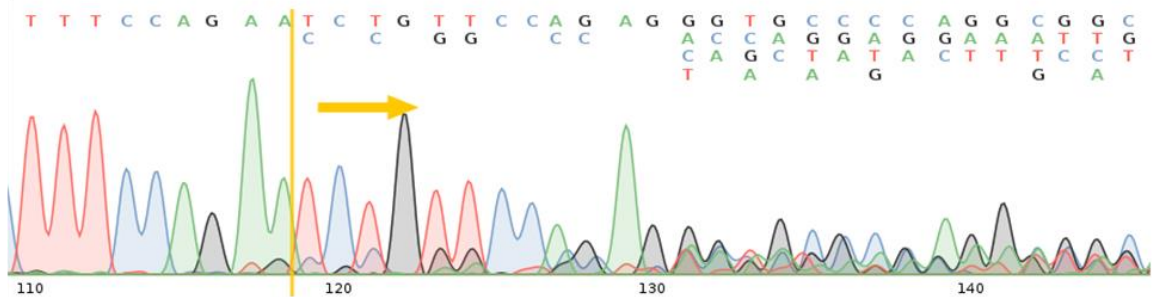
Clone 1.5



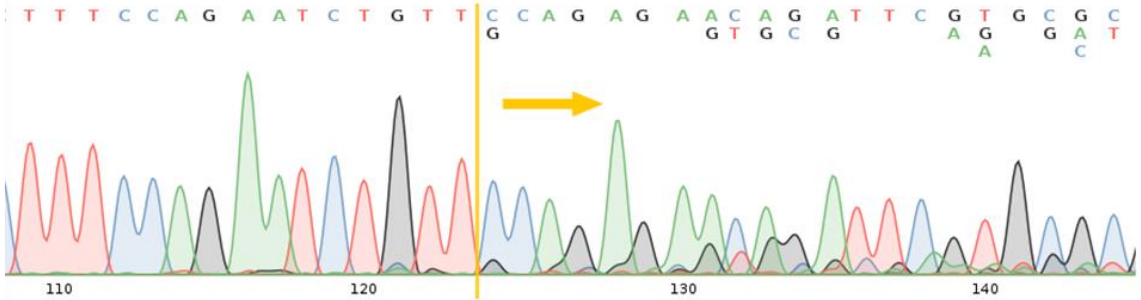
Clone 2.D7



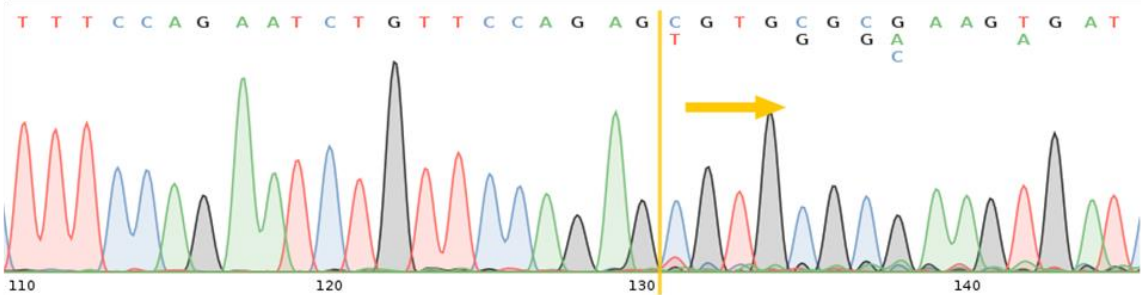
Clone 1.D10



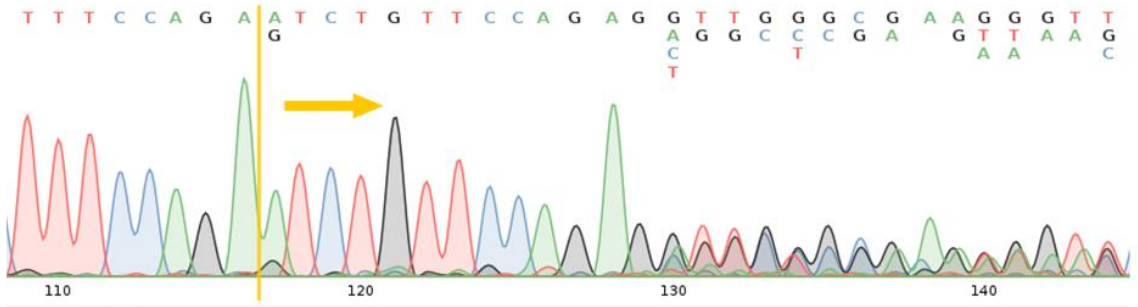
Clone 2.F11



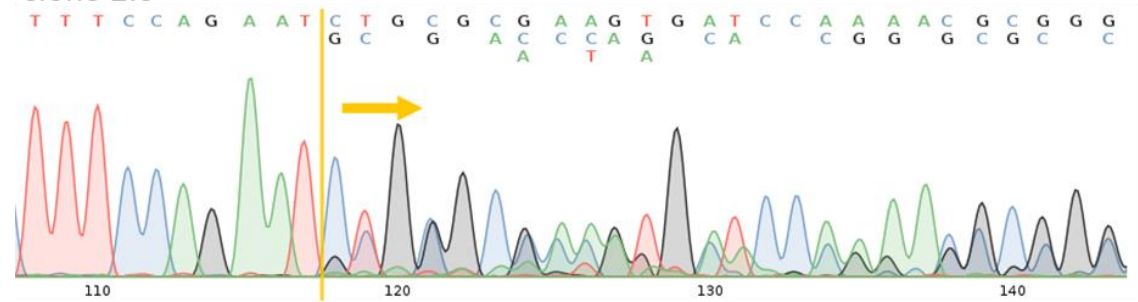
Clone 1.C9



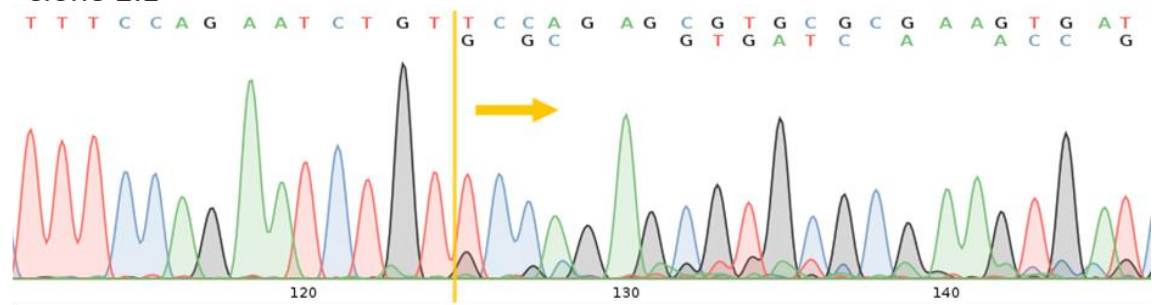
Clone 2.2



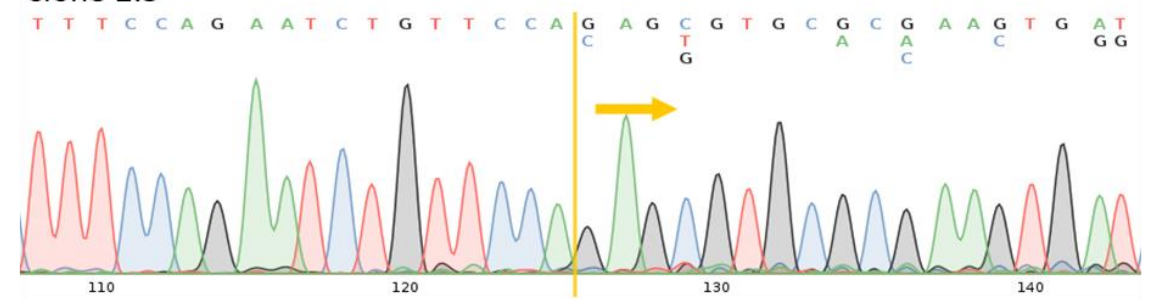
Clone 2.6



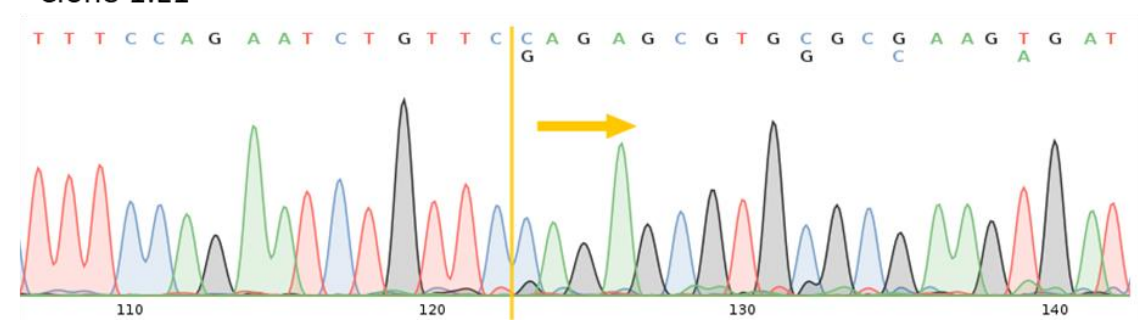
Clone 2.1



Clone 2.3

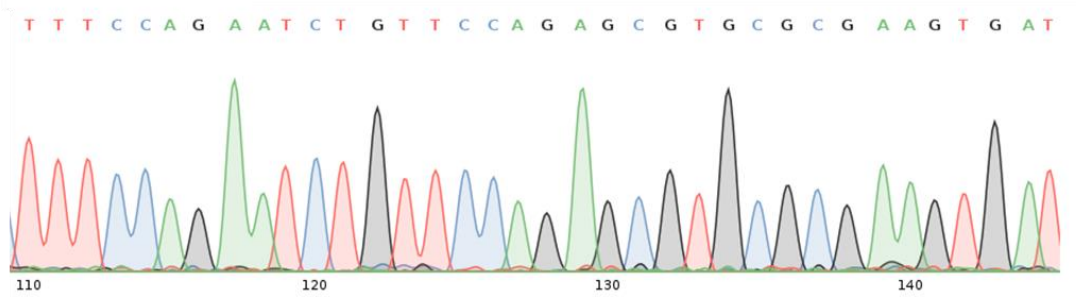


Clone 1.E1

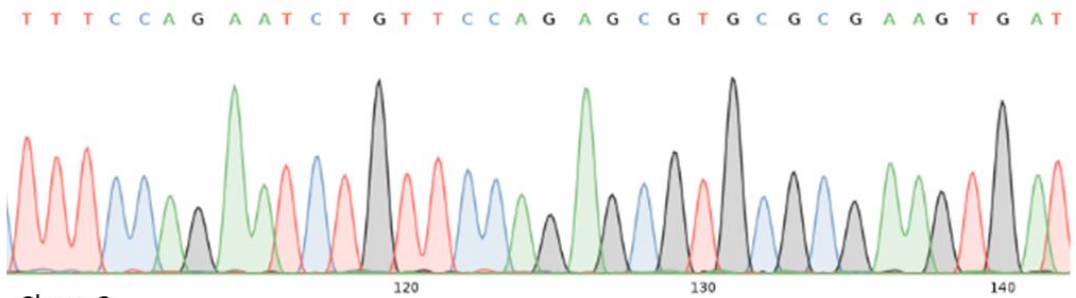


Appendix 2.2 Sequences of BPH-1 PpmO clones targeted with AR CRISPR/Cas9 lentivirus. Yellow arrow indicates the start of the edit site.

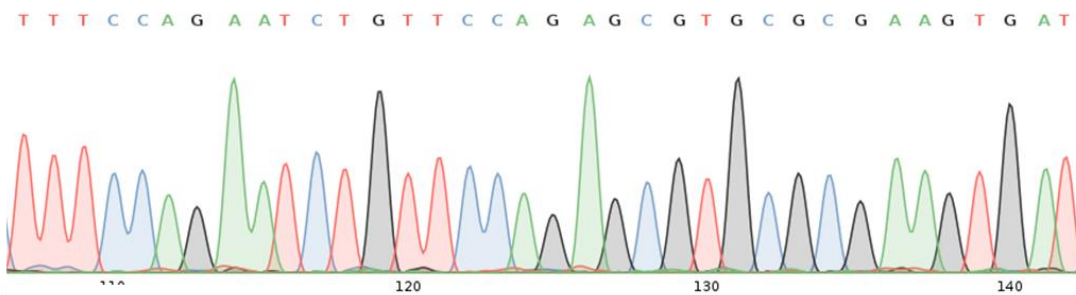
WT



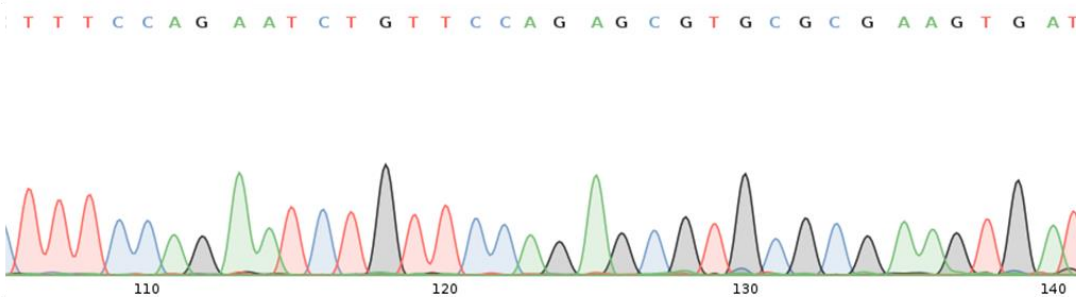
Clone 1



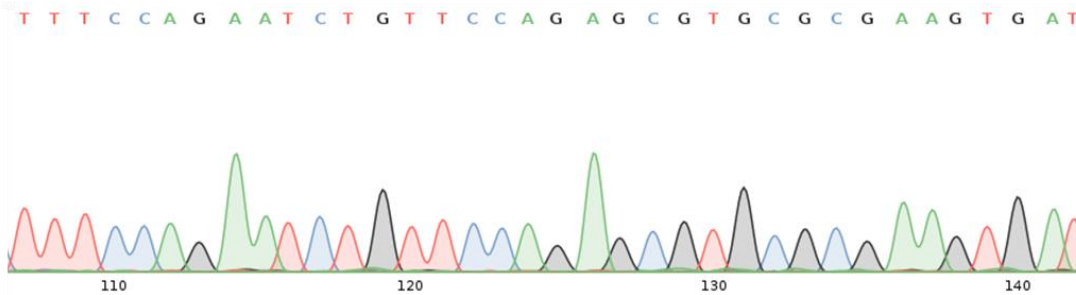
Clone 2



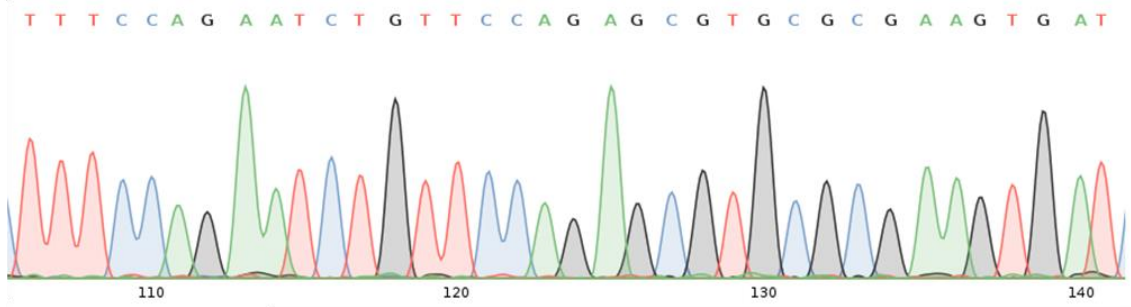
Clone 3



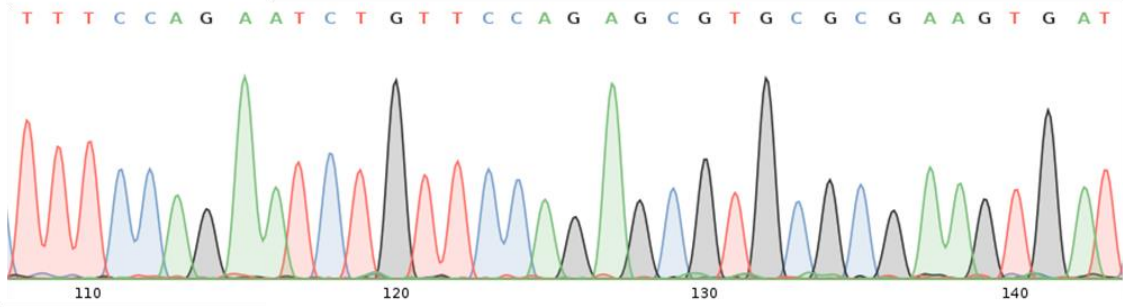
Clone 5



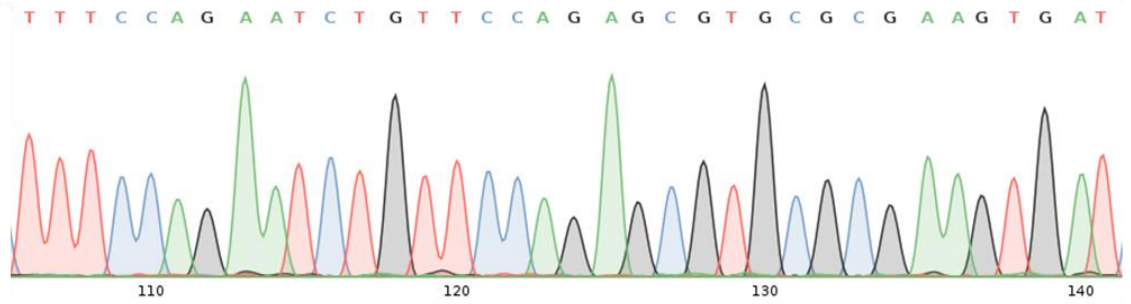
Clone 6



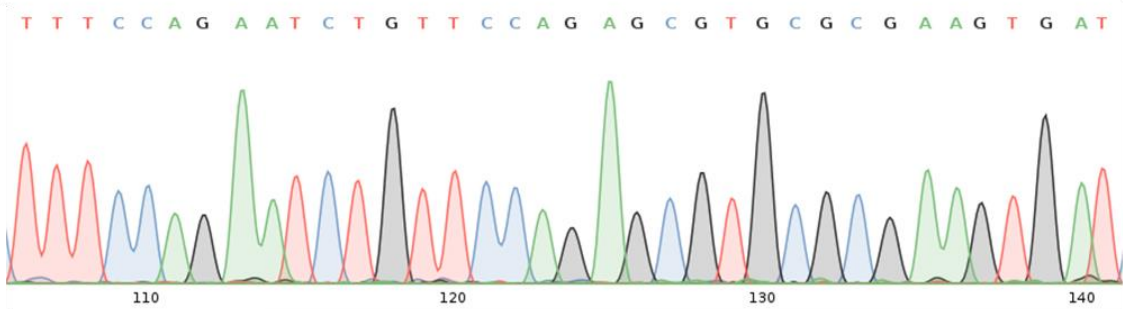
Clone 8



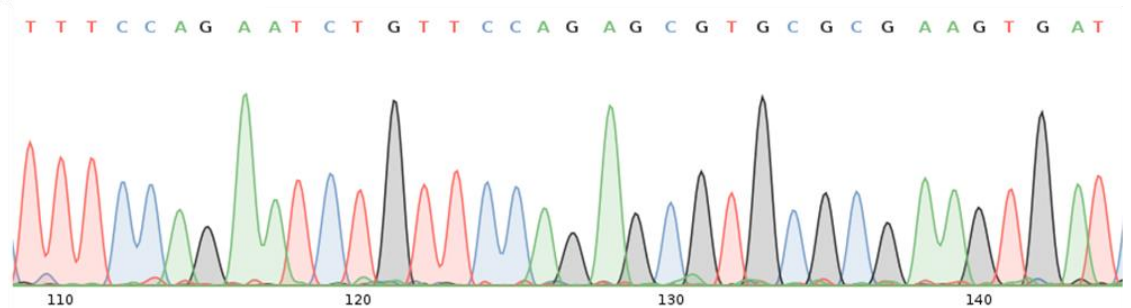
Clone 10



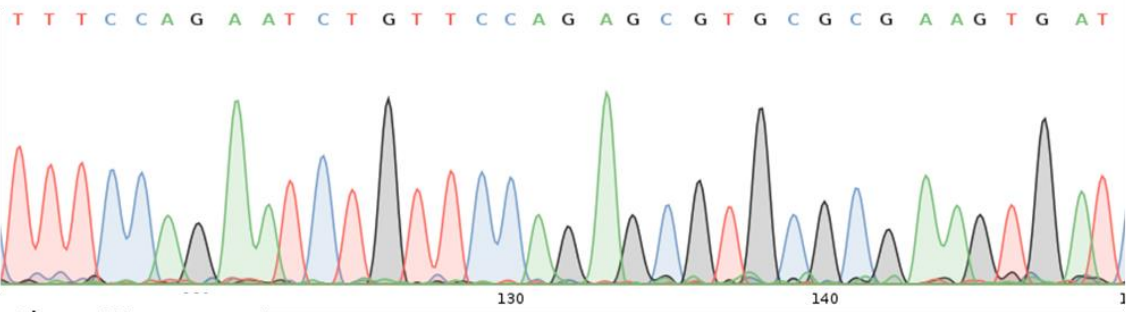
Clone 11



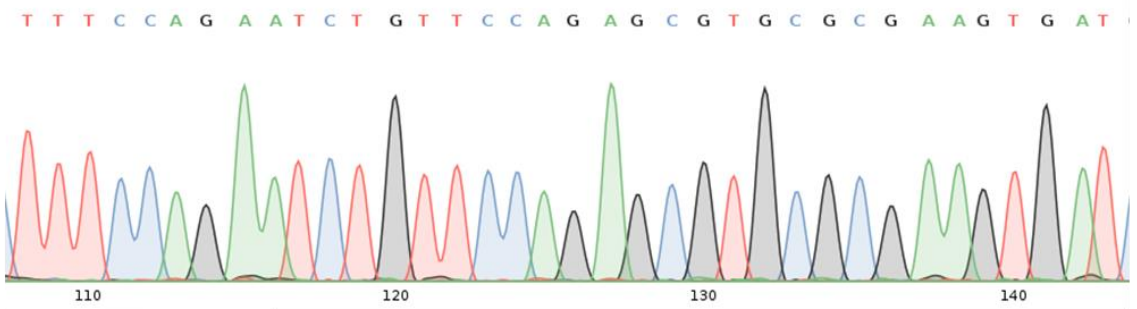
Clone 12



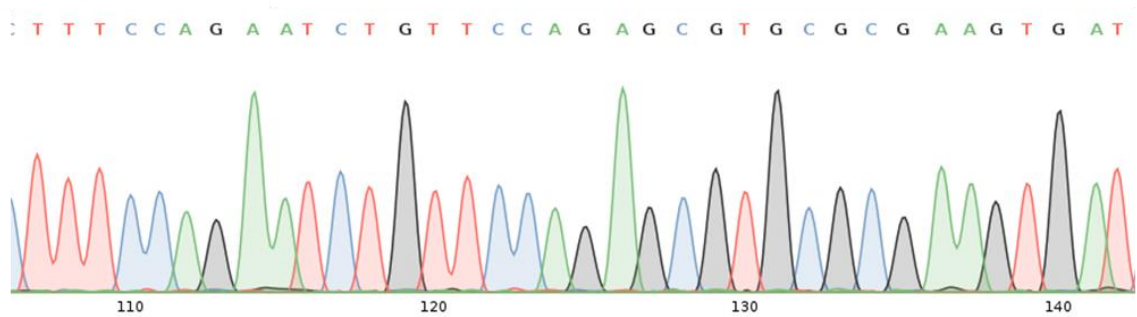
Clone 14



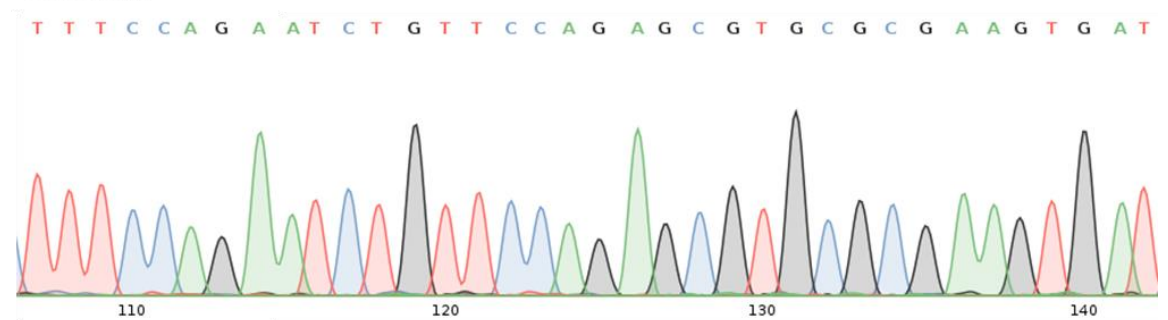
Clone 15



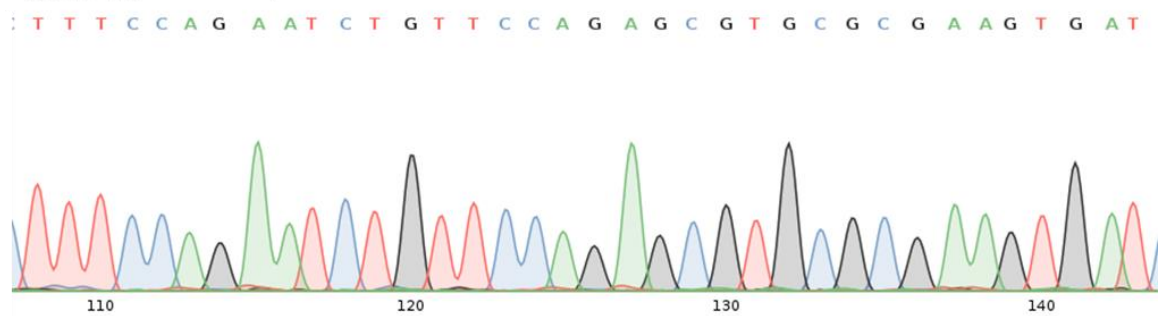
Clone 16



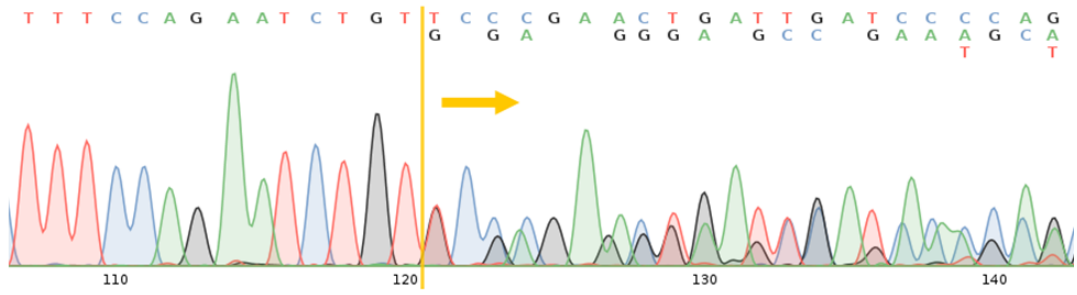
Clone 18



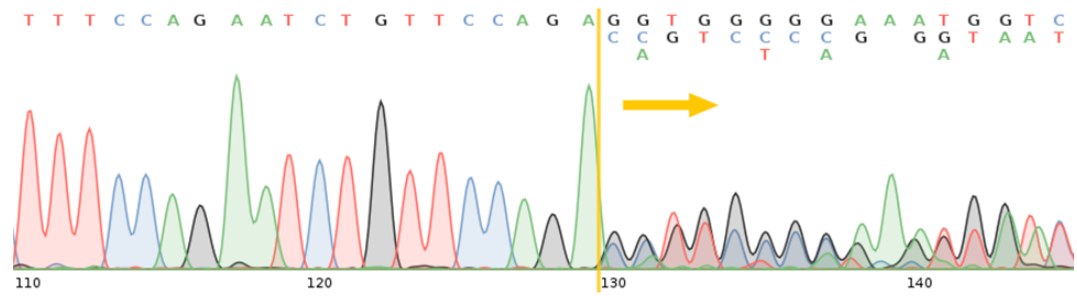
Clone 20



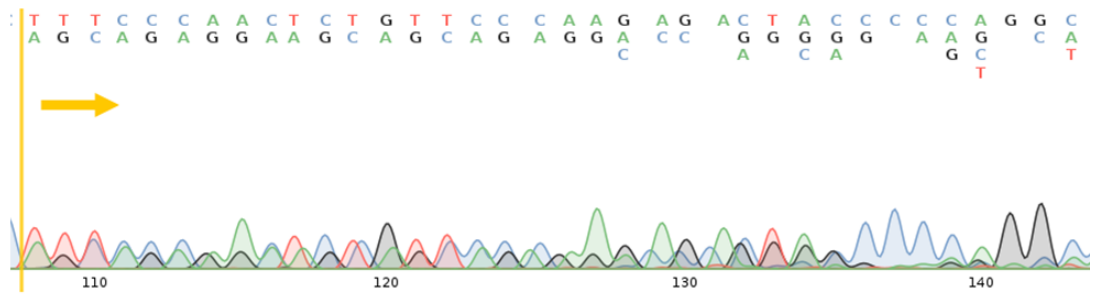
Clone 4



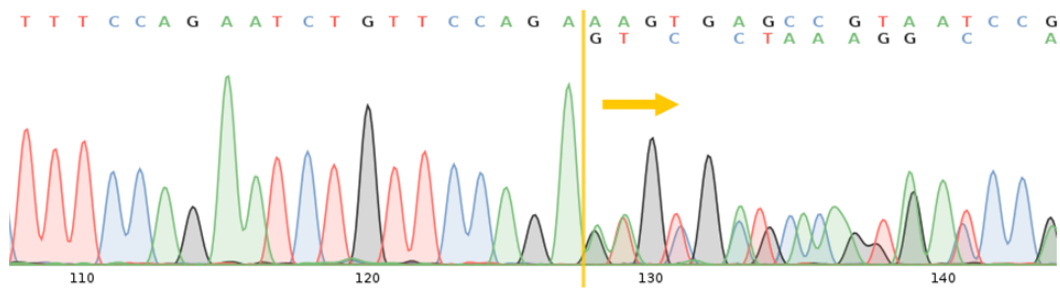
Clone 7



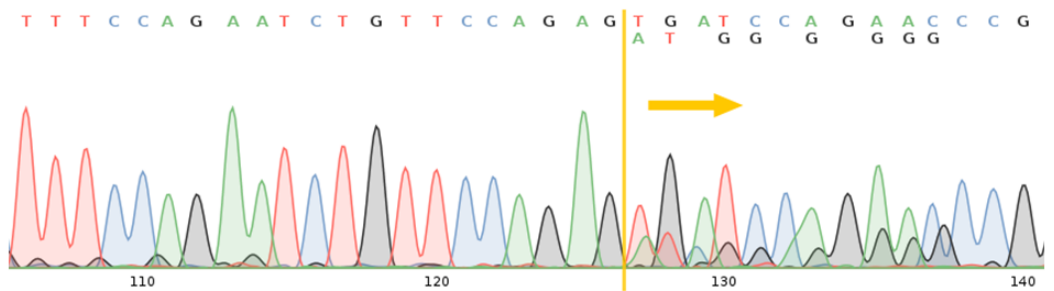
Clone 13



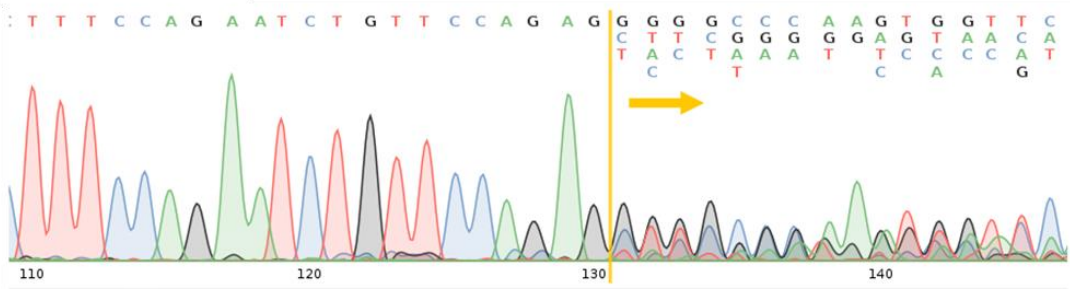
Clone 17



Clone 19



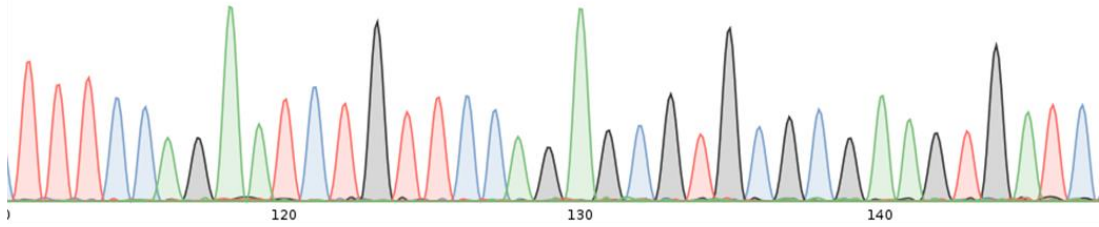
Clone 21



Appendix 2.3 Sequences of P4E6 clones targeted with AR CRISPR/Cas9 lentivirus. Yellow arrow indicates the start of the edit site.

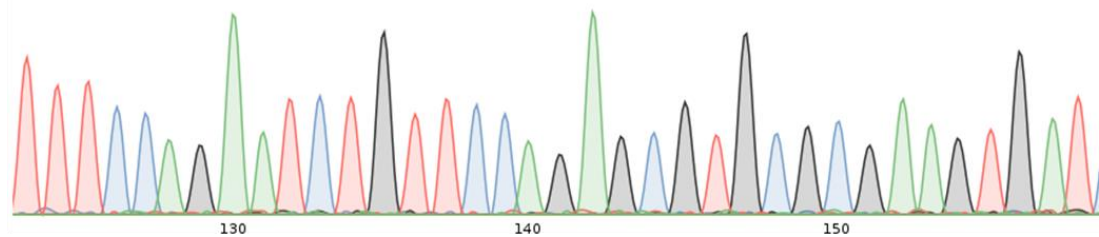
WT

T T T C C A G A A T C T G T T C C A G A G C G T G C G C G A A G T G A T C



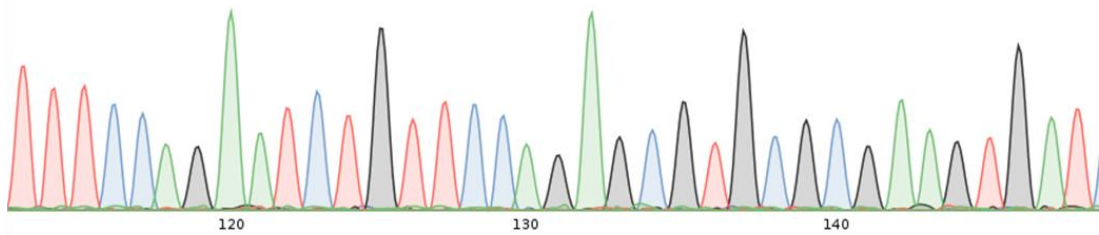
Clone 1

T T T C C A G A A T C T G T T C C A G A G C G T G C G C G A A G T G A T



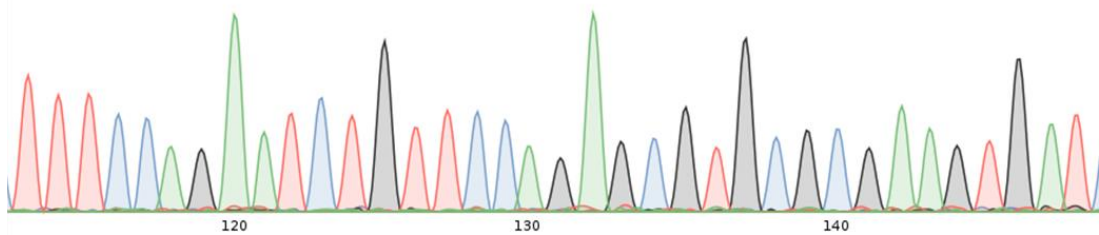
Clone 2

T T T C C A G A A T C T G T T C C A G A G C G T G C G C G A A G T G A T



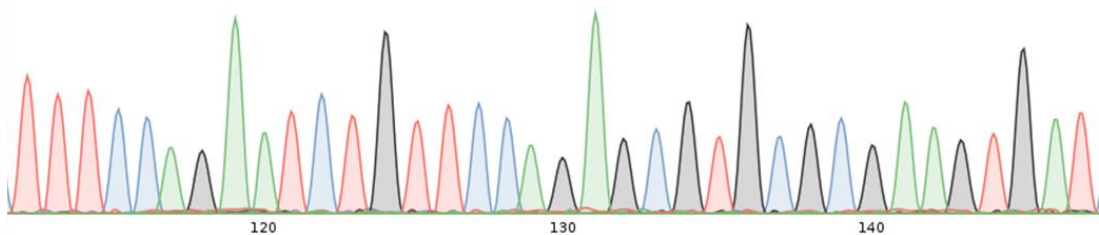
Clone 3

T T T C C A G A A T C T G T T C C A G A G C G T G C G C G A A G T G A T

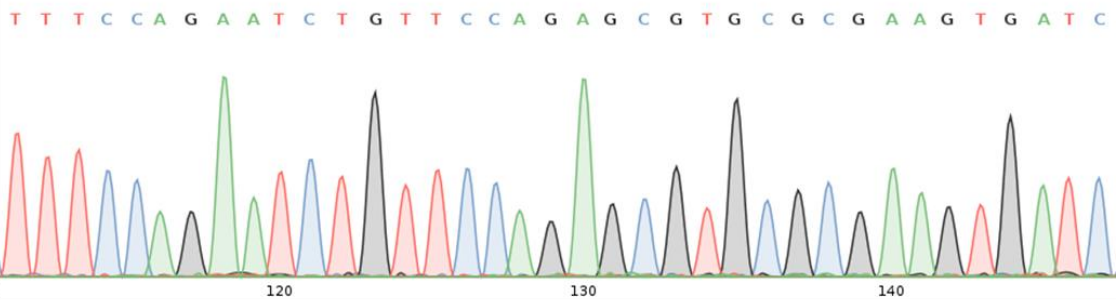


Clone 4

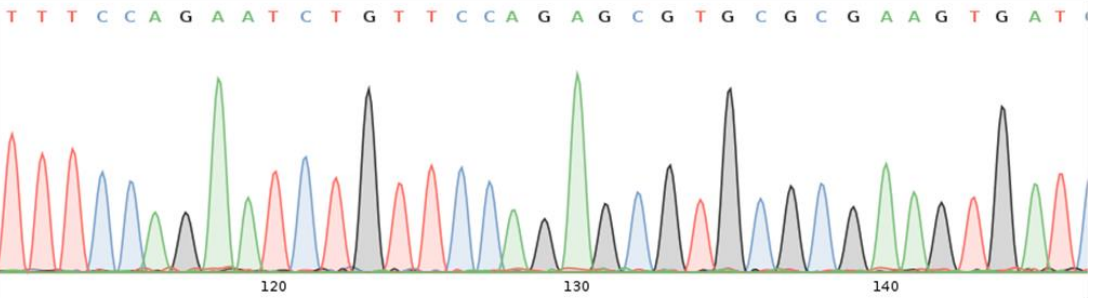
T T T C C A G A A T C T G T T C C A G A G C G T G C G C G A A G T G A T



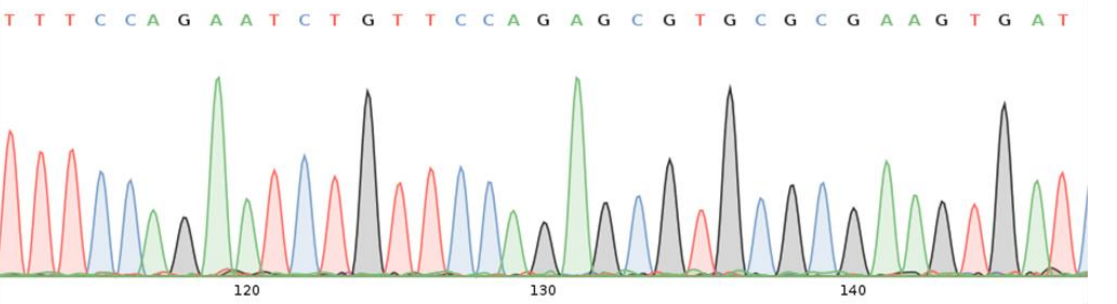
Clone 13



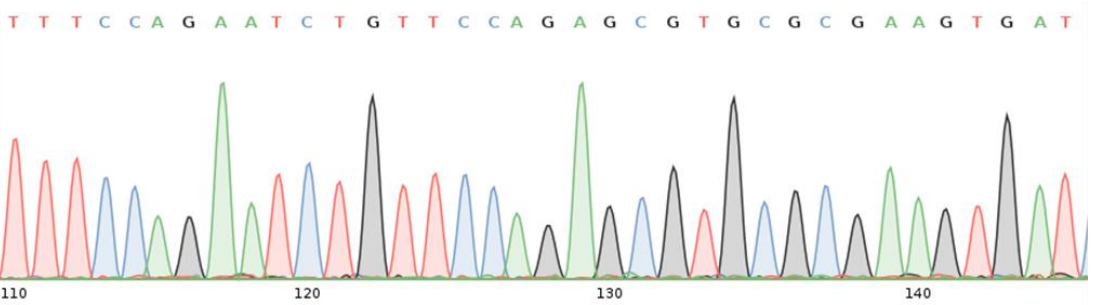
Clone 14



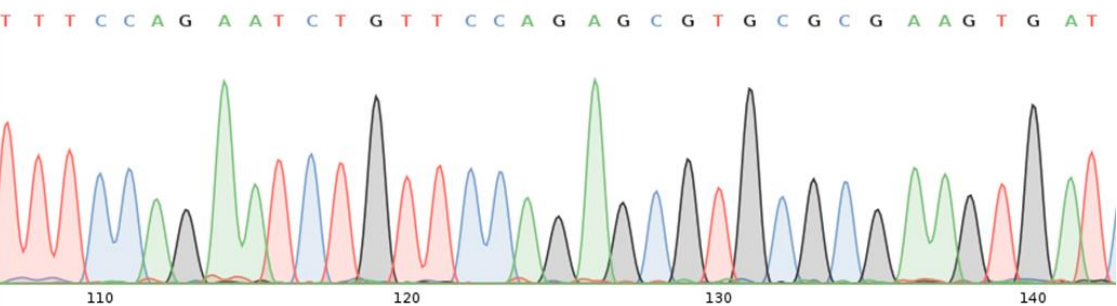
Clone 20



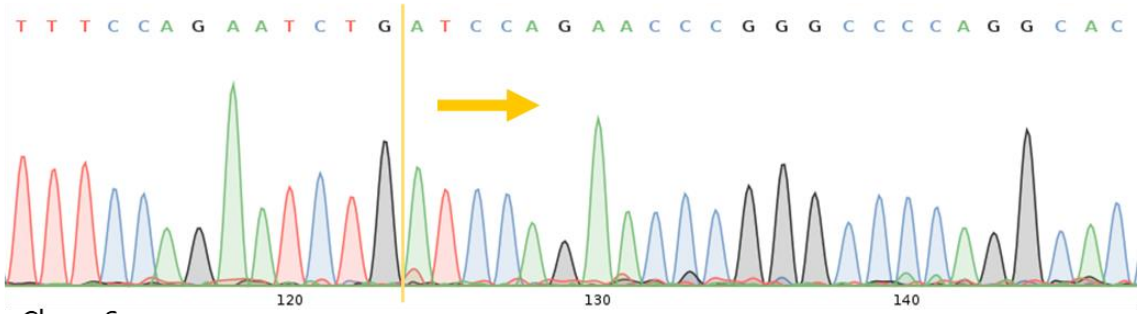
Clone 21



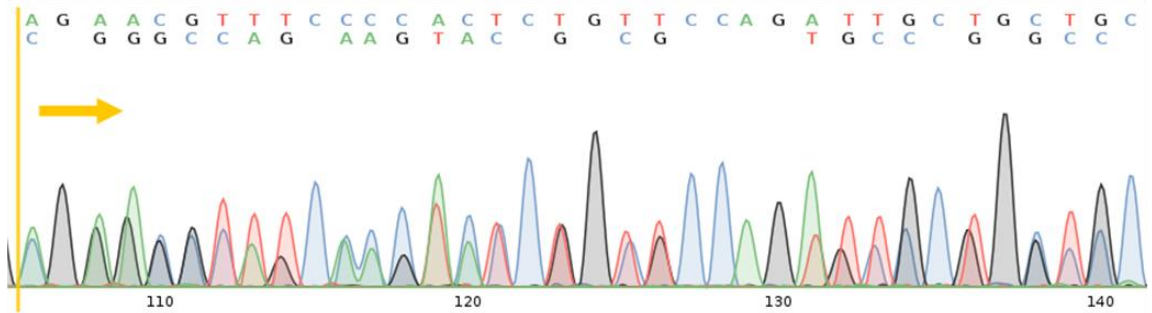
Clone 24



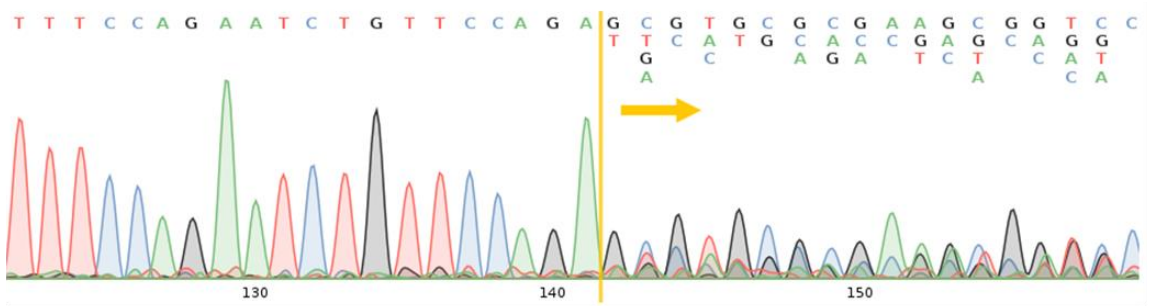
Clone 5



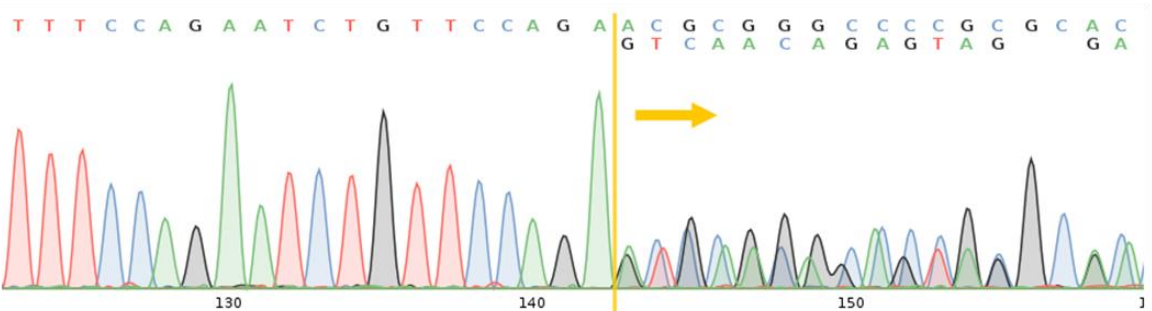
Clone 6



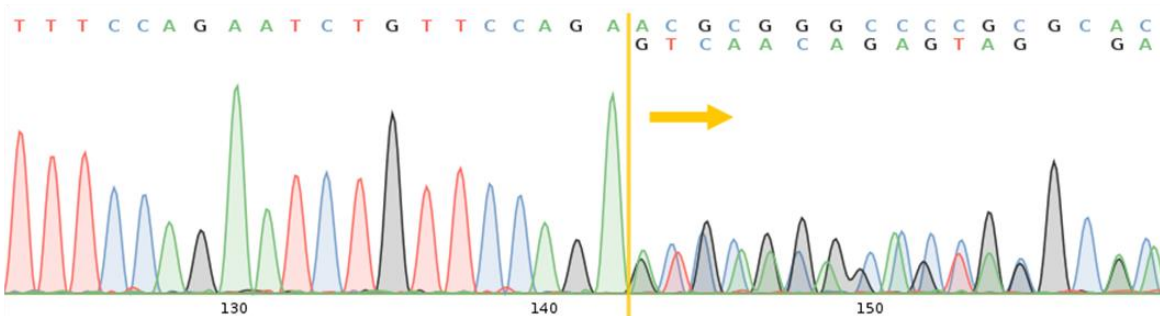
Clone 7



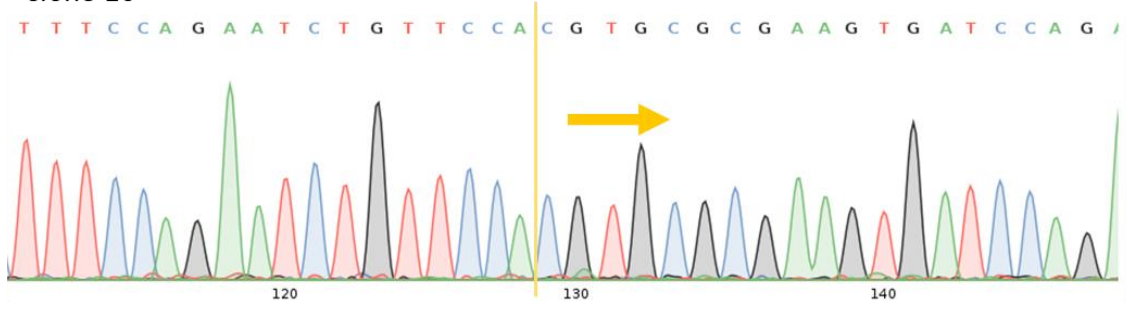
Clone 8



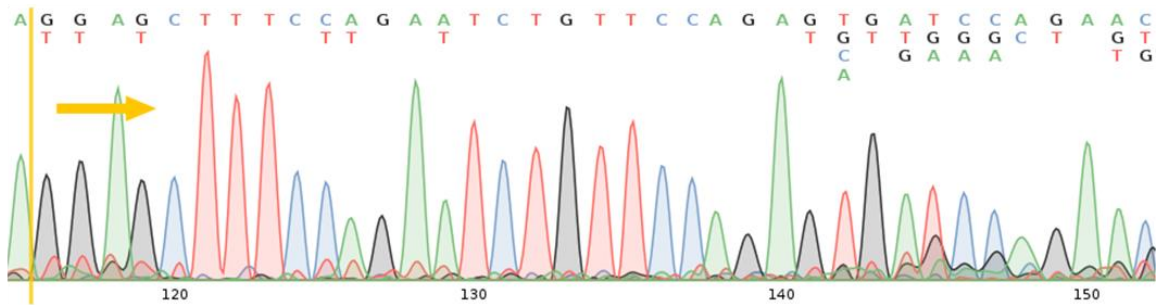
Clone 9



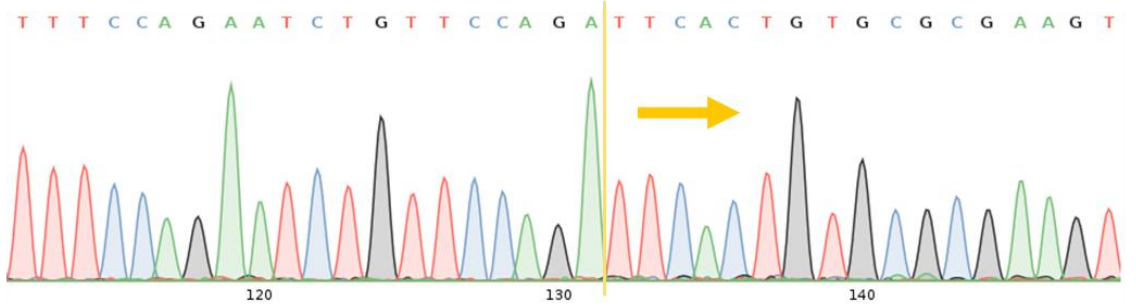
Clone 10



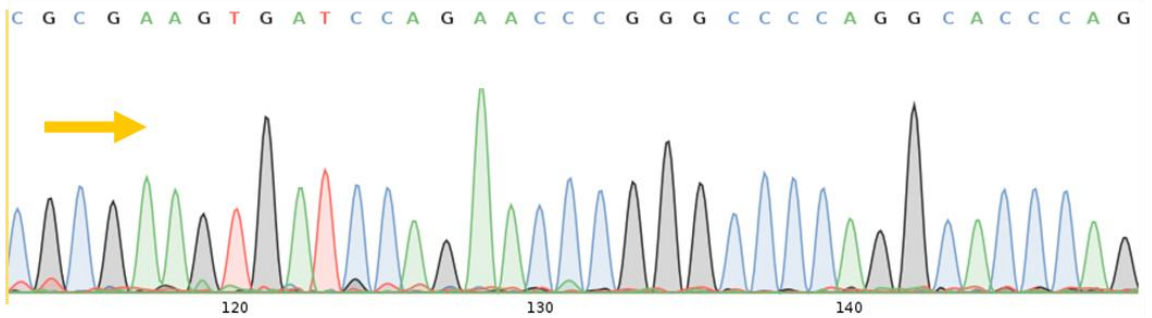
Clone 11



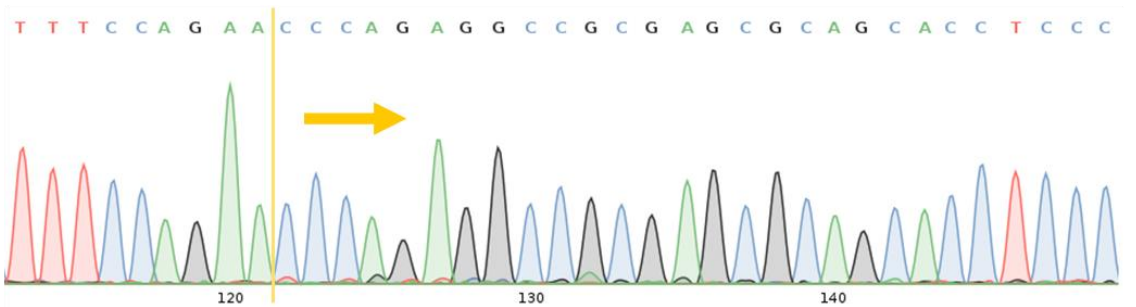
Clone 15



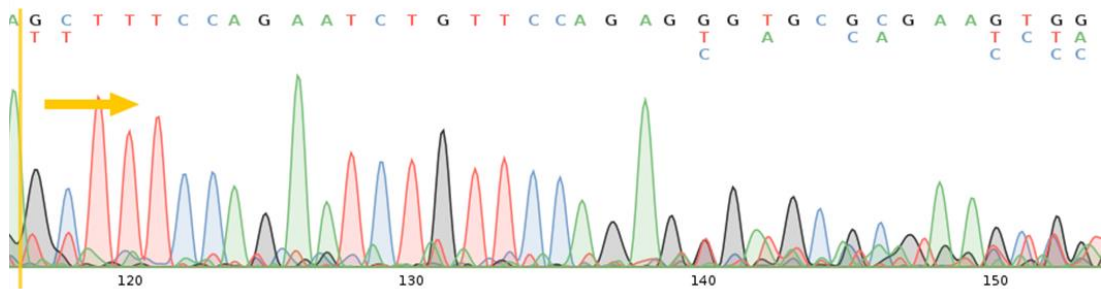
Clone 16



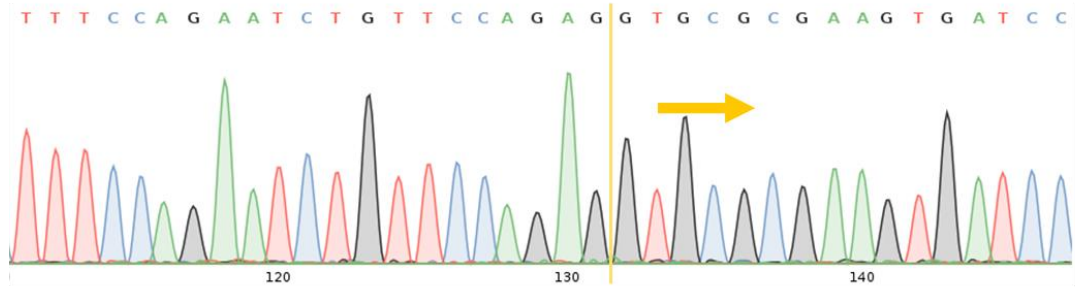
Clone 17



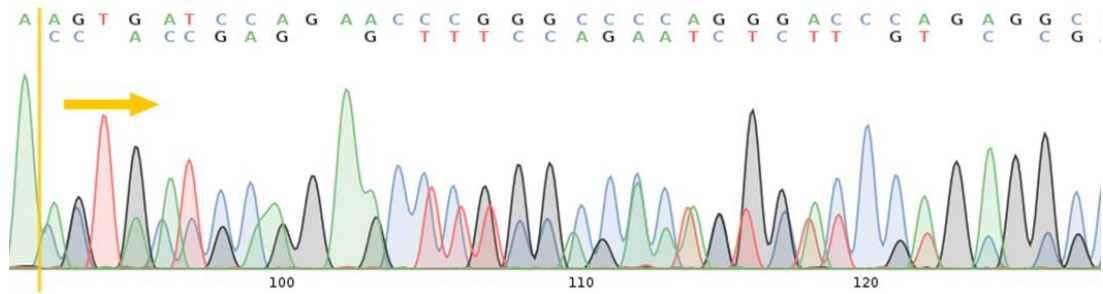
Clone 18



Clone 22



Clone 23



Abbreviations

3D-CRT	3D-dimensional conformal radiation therapy
ADT	Androgen deprivation therapy
ALDH	Aldehyde dehydrogenase
APES	3-aminopropyltriethoxysilane
AR	Androgen receptor
ARE	Androgen response elements
ARVs	AR splice variants
ATCC	American type culture collection
ATP	Adenosine triphosphate
BM	Basement membrane
bp	Base pairs
BPH	Benign prostatic hyperplasia
CaCl ₂	Calcium chloride
CAFs	Carcinoma associated fibroblasts

CAR	Chimeric antigen receptor
CARNs	Castration resistant NKX3.1 expressing cells
CB	Committed basal cells
cDNA	Complementary DNA
CRPC	Castration-resistant prostate cancer
crRNAs	Crispr RNA
CSC	Cancer stem cell
CT	Threshold cycle
D10	DMEM + 10% FCS + 2 mm L-Glutamine
DAB	Diaminobenzidene
DAPI	4',6-diamidino-2-phenylindole
DBD	DNA binding domain
dCas9	"dead" Cas9
DHT	Dihydrotestosterone
DMEM	Dulbecco's modified eagle's medium

DMS	Dimethyl sulfoxide
DNA	Deoxyribonucleic acid
dNTP	Deoxyribonucleotide triphosphate
DSB	Double stranded break
EBRT	External beam radiation therapy
ECL	Enhanced chemiluminescence
ECM	Extracellular matrix
EDTA	Ethylenediaminetetraacetic acid
EGF	Epidermal growth factor
EMT	Epithelial-to-mesenchymal transition
FCS	Foetal calf serum
FGF	Fibroblast growth factor
g	Gram
gDNA	Genomic DNA
GnRH	Gonadotropin-releasing hormone

gRNA	Guide RNA
HDR	Homology-directed repair
HIER	Heat-induced epitope retrieval
HIFU	High-intensity focused ultrasound
HR	Hour
HRP	Horseradish peroxidase
Hsp	Heat shock proteins
ICC	Immunocytochemistry
IGF	Insulin-like growth factor
IHC	Immunohistochemistry
IMRT	Image-guided intensity-modulated radiation therapy
K2	KSFM media + 2% FCS + 2 mm L-Glutamine + BPE + EGF
kDa	Kilo dalton
KGF	Keratin growth factor
KO	Knock-out

KSFM	Keratinocyte serum-free medium
LBD	Ligand-binding domain
LHRH	Luteinising hormone releasing hormone
LT	Large T antigen
M	Molar
mg	Milligram
MgCl ₂	Magnesium chloride
min	Minute
ml	Millilitre
mM	Millimolar
mRNA	Messenger RNA
NE	Neuroendocrine
ng	Nanogram
NHEJ	Non-homologous end joining
nm	Nanometre

NSE	Neurone specific enolase
NTD	Transcriptional activation domain
PAMs	Protospacer adjacent motifs
PAP	Prostatic acid phosphatase
PBS	Phosphate buffered saline
PCa	Prostate cancer
PCR	Polymerase chain reaction
PFA	Paraformaldehyde
PIA	Proliferative inflammatory atrophy
PIN	Prostatic intraepithelial neoplasia
PSA	Prostate specific antigen
qRT-PCR	Quantitative reverse-transcriptase PCR
R10	RPMI + 10% FCS + 2 mm L-Glutamine
R5	RPMI + 5% FCS + 2 mm L-Glutamine
RA	Retinoic acid

RAR	RA receptor
RARE	Retinoic acid response elements
RPM	Revolutions per minute
RPMI	Roswell Park Memorial Institute medium
RT	Reverse transcriptase
RVD	Repeat variable diresidue
RXR	Retinoic X receptors
SC	Stem cell
T25	25cm ² tissue culture flask
T75	75cm ² tissue culture flask
TA	Transit amplifying cells
TALENs	Transcription-activator-like effector nucleases
TALs	Transcription-activator-like effectors
TBST	TBS + tween-20
tracrRNA	Trans-activating RNA

TRUS	Transrectal ultrasound
TURP	Transurethral resection
UGE	Urogenital sinus epithelium
UGM	Urogenital sinus mesenchyme
v/v	Volume per volume
w/v	Weight per volume
WT	Wild type
ZF	Zinc finger
ZFN	Zinc finger nucleases
β -Me	β -mercaptoethanol
μ g	Microgram
μ l	Microlitre
μ m	Micrometre
μ M	Micromolar

References

- ACKERMAN, C. M., LOWE, L. P., LEE, H., HAYES, M. G., DYER, A. R., METZGER, B. E., LOWE, W. L., URBANEK, M. & HAPO STUDY COOPERATIVE RESEARCH, G. 2012. Ethnic variation in allele distribution of the androgen receptor (AR) (CAG)_n repeat. *J Androl*, 33, 210-5.
- ADCOCK, A., TRIVEDI, G., EDMONDSON, R., SPEARMAN, C. & YANG, L. 2015. Three-Dimensional (3D) Cell Cultures in Cell-based Assays for in-vitro Evaluation of Anticancer Drugs. *Journal of Analytical & Bioanalytical Techniques*, 6.
- AGARWAL, S., HYNES, P. G., TILLMAN, H. S., LAKE, R., ABOU-KHEIR, W. G., FANG, L., CASEY, O. M., AMERI, A. H., MARTIN, P. L., YIN, J. J., IAQUINTA, P. J., KARTHAUS, W. R., CLEVERS, H. C., SAWYERS, C. L. & KELLY, K. 2015. Identification of Different Classes of Luminal Progenitor Cells within Prostate Tumors. *Cell Reports*, 13, 2147-2158.
- AHRENS-FATH, I., POLITZ, O., GESERICK, C. & HAENDLER, B. 2005. Androgen receptor function is modulated by the tissue-specific AR45 variant. *Febs Journal*, 272, 74-84.
- AL-HAJJ, M., BECKER, M. W., WICHA, M., WEISSMAN, I. & CLARKE, M. F. 2004. Therapeutic implications of cancer stem cells. *Curr Opin Genet Dev*, 14, 43-7.
- ANTON, T. & BULTMANN, S. 2017. Site-specific recruitment of epigenetic factors with a modular CRISPR/Cas system. *Nucleus*, 8, 279-286.
- ARCHER, L. K., FRAME, F. M. & MAITLAND, N. J. 2017. Stem cells and the role of ETS transcription factors in the differentiation hierarchy of normal and malignant prostate epithelium. *J Steroid Biochem Mol Biol*, 166, 68-83.
- ASIM, M., BIN HAFEEZ, B., SIDDIQUI, I. A., GERLACH, C., PATZ, M., MUKHTAR, H. & BANIAHMAD, A. 2011. Ligand-dependent Corepressor Acts as a Novel Androgen Receptor Corepressor, Inhibits Prostate Cancer Growth, and Is Functionally Inactivated by the Src Protein Kinase. *Journal of Biological Chemistry*, 286, 37108-37117.
- BACA, S. C., PRANDI, D., LAWRENCE, M. S., MOSQUERA, J. M., ROMANEL, A., DRIER, Y., PARK, K., KITABAYASHI, N., MACDONALD, T. Y., GHANDI, M., VAN ALLEN, E., KRYUKOV, G. V., SBONER, A., THEURILLAT, J. P., SOONG, T. D., NICKERSON, E., AUCLAIR, D., TEWARI, A., BELTRAN, H., ONOFRIO, R. C., BOYSEN, G., GUIDUCCI, C., BARBIERI, C. E., CIBULSKIS, K., SIVACHENKO, A., CARTER, S. L., SAKSENA, G., VOET, D., RAMOS, A. H., WINCKLER, W., CIPICCHIO, M., ARDLIE, K., KANTOFF, P. W., BERGER, M. F., GABRIEL, S. B., GOLUB, T. R., MEYERSON, M., LANDER, E. S., ELEMENTO, O., GETZ, G., DEMICHELIS, F., RUBIN, M. A. & GARRAWAY, L. A. 2013. Punctuated evolution of prostate cancer genomes. *Cell*, 153, 666-77.
- BARSKY, S., SIEGAL, G., JANNOTTA, F., LIOTTA, L. 1983. Loss of basement membrane components by invasive tumors but not by their benign counterparts. *Lab Invest.*, 42, 140-147.
- BATLLE, E. & CLEVERS, H. 2017. Cancer stem cells revisited. *Nat Med*, 23, 1124-1134.
- BAUMAN, G., RUMBLE, R. B., CHEN, J., LOBLAW, A., WARDE, P. & MEMBERS OF THE, I. I. E. P. 2012. Intensity-modulated radiotherapy in the treatment of prostate cancer. *Clin Oncol (R Coll Radiol)*, 24, 461-73.

- BELLO-DEOCAMPO, D., KLEINMAN, H. K., DEOCAMPO, N. D. & WEBBER, M. M. 2001. Laminin-1 and alpha6beta1 integrin regulate acinar morphogenesis of normal and malignant human prostate epithelial cells. *Prostate*, 46, 142-53.
- BELTRAN, H., BEER, T. M., CARDUCCI, M. A., DE BONO, J., GLEAVE, M., HUSSAIN, M., KELLY, W. K., SAAD, F., STERNBERG, C., TAGAWA, S. T. & TANNOCK, I. F. 2011. New therapies for castration-resistant prostate cancer: efficacy and safety. *Eur Urol*, 60, 279-90.
- BERGER, R., FEBBO, P. G., MAJUMDER, P. K., ZHAO, J. J., MUKHERJEE, S., SIGNORETTI, S., CAMPBELL, K. T., SELLERS, W. R., ROBERTS, T. M., LODA, M., GOLUB, T. R. & HAHN, W. C. 2004. Androgen-induced differentiation and tumorigenicity of human prostate epithelial cells. *Cancer Res*, 64, 8867-75.
- BERRY, P. A., MAITLAND, N. J. & COLLINS, A. T. 2008. Androgen receptor signalling in prostate: effects of stromal factors on normal and cancer stem cells. *Mol Cell Endocrinol*, 288, 30-7.
- BERTHON, P., WALLER, A. S., VILLETTE, J. M., LORIDON, L., CUSSENOT, O. & MAITLAND, N. J. 1997. Androgens are not a direct requirement for the proliferation of human prostatic epithelium in vitro. *International Journal of Cancer*, 73, 910-916.
- BIBIKOVA, M., CARROLL, D., SEGAL, D. J., TRAUTMAN, J. K., SMITH, J., KIM, Y. G. & CHANDRASEGARAN, S. 2001. Stimulation of homologous recombination through targeted cleavage by chimeric nucleases. *Molecular and Cellular Biology*, 21, 289-297.
- BIKARD, D., JIANG, W. Y., SAMAI, P., HOCHSCHILD, A., ZHANG, F. & MARRAFFINI, L. A. 2013. Programmable repression and activation of bacterial gene expression using an engineered CRISPR-Cas system. *Nucleic Acids Research*, 41, 7429-7437.
- BOCH, J. & BONAS, U. 2010. Xanthomonas AvrBs3 Family-Type III Effectors: Discovery and Function. *Annual Review of Phytopathology, Vol 48*, 48, 419-436.
- BOCH, J., SCHOLZE, H., SCHORNACK, S., LANDGRAF, A., HAHN, S., KAY, S., LAHAYE, T., NICKSTADT, A. & BONAS, U. 2009. Breaking the Code of DNA Binding Specificity of TAL-Type III Effectors. *Science*, 326, 1509-1512.
- BONKHOF, H. & REMBERGER, K. 1993. Widespread Distribution of Nuclear Androgen Receptors in the Basal-Cell Layer of the Normal and Hyperplastic Human Prostate. *Virchows Archiv a-Pathological Anatomy and Histopathology*, 422, 35-38.
- BONNET, D. & DICK, J. E. 1997. Human acute myeloid leukemia is organized as a hierarchy that originates from a primitive hematopoietic cell. *Nature Medicine*, 3, 730-737.
- BOUKAMP, P., PETRUSSEVSKA, R. T., BREITKREUTZ, D., HORNUNG, J., MARKHAM, A. & FUSENIG, N. E. 1988. Normal Keratinization in a Spontaneously Immortalized Aneuploid Human Keratinocyte Cell-Line. *Journal of Cell Biology*, 106, 761-771.
- BRINKMANN, V., FOROUTAN, H., SACHS, M., WEIDNER, K. M. & BIRCHMEIER, W. 1995. Hepatocyte Growth-Factor Scatter Factor Induces a Variety of Tissue-Specific Morphogenic Programs in Epithelial-Cells. *Journal of Cell Biology*, 131, 1573-1586.

- BRYANT, S. L., FRANCIS, J. C., LOKODY, I. B., WANG, H., RISBRIDGER, G. P., LOVELAND, K. L. & SWAIN, A. 2014. Sex specific retinoic acid signaling is required for the initiation of urogenital sinus bud development. *Developmental Biology*, 395, 209-217.
- CANCER RESEARCH UK. Available: <https://www.cancerresearchuk.org/health-professional/cancer-statistics/statistics-by-cancer-type/prostate-cancer> [Accessed 29/07/2018].
- CARROLL, D. 2011. Genome Engineering With Zinc-Finger Nucleases. *Genetics*, 188, 773-782.
- CHAN, C. H., GODINHO, L. N., THOMAIDOU, D., TAN, S. S., GULISANO, M. & PARNAVELAS, J. G. 2001. Emx1 is a marker for pyramidal neurons of the cerebral cortex. *Cerebral Cortex*, 11, 1191-1198.
- CHEN, N. & ZHOU, Q. 2016. The evolving Gleason grading system. *Chin J Cancer Res*, 28, 58-64.
- CHEN, S. D., SANJANA, N. E., ZHENG, K. J., SHALEM, O., LEE, K., SHI, X., SCOTT, D. A., SONG, J., PAN, J. Q., WEISSLEDER, R., LEE, H., ZHANG, F. & SHARP, P. A. 2015. Genome-wide CRISPR Screen in a Mouse Model of Tumor Growth and Metastasis. *Cell*, 160, 1246-1260.
- CHEN, Y. M., CANG, S. D., HAN, L. Y., LIU, C., YANG, P., SOLANGI, Z., LU, Q. Y., LIU, D. L. & CHIAO, J. W. 2016. Establishment of prostate cancer spheres from a prostate cancer cell line after phenethyl isothiocyanate treatment and discovery of androgen-dependent reversible differentiation between sphere and neuroendocrine cells. *Oncotarget*, 7, 26567-26579.
- CHOO, Y. & KLUG, A. 1994. Selection of DNA-Binding Sites for Zinc Fingers Using Rationally Randomized DNA Reveals Coded Interactions. *Proceedings of the National Academy of Sciences of the United States of America*, 91, 11168-11172.
- CHUA, C. W., EPSI, N. J., LEUNG, E. Y., XUAN, S. H., LEI, M., LI, B. I., BERGREN, S. K., HIBSHOOSH, H., MITROFANOVA, A. & SHEN, M. M. 2018. Differential requirements of androgen receptor in luminal progenitors during prostate regeneration and tumor initiation. *Elife*, 7.
- CHUA, C. W., SHIBATA, M., LEI, M., TOIVANEN, R., BARLOW, L. J., BERGREN, S. K., BADANI, K. K., MC KIERNAN, J. M., BENSON, M. C., HIBSHOOSH, H. & SHEN, M. M. 2014. Single luminal epithelial progenitors can generate prostate organoids in culture. *Nature Cell Biology*, 16, 951-961.
- CLARK, J., MERSON, S., JHAVAR, S., FLOHR, P., EDWARDS, S., FOSTER, C. S., EELES, R., MARTIN, F. L., PHILLIPS, D. H., CRUNDWELL, M., CHRISTMAS, T., THOMPSON, A., FISHER, C., KOVACS, G. & COOPER, C. S. 2007. Diversity of TMPRSS2-ERG fusion transcripts in the human prostate. *Oncogene*, 26, 2667-2673.
- CLEGG, N. J., WONGVIPAT, J., JOSEPH, J. D., TRAN, C., OUK, S., DILHAS, A., CHEN, Y., GRILLOT, K., BISCHOFF, E. D., CAL, L., APARICIO, A., DOROW, S., ARORA, V., SHAO, G., QIAN, J., ZHAO, H., YANG, G. B., CAO, C. Y., SENSINTAFFAR, J., WASIELEWSKA, T., HERBERT, M. R., BONNEFOUS, C., DARIMONT, B., SCHER, H. I., SMITH-JONES, P., KLANG, M., SMITH, N. D., DE STANCHINA, E., WU, N., OUFELLI, O., RIX, P. J., HEYMAN, R. A., JUNG, M. E., SAWYERS, C. L. & HAGER, J. H. 2012. ARN-509: A Novel Antiandrogen for Prostate Cancer Treatment. *Cancer Research*, 72, 1494-1503.

- CLEMONS, J., GLODE, L. M., GAO, D. X. & FLAIG, T. W. 2013. Low-dose diethylstilbestrol for the treatment of advanced prostate cancer. *Urologic Oncology-Seminars and Original Investigations*, 31, 198-204.
- COHEN, J. K. & MILLER, R. J. 1994. Thermal Protection of Urethra during Cryosurgery of Prostate. *Cryobiology*, 31, 313-316.
- COLLINS, A. T., BERRY, P. A., HYDE, C., STOWER, M. J. & MAITLAND, N. J. 2005. Prospective identification of tumorigenic prostate cancer stem cells. *Cancer Research*, 65, 10946-10951.
- DART, D. A., WAXMAN, J., ABOAGYE, E. O. & BEVAN, C. L. 2013. Visualising androgen receptor activity in male and female mice. *PLoS One*, 8, e71694.
- DE BONO, J. S., LOGOTHETIS, C. J., MOLINA, A., FIZAZI, K., NORTH, S., CHU, L., CHI, K. N., JONES, R. J., GOODMAN, O. B., SAAD, F., STAFFURTH, J. N., MAINWARING, P., HARLAND, S., FLAIG, T. W., HUTSON, T. E., CHENG, T., PATTERSON, H., HAINSWORTH, J. D., RYAN, C. J., STERNBERG, C. N., ELLARD, S. L., FLECHON, A., SALEH, M., SCHOLZ, M., EFSTATHIOU, E., ZIVI, A., BIANCHINI, D., LORIOT, Y., CHIEFFO, N., KHEOH, T., HAQQ, C. M., SCHER, H. I. & INVESTIGATORS, C.-A.-. 2011. Abiraterone and Increased Survival in Metastatic Prostate Cancer. *New England Journal of Medicine*, 364, 1995-2005.
- DE LA TAILLE, A., HAYEK, O., BENSON, M. C., BAGIELLA, E., OLSSON, C. A., FATAL, M. & KATZ, A. E. 2000. Salvage cryotherapy for recurrent prostate cancer after radiation therapy: the Columbia experience. *Urology*, 55, 79-84.
- DECAPRIO, J. A., LUDLOW, J. W., FIGGE, J., SHEW, J. Y., HUANG, C. M., LEE, W. H., MARSILIO, E., PAUCHA, E. & LIVINGSTON, D. M. 1988. SV40 large tumor antigen forms a specific complex with the product of the retinoblastoma susceptibility gene. *Cell*, 54, 275-83.
- DEHAIRS, J., TALEBI, A., CHERIFI, Y. & SWINNEN, J. V. 2016. CRISP-ID: decoding CRISPR mediated indels by Sanger sequencing. *Sci Rep*, 6, 28973.
- DERMER, G. B. 1978. Basal cell proliferation in benign prostatic hyperplasia. *Cancer*, 41, 1857-62.
- DESHAYES, E., ROUMIGUIE, M., THIBAUT, C., BEUZEBOC, P., CACHIN, F., HENNEQUIN, C., HUGLO, D., ROZET, F., KASSAB-CHAHMI, D., REBILLARD, X. & HOUEDE, N. 2017. Radium 223 dichloride for prostate cancer treatment. *Drug Des Devel Ther*, 11, 2643-2651.
- DI SANT'AGNESE, P. A. 1998. Neuroendocrine cells of the prostate and neuroendocrine differentiation in prostatic carcinoma: A review of morphologic aspects. *Urology*, 51, 121-124.
- ERAMO, A., LOTTI, F., SETTE, G., PILOZZI, E., BIFFONI, M., DI VIRGILIO, A., CONTICELLO, C., RUCO, L., PESCHLE, C. & DE MARIA, R. 2008. Identification and expansion of the tumorigenic lung cancer stem cell population. *Cell Death Differ*, 15, 504-14.
- FRAME, F., NOBLE, A., KLEIN, S., WALKER, H., SUMAN, R., KASPROWICZ, R., MANN, V., SIMMS, M. & MAITLAND, N. 2017. Tumor heterogeneity and therapy resistance - implications for future treatments of prostate cancer. *J Cancer Metastasis Treat* 3, 302-314.
- FRAME, F., PELLACANI, D., COLLINS, A. T., SIMMS, M. S., MANN, V. M., JONES, G. D., MEUTH, M., BRISTOW, R. G. & MAITLAND, N. J. 2013. HDAC inhibitor confers radiosensitivity to prostate stem-like cells. *Br J Cancer*, 109, 3023-33.

- FRAME, F. M., HAGER, S., PELLACANI, D., STOWER, M. J., WALKER, H. F., BURNS, J. E., COLLINS, A. T. & MAITLAND, N. J. 2010. Development and limitations of lentivirus vectors as tools for tracking differentiation in prostate epithelial cells. *Experimental Cell Research*, 316, 3161-3171.
- GADDIPATI, J. P., MCLEOD, D. G., HEIDENBERG, H. B., SESTERHENN, I. A., FINGER, M. J., MOUL, J. W. & SRIVASTAVA, S. 1994. Frequent detection of codon 877 mutation in the androgen receptor gene in advanced prostate cancers. *Cancer Res*, 54, 2861-4.
- GLEASON, D. 1966. Classification of prostatic carcinomas. . *Cancer Chemother reports*, 50, 125-128.
- GOLDSTEIN, A. S., HUANG, J. T., GUO, C. Y., GARRAWAY, I. P. & WITTE, O. N. 2010. Identification of a Cell of Origin for Human Prostate Cancer. *Science*, 329, 568-571.
- GOTTLIEB, B., BEITEL, L. K., NADARAJAH, A., PALIOURAS, M. & TRIFIRO, M. 2012. The Androgen Receptor Gene Mutations Database: 2012 Update. *Human Mutation*, 33, 887-894.
- GREY, B. R., OATES, J. E., BROWN, M. D. & CLARKE, N. W. 2009. Cd133: A Marker of Transit Amplification Rather Than Stem Cell Phenotype in the Prostate? *Bju International*, 103, 856-858.
- GUZMAN-RAMIREZ, N., VOLLER, M., WETTERWALD, A., GERMANN, M., CROSS, N. A., RENTSCH, C. A., SCHALKEN, J., THALMANN, G. N. & CECCHINI, M. G. 2009. In Vitro Propagation and Characterization of Neoplastic Stem/Progenitor-Like Cells From Human Prostate Cancer Tissue. *Prostate*, 69, 1683-1693.
- HANAHAH, D. & WEINBERG, R. A. 2011. Hallmarks of Cancer: The Next Generation. *Cell*, 144, 646-674.
- HAYWARD, S. W., DAHIYA, R., CUNHA, G. R., BARTEK, J., DESHPANDE, N. & NARAYAN, P. 1995. Establishment and characterization of an immortalized but non-transformed human prostate epithelial cell line: BPH-1. *In Vitro Cell Dev Biol Anim*, 31, 14-24.
- HAYWARD, S. W., WANG, Y., CAO, M., HOM, Y. K., ZHANG, B., GROSSFELD, G. D., SUDILOVSKY, D. & CUNHA, G. R. 2001. Malignant transformation in a nontumorigenic human prostatic epithelial cell line. *Cancer Res*, 61, 8135-42.
- HE, W. W., SCIAVOLINO, P. J., WING, J., AUGUSTUS, M., HUDSON, P., MEISSNER, P. S., CURTIS, R. T., SHELL, B. K., BOSTWICK, D. G., TINDALL, D. J., GELMANN, E. P., ABATESHEN, C. & CARTER, K. C. 1997. A novel human prostate-specific, androgen-regulated homeobox gene (NKX3.1) that maps to 8p21, a region frequently deleted in prostate cancer. *Genomics*, 43, 69-77.
- HEIDENREICH, A., BASTIAN, P. J., BELLMUNT, J., BOLLA, M., JONIAU, S., VAN DER KWAST, T., MASON, M., MATVEEV, V., WIEGEL, T., ZATTONI, F. & MOTTET, N. 2014. EAU Guidelines on Prostate Cancer. Part 1: Screening, Diagnosis, and Local Treatment with Curative Intent-Update 2013. *European Urology*, 65, 124-137.
- HENDRIKS, W. T., WARREN, C. R. & COWAN, C. A. 2016. Genome Editing in Human Pluripotent Stem Cells: Approaches, Pitfalls, and Solutions. *Cell Stem Cell*, 18, 53-65.

- HENNINGS, H., MICHAEL, D., CHENG, C., STEINERT, P., HOLBROOK, K. & YUSPA, S. H. 1980. Calcium regulation of growth and differentiation of mouse epidermal cells in culture. *Cell*, 19, 245-54.
- HENSHALL, S. M., QUINN, D. I., LEE, C. S., HEAD, D. R., GOLOVSKY, D., BRENNER, P. C., DELPRADO, W., STRICKER, P. D., GRYGIEL, J. J. & SUTHERLAND, R. L. 2001. Altered expression of androgen receptor in the malignant epithelium and adjacent stroma is associated with early relapse in prostate cancer. *Cancer Research*, 61, 423-427.
- HILLE, F. & CHARPENTIER, E. 2016. CRISPR-Cas: biology, mechanisms and relevance. *Philos Trans R Soc Lond B Biol Sci*, 371.
- HILTON, I. B., D'IPPOLITO, A. M., VOCKLEY, C. M., THAKORE, P. I., CRAWFORD, G. E., REDDY, T. E. & GERSBACH, C. A. 2015. Epigenome editing by a CRISPR-Cas9-based acetyltransferase activates genes from promoters and enhancers. *Nature Biotechnology*, 33, 510-U225.
- HIRST, C. J., CABRERA, C. & KIRBY, M. 2012. Epidemiology of castration resistant prostate cancer: A longitudinal analysis using a UK primary care database. *Cancer Epidemiology*, 36, E349-E353.
- HOFFMAN, R. M., GILLILAND, F. D., ADAMS-CAMERON, M., HUNT, W. C. & KEY, C. R. 2002. Prostate-specific antigen testing accuracy in community practice. *BMC Fam Pract*, 3, 19.
- HORNBERG, E., YLITALO, E. B., CRNALIC, S., ANTTI, H., STATTIN, P., WIDMARK, A., BERGH, A. & WIKSTROM, P. 2011. Expression of Androgen Receptor Splice Variants in Prostate Cancer Bone Metastases is Associated with Castration-Resistance and Short Survival. *Plos One*, 6.
- HOROSZEWICZ, J. S., LEONG, S. S., KAWINSKI, E., KARR, J. P., ROSENTHAL, H., CHU, T. M., MIRAND, E. A. & MURPHY, G. P. 1983. Lncap Model of Human Prostatic Carcinoma. *Cancer Research*, 43, 1809-1818.
- HU, J., WANG, G. & SUN, T. 2017. Dissecting the roles of the androgen receptor in prostate cancer from molecular perspectives. *Tumour Biol*, 39, 1010428317692259.
- HU, R., DUNN, T. A., WEI, S. Z., ISHARWAL, S., VELTRI, R. W., HUMPHREYS, E., HAN, M., PARTIN, A. W., VESSELLA, R. L., ISAACS, W. B., BOVA, G. S. & LUO, J. 2009. Ligand-Independent Androgen Receptor Variants Derived from Splicing of Cryptic Exons Signify Hormone-Refractory Prostate Cancer. *Cancer Research*, 69, 16-22.
- HUANG, L. F., YUAN, Z. J., LIU, P. J. & ZHOU, T. S. 2015. Effects of promoter leakage on dynamics of gene expression. *Bmc Systems Biology*, 9.
- HUDSON, D. L., GUY, A. T., FRY, P., O'HARE, M. J., WATT, F. M. & MASTERS, J. R. W. 2001. Epithelial cell differentiation pathways in the human prostate: Identification of intermediate phenotypes by keratin expression. *Journal of Histochemistry & Cytochemistry*, 49, 271-278.
- HUGGINS, M. L. 1941. A New Society for X-Ray and Electron Diffraction Research Workers. *Science*, 93, 489-90.
- ISAACS, J. T. & COFFEY, D. S. 1989. Etiology and disease process of benign prostatic hyperplasia. *Prostate Suppl*, 2, 33-50.
- IVERSEN, P., TYRRELL, C. J., KAISARY, A. V., ANDERSON, J. B., VAN POPPEL, H., TAMMELA, T. L., CHAMBERLAIN, M., CARROLL, K. & MELEZINEK, I. 2000.

- Bicalutamide monotherapy compared with castration in patients with nonmetastatic locally advanced prostate cancer: 6.3 years of followup. *J Urol*, 164, 1579-82.
- IZADPANAH, R., KAUSHAL, D., KRIEDT, C., TSIEN, F., PATEL, B., DUFOUR, J. & BUNNELL, B. A. 2008. Long-term in vitro expansion alters the biology of adult mesenchymal stem cells. *Cancer Res*, 68, 4229-38.
- JACOB, F. & MONOD, J. 1961. Genetic regulatory mechanisms in the synthesis of proteins. *J Mol Biol*, 3, 318-56.
- JAMES, N., SYDES, M., MASON, M., CLARKE, N., DEARNALEY, D., SPEARS, M., MILLMAN, R., PARKER, C., RITCHIE, A., RUSSELL, J., STAFFURTH, J., JONES, R., TOLAN, S., WAGSTAFF, J., PROTHEROE, A., SRINIVASAN, R., BIRTLE, A., O'SULLIVAN, J., CATHOMAS, R. & PARMAR, M. 2015. Docetaxel and/or zoledronic acid for hormone-naïve prostate cancer: First overall survival results from STAMPEDE (NCT00268476). *Journal of Clinical Oncology*, 33, 5001-5001.
- JIAO, J., HINDOYAN, A., WANG, S., TRAN, L. M., GOLDSTEIN, A. S., LAWSON, D., CHEN, D., LI, Y., GUO, C., ZHANG, B., FAZLI, L., GLEAVE, M., WITTE, O. N., GARRAWAY, I. P. & WU, H. 2012. Identification of CD166 as a surface marker for enriching prostate stem/progenitor and cancer initiating cells. *PLoS One*, 7, e42564.
- JOHNSTONE, B., HERING, T. M., CAPLAN, A. I., GOLDBERG, V. M. & YOO, J. U. 1998. In vitro chondrogenesis of bone marrow-derived mesenchymal progenitor cells. *Exp Cell Res*, 238, 265-72.
- KANTOFF, P. W., HIGANO, C. S., SHORE, N. D., BERGER, E. R., SMALL, E. J., PENSON, D. F., REDFERN, C. H., FERRARI, A. C., DREICER, R., SIMS, R. B., XU, Y., FROHLICH, M. W., SCHELLHAMMER, P. F. & INVESTIGATORS, I. S. 2010. Sipuleucel-T immunotherapy for castration-resistant prostate cancer. *N Engl J Med*, 363, 411-22.
- KARANTANOS, T., CORN, P. G. & THOMPSON, T. C. 2013. Prostate cancer progression after androgen deprivation therapy: mechanisms of castrate resistance and novel therapeutic approaches. *Oncogene*, 32, 5501-11.
- KAWAI, J., HIROSE, K., FUSHIKI, S., HIROTSUNE, S., OZAWA, N., HARA, A., HAYASHIZAKI, Y. & WATANABE, S. 1994. Comparison of DNA Methylation Patterns among Mouse-Cell Lines by Restriction Landmark Genomic Scanning. *Molecular and Cellular Biology*, 14, 7421-7427.
- KAWAMURA, N., NIMURA, K., NAGANO, H., YAMAGUCHI, S., NONOMURA, N. & KANEDA, Y. 2015. CRISPR/Cas9-mediated gene knockout of NANOG and NANOGP8 decreases the malignant potential of prostate cancer cells. *Oncotarget*, 6, 22361-22374.
- KEARNS, N. A., PHAM, H., TABAK, B., GENGA, R. M., SILVERSTEIN, N. J., GARBER, M. & MAEHR, R. 2015. Functional annotation of native enhancers with a Cas9-histone demethylase fusion. *Nat Methods*, 12, 401-403.
- KIM, H. & KIM, J. S. 2014. A guide to genome engineering with programmable nucleases. *Nat Rev Genet*, 15, 321-34.
- KIM, J. & COETZEE, G. A. 2004. Prostate specific antigen gene regulation by androgen receptor. *J Cell Biochem*, 93, 233-41.
- KLINGELHUTZ, A. J., FOSTER, S. A. & MCDUGALL, J. K. 1996. Telomerase activation by the E6 gene product of human papillomavirus type 16. *Nature*, 380, 79-82.

- KOGAN, I., GOLDFINGER, N., MILYAVSKY, M., COHEN, M., SHATS, I., DOBLER, G., KLOCKER, H., WASYLYK, B., VOLLER, M., AALDERS, T., SCHALKEN, J. A., OREN, M. & ROTTER, V. 2006. hTERT-immortalized prostate epithelial and stromal-derived cells: an authentic in vitro model for differentiation and carcinogenesis. *Cancer Res*, 66, 3531-40.
- KOLLMEIER, M. A. & ZELEFSKY, M. J. 2012. How to select the optimal therapy for early-stage prostate cancer. *Critical Reviews in Oncology Hematology*, 84, E6-E15.
- KORENCHUK, S., LEHR, J. E., MCLEAN, L., LEE, Y. G., WHITNEY, S., VESSELLA, R., LIN, D. L. & PIENTA, K. J. 2001. VCaP, a cell-based model system of human prostate cancer. *In Vivo*, 15, 163-168.
- KOSICKI, M., TOMBERG, K. & BRADLEY, A. 2018. Repair of double-strand breaks induced by CRISPR-Cas9 leads to large deletions and complex rearrangements. *Nat Biotechnol*, 36, 765-771.
- KOUDINOVA, N. V., PINTHUS, J. H., BRANDIS, A., BRENNER, O., BENDEL, P., RAMON, J., ESHHAR, Z., SCHERZ, A. & SALOMON, Y. 2003. Photodynamic therapy with Pd-Bacteriopheophorbide (TOOKAD): successful in vivo treatment of human prostatic small cell carcinoma xenografts. *Int J Cancer*, 104, 782-9.
- KOUKOURAKIS, G., KELEKIS, N., ARMONIS, V. & KOULOULIAS, V. 2009. Brachytherapy for prostate cancer: a systematic review. *Adv Urol*, 327945.
- KUNDERFRANCO, P., MELLO-GRAND, M., CANGEMI, R., PELLINI, S., MENSAH, A., ALBERTINI, V., MALEK, A., CHIORINO, G., CATAPANO, C. V. & CARBONE, G. M. 2010. ETS transcription factors control transcription of EZH2 and epigenetic silencing of the tumor suppressor gene Nkx3.1 in prostate cancer. *PLoS One*, 5, e10547.
- KWABI-ADDO, B., OZEN, M. & ITTMANN, M. 2004. The role of fibroblast growth factors and their receptors in prostate cancer. *Endocrine-Related Cancer*, 11, 709-724.
- KYPRIANOU, N. & ISAACS, J. T. 1988. Activation of programmed cell death in the rat ventral prostate after castration. *Endocrinology*, 122, 552-62.
- LAI, K. P., YAMASHITA, S., VITKUS, S., SHYR, C. R., YEH, S. & CHANG, C. 2012. Suppressed prostate epithelial development with impaired branching morphogenesis in mice lacking stromal fibromuscular androgen receptor. *Mol Endocrinol*, 26, 52-66.
- LAMB, L. E., KNUDSEN, B. S. & MIRANTI, C. K. 2010. E-cadherin-mediated survival of androgen-receptor-expressing secretory prostate epithelial cells derived from a stratified in vitro differentiation model. *J Cell Sci*, 123, 266-76.
- LANG, S. H., SMITH, J., HYDE, C., MACINTOSH, C., STOWER, M. & MAITLAND, N. J. 2006. Differentiation of prostate epithelial cell cultures by Matrigel/stromal cell glandular reconstruction. *In Vitro Cellular & Developmental Biology-Animal*, 42, 273-280.
- LANG, S. H., STARK, M., COLLINS, A., PAUL, A. B., STOWER, M. J. & MAITLAND, N. J. 2001. Experimental prostate epithelial morphogenesis in response to stroma and three-dimensional matrigel culture. *Cell Growth & Differentiation*, 12, 631-640.
- LANG, S. H., STOWER, M. & MAITLAND, N. J. 2000. In vitro modelling of epithelial and stromal interactions in non-malignant and malignant prostates. *British Journal of Cancer*, 82, 990-997.

- LEE, S. O., TIAN, J., HUANG, C. K., MA, Z. F., LAI, K. P., HSIAO, H. M., JIANG, M., YEH, S. Y. & CHANG, C. S. 2012. Suppressor role of androgen receptor in proliferation of prostate basal epithelial and progenitor cells. *Journal of Endocrinology*, 213, 173-182.
- LI, C., DU, Y., YANG, Z., HE, L. Y., WANG, Y. Y., HAO, L., DING, M. X., YAN, R. P., WANG, J. S. & FAN, Z. S. 2016. GALNT1-Mediated Glycosylation and Activation of Sonic Hedgehog Signaling Maintains the Self-Renewal and Tumor-Initiating Capacity of Bladder Cancer Stem Cells. *Cancer Research*, 76, 1273-1283.
- LI, C., HEIDT, D. G., DALERBA, P., BURANT, C. F., ZHANG, L., ADSAY, V., WICHA, M., CLARKE, M. F. & SIMEONE, D. M. 2007. Identification of pancreatic cancer stem cells. *Cancer Res*, 67, 1030-7.
- LI, Y., HWANG, T. H., OSETH, L. A., HAUGE, A., VESSELLA, R. L., SCHMECHEL, S. C., HIRSCH, B., BECKMAN, K. B., SILVERSTEIN, K. A. & DEHM, S. M. 2012. AR intragenic deletions linked to androgen receptor splice variant expression and activity in models of prostate cancer progression. *Oncogene*, 31, 4759-4767.
- LING, M. T., CHAN, K. W. & CHOO, C. K. 2001. Androgen induces differentiation of a human papillomavirus 16 E6/E7 immortalized prostate epithelial cell line. *Journal of Endocrinology*, 170, 287-296.
- LIU, A. Y., TRUE, L. D., LATRAY, L., NELSON, P. S., ELLIS, W. J., VESSELLA, R. L., LANGE, P. H., HOOD, L. & VANDENENGH, G. 1997. Cell-cell interaction in prostate gene regulation and cytodifferentiation. *Proceedings of the National Academy of Sciences of the United States of America*, 94, 10705-10710.
- LIU, J., PASCAL, L. E., ISHARWAL, S., METZGER, D., GARCIA, R. R., PILCH, J., KASPER, S., WILLIAMS, K., BASSE, P. H., NELSON, J. B., CHAMBON, P. & WANG, Z. 2011. Regenerated Luminal Epithelial Cells Are Derived from Preexisting Luminal Epithelial Cells in Adult Mouse Prostate. *Molecular Endocrinology*, 25, 1849-1857.
- LIVERMORE, K. E., MUNKLEY, J. & ELLIOT, D. J. 2016. Androgen receptor and prostate cancer. *Aims Molecular Science*, 3, 280-299.
- LUCIA, M. S. & LAMBERT, J. R. 2008. Growth factors in benign prostatic hyperplasia: basic science implications. *Curr Urol Rep*, 9, 272-8.
- MA, D. Z., GAO, P. F., QIAN, L. L., WANG, Q. Q., CAI, C. B., JIANG, S. W., XIAO, G. J. & CUI, W. T. 2015. Over-Expression of Porcine Myostatin Missense Mutant Leads to A Gender Difference in Skeletal Muscle Growth between Transgenic Male and Female Mice. *International Journal of Molecular Sciences*, 16, 20020-20032.
- MADERSBACHER, S., PEDEVILLA, M., VINGERS, L., SUSANI, M. & MARBERGER, M. 1995. Effect of High-Intensity Focused Ultrasound on Human Prostate-Cancer in-Vivo. *Cancer Research*, 55, 3346-3351.
- MAEDER, M. L., LINDER, S. J., CASCIO, V. M., FU, Y., HO, Q. H. & JOUNG, J. K. 2013. CRISPR RNA-guided activation of endogenous human genes. *Nat Methods*, 10, 977-9.
- MAITLAND, N. J. 2013. Stem Cells in the Normal and Malignant Prostate. In: TINDALL, D. J. (ed.) *Prostate Cancer: Biochemistry, Molecular Biology and Genetics*. New York, NY: Springer New York.
- MAITLAND, N. J. & COLLINS, A. T. 2008. Prostate cancer stem cells: a new target for therapy. *J Clin Oncol*, 26, 2862-70.

- MAITLAND, N. J., MACINTOSH, C. A., HALL, J., SHARRARD, M., QUINN, G. & LANG, S. 2001. In vitro models to study cellular differentiation and function in human prostate cancers. *Radiat Res*, 155, 133-142.
- MALI, P., ESVELT, K. M. & CHURCH, G. M. 2013. Cas9 as a versatile tool for engineering biology. *Nature Methods*, 10, 957-963.
- MARTINCORENA, I., RAINE, K. M., GERSTUNG, M., DAWSON, K. J., HAASE, K., VAN LOO, P., DAVIES, H., STRATTON, M. R. & CAMPBELL, P. J. 2017. Universal Patterns of Selection in Cancer and Somatic Tissues. *Cell*, 171, 1029-+.
- MCCUTCHEON, S. R., CHIU, K. L., LEWIS, D. D. & TAN, C. 2018. CRISPR-Cas Expands Dynamic Range of Gene Expression From T7RNAP Promoters. *Biotechnology Journal*, 13.
- MCNEAL, J. E. 1981. The Zonal Anatomy of the Prostate. *Prostate*, 2, 35-49.
- MEISSNER, A., MIKKELSEN, T. S., GU, H. C., WERNIG, M., HANNA, J., SIVACHENKO, A., ZHANG, X. L., BERNSTEIN, B. E., NUSBAUM, C., JAFFE, D. B., GNIRKE, A., JAENISCH, R. & LANDER, E. S. 2008. Genome-scale DNA methylation maps of pluripotent and differentiated cells. *Nature*, 454, 766-U91.
- MIKI, J., FURUSATO, B., LI, H. Z., GU, Y. P., TAKAHASHI, H., EGAWA, S., SESTERHENN, I. A., MCLEOD, D. G., SRIVASTAVA, S. & RHIM, J. S. 2007. Identification of putative stem cell markers, CD133 and CXCR4, in hTERT-immortalized primary nonmalignant and malignant tumor-derived human prostate epithelial cell lines and in prostate cancer specimens. *Cancer Research*, 67, 3153-3161.
- MJONES, P., SAGATUN, L., NORDRUM, I. S. & WALDUM, H. L. 2017. Neuron-Specific Enolase as an Immunohistochemical Marker Is Better Than Its Reputation. *Journal of Histochemistry & Cytochemistry*, 65, 687-703.
- MOORE, C. M., PENDSE, D. & EMBERTON, M. 2009. Photodynamic therapy for prostate cancer--a review of current status and future promise. *Nat Clin Pract Urol*, 6, 18-30.
- MOSCOU, M. J. & BOGDANOVA, A. J. 2009. A simple cipher governs DNA recognition by TAL effectors. *Science*, 326, 1501.
- MOSES, C., GARCIA-BLOJ, B., HARVEY, A. R. & BLANCAFORT, P. 2018. Hallmarks of cancer: The CRISPR generation. *Eur J Cancer*, 93, 10-18.
- MYERS, R. B. & GRIZZLE, W. E. 1996. Biomarker expression in prostatic intraepithelial neoplasia. *Eur Urol*, 30, 153-66.
- NIU, Y. J., ALTUWAIJRI, S., LAI, K. P., WU, C. T., RICKE, W. A., MESSING, E. M., YAO, J., YEH, S. & CHANG, C. 2008. Androgen receptor is a tumor suppressor and proliferator in prostate cancer. *Proceedings of the National Academy of Sciences of the United States of America*, 105, 12182-12187.
- NOMURA, T. & MIMATA, H. 2012. Focal therapy in the management of prostate cancer: an emerging approach for localized prostate cancer. *Adv Urol*, 2012, 391437.
- NOWELL, P. C. 1976. The clonal evolution of tumor cell populations. *Science*, 194, 23-8.
- OBORT, A., AJADI, M. & AKINLOYE, O. 2013. Prostate-Specific Antigen: Any Successor in Sight? *Rev Urol*, 15, 97-107.
- OJEH, N., PASTAR, I., TOMIC-CANIC, M. & STOJADINOVIC, O. 2015. Stem Cells in Skin Regeneration, Wound Healing, and Their Clinical Applications. *International Journal of Molecular Sciences*, 16, 25476-25501.

- OLDRIDGE, E. E., PELLACANI, D., COLLINS, A. T. & MAITLAND, N. J. 2012. Prostate cancer stem cells: Are they androgen-responsive? *Molecular and Cellular Endocrinology*, 360, 14-24.
- OLSEN, J. R., AZEEM, W., HELLEM, M. R., MARVYIN, K., HUA, Y. P., QU, Y., LI, L. S., LIN, B. Y., KE, X. S., OYAN, A. M. & KALLAND, K. H. 2016. Context dependent regulatory patterns of the androgen receptor and androgen receptor target genes. *Bmc Cancer*, 16.
- PACKER, J. R. & MAITLAND, N. J. 2016. The molecular and cellular origin of human prostate cancer. *Biochimica Et Biophysica Acta-Molecular Cell Research*, 1863, 1238-1260.
- PAL, S., GUPTA, R. & DAVULURI, R. V. 2012. Alternative transcription and alternative splicing in cancer. *Pharmacology & Therapeutics*, 136, 283-294.
- PALLER, C. J. & ANTONARAKIS, E. S. 2011. Cabazitaxel: a novel second-line treatment for metastatic castration-resistant prostate cancer. *Drug Des Devel Ther*, 5, 117-24.
- PAVLETICH, N. P. & PABO, C. O. 1991. Zinc Finger DNA Recognition - Crystal-Structure of a Zif268-DNA Complex at 2.1-Å. *Science*, 252, 809-817.
- PELLACANI, D., KESTORAS, D., DROOP, A. P., FRAME, F. M., BERRY, P. A., LAWRENCE, M. G., STOWER, M. J., SIMMS, M. S., MANN, V. M., COLLINS, A. T., RISBRIDGER, G. P. & MAITLAND, N. J. 2014. DNA hypermethylation in prostate cancer is a consequence of aberrant epithelial differentiation and hyperproliferation. *Cell Death and Differentiation*, 21, 761-773.
- PERSAD, R. 2002. Leuprorelin acetate in prostate cancer: A European update. *International Journal of Clinical Practice*, 56, 389-396.
- PILLAI, S., BIKLE, D. D., MANCIANTI, M. L., CLINE, P. & HINCENBERGS, M. 1990. Calcium Regulation of Growth and Differentiation of Normal Human Keratinocytes - Modulation of Differentiation Competence by Stages of Growth and Extracellular Calcium. *Journal of Cellular Physiology*, 143, 294-302.
- PLANZ, B., WANG, Q. F., KIRLEY, S. D., LIN, C. W. & MCDUGAL, W. S. 1998. Androgen responsiveness of stromal cells of the human prostate: Regulation of cell proliferation and keratinocyte growth factor by androgen. *Journal of Urology*, 160, 1850-1855.
- POLSON, E. S., LEWIS, J. L., CELIK, H., MANN, V. M., STOWER, M. J., SIMMS, M. S., RODRIGUES, G., COLLINS, A. T. & MAITLAND, N. J. 2013. Monoallelic expression of TMPRSS2/ERG in prostate cancer stem cells. *Nature Communications*, 4.
- PRINS, G. S., BIRCH, L. & GREENE, G. L. 1991. Androgen Receptor Localization in Different Cell-Types of the Adult-Rat Prostate. *Endocrinology*, 129, 3187-3199.
- PUTZI, M. J. & DE MARZO, A. M. 2000. Morphologic transitions between proliferative inflammatory atrophy and high-grade prostatic intraepithelial neoplasia. *Urology*, 56, 828-832.
- QI, L. S., LARSON, M. H., GILBERT, L. A., DOUDNA, J. A., WEISSMAN, J. S., ARKIN, A. P. & LIM, W. A. 2013. Repurposing CRISPR as an RNA-Guided Platform for Sequence-Specific Control of Gene Expression. *Cell*, 152, 1173-1183.
- QIN, Z. Q., LI, X., HAN, P., ZHENG, Y. X., LIU, H. Y., TANG, J. Y., YANG, C. D., ZHANG, J. Z., WANG, K. P., QI, X. K., TANG, M., WANG, W. & ZHANG, W. 2017. Association between polymorphic CAG repeat lengths in the androgen receptor gene and

- susceptibility to prostate cancer A systematic review and meta-analysis. *Medicine*, 96.
- RANE, J. K., DROOP, A. P., PELLACANI, D., POLSON, E. S., SIMMS, M. S., COLLINS, A. T., CAVES, L. S. D. & MAITLAND, N. J. 2014. Conserved Two-Step Regulatory Mechanism of Human Epithelial Differentiation. *Stem Cell Reports*, 2, 180-188.
- RAY, F. A., PEABODY, D. S., COOPER, J. L., CRAM, L. S. & KRAEMER, P. M. 1990. Sv40-T Antigen Alone Drives Karyotype Instability That Precedes Neoplastic Transformation of Human-Diploid Fibroblasts. *Journal of Cellular Biochemistry*, 42, 13-31.
- RICCI-VITIANI, L., LOMBARDI, D. G., PILOZZI, E., BIFFONI, M., TODARO, M., PESCHLE, C. & DE MARIA, R. 2007. Identification and expansion of human colon-cancer-initiating cells. *Nature*, 445, 111-115.
- RICHARDSON, G. D., ROBSON, C. N., LANG, S. H., NEAL, D. E., MAITLAND, N. J. & COLLINS, A. T. 2004. CD133, a novel marker for human prostatic epithelial stem cells. *Journal of Cell Science*, 117, 3539-3545.
- RISSTALPERS, C., VERLEUNMOOIJMAN, M. C. T., TRAPMAN, J. & BRINKMANN, A. O. 1993. Threonine on Amino-Acid Position-868 in the Human Androgen Receptor Is Essential for Androgen-Binding Specificity and Functional-Activity. *Biochemical and Biophysical Research Communications*, 196, 173-180.
- RIVERA-GONZALEZ, G. C., DROOP, A. P., RIPPON, H. J., TIEMANN, K., PELLACANI, D., GEORGOPOULOS, L. J. & MAITLAND, N. J. 2012. Retinoic acid and androgen receptors combine to achieve tissue specific control of human prostatic transglutaminase expression: a novel regulatory network with broader significance. *Nucleic Acids Research*, 40, 4825-4840.
- RUSKA, K. M., SAUVAGEOT, J. & EPSTEIN, J. I. 1998. Histology and cellular kinetics of prostatic atrophy. *American Journal of Surgical Pathology*, 22, 1073-1077.
- SANDER, J. D. & JOUNG, J. K. 2014. CRISPR-Cas systems for editing, regulating and targeting genomes. *Nature Biotechnology*, 32, 347-355.
- SCHEFFNER, M., WERNESS, B. A., HUIBREGTSE, J. M., LEVINE, A. J. & HOWLEY, P. M. 1990. The E6 Oncoprotein Encoded by Human Papillomavirus Type-16 and Type-18 Promotes the Degradation of P53. *Cell*, 63, 1129-1136.
- SCHER, H. I., FIZAZI, K., SAAD, F., TAPLIN, M. E., STERNBERG, C. N., MILLER, K., DE WIT, R., MULDER, P., CHI, K. N., SHORE, N. D., ARMSTRONG, A. J., FLAIG, T. W., FLECHON, A., MAINWARING, P., FLEMING, M., HAINSWORTH, J. D., HIRMAND, M., SELBY, B., SEELY, L., DE BONO, J. S. & INVESTIGATORS, A. 2012. Increased Survival with Enzalutamide in Prostate Cancer after Chemotherapy. *New England Journal of Medicine*, 367, 1187-1197.
- SCHUMANN, K., LIN, S., BOYER, E., SIMEONOV, D. R., SUBRAMANIAM, M., GATE, R. E., HALIBURTON, G. E., YEE, C. J., BLUESTONE, J. A., DOUDNA, J. A. & MARSON, A. 2015. Generation of knock-in primary human T cells using Cas9 ribonucleoproteins. *Proceedings of the National Academy of Sciences of the United States of America*, 112, 10437-10442.
- SHARMA, P. & SCHREIBER-AGUS, N. 1999. Mouse models of prostate cancer. *Oncogene*, 18, 5349-55.
- SHERWOOD, E. R., BERG, L. A., MITCHELL, N. J., MCNEAL, J. E., KOZLOWSKI, J. M. & LEE, C. 1990. Differential cytokeratin expression in normal, hyperplastic and malignant epithelial cells from human prostate. *J Urol*, 143, 167-71.

- SHI, J., WANG, E., MILAZZO, J. P., WANG, Z., KINNEY, J. B. & VAKOC, C. R. 2015. Discovery of cancer drug targets by CRISPR-Cas9 screening of protein domains. *Nat Biotechnol*, 33, 661-7.
- SIMANAINEN, U., ALLAN, C. M., LIM, P., MCPHERSON, S., JIMENEZ, M., ZAJAC, J. D., DAVEY, R. A. & HANDELSMAN, D. J. 2007. Disruption of prostate epithelial androgen receptor impedes prostate lobe-specific growth and function. *Endocrinology*, 148, 2264-72.
- SMITH, B. A., SOKOLOV, A., UZUNANGELOV, V., BAERTSCH, R., NEWTON, Y., GRAIM, K., MATHIS, C., CHENG, D., STUART, J. M. & WITTE, O. N. 2015. A basal stem cell signature identifies aggressive prostate cancer phenotypes. *Proc Natl Acad Sci U S A*, 112, E6544-52.
- SMITH, M., BIGGAR, S. & HUSSAIN, M. 1995. Prostate-Specific Antigen Messenger-Rna Is Expressed in Non-Prostate Cells - Implications for Detection of Micrometastases. *Cancer Research*, 55, 2640-2644.
- SOMMERFELD, H. J., MEEKER, A. K., PIATYSZEK, M. A., BOVA, G. S., SHAY, J. W. & COFFEY, D. S. 1996. Telomerase activity: A prevalent marker of malignant human prostate tissue. *Cancer Research*, 56, 218-222.
- STEINBERG, M. 2009. Degarelix: A Gonadotropin-Releasing Hormone Antagonist for the Management of Prostate Cancer. *Clinical Therapeutics*, 31, 2312-2331.
- STEINESTEL, J., LUEDEKE, M., ARNDT, A., SCHNOELLER, T., LENNERZ, J. K., MAIER, C., CRONAUER, M., STEINESTEL, K., BOEGEMANN, M. & SCHRADER, A. J. 2015. Detecting predictive androgen receptor modifications in circulating prostate cancer cells. *Journal of Clinical Oncology*, 33.
- STEWART, N., BACCHETTI, S. 1991. Expression of SV40 large T antigen, but not small t antigen, is required for the induction of chromosomal aberrations in transformed human cells. *Virology*, 180, 49-57.
- SUN, S. H., SPRENGER, C. C. T., VESSELLA, R. L., HAUGK, K., SORIANO, K., MOSTAGHEL, E. A., PAGE, S. T., COLEMAN, I. M., NGUYEN, H. M., SUN, H. Y., NELSON, P. S. & PLYMATE, S. R. 2010. Castration resistance in human prostate cancer is conferred by a frequently occurring androgen receptor splice variant. *Journal of Clinical Investigation*, 120, 2715-2730.
- SWIFT, S. L., BURNS, J. E. & MAITLAND, N. J. 2010. Altered Expression of Neurotensin Receptors Is Associated with the Differentiation State of Prostate Cancer. *Cancer Research*, 70, 347-356.
- TAKAO, A., YOSHIKAWA, K., KARNAN, S., OTA, A., UEMURA, H., DE VELASCO, M. A., KURA, Y., SUZUKI, S., UEDA, R., NISHINO, T. & HOSOKAWA, Y. 2018. Generation of PTENknockout (*/*) murine prostate cancer cells using the CRISPR/Cas9 system and comprehensive gene expression profiling. *Oncol Rep*, 40, 2455-2466.
- TAUROZZI, A. 2016. *Genetic and Epigenetic Profiling of Human Prostate Cancer Cell-Subsets*. PhD, University of York.
- TOIVANEN, R. & SHEN, M. M. 2017. Prostate organogenesis: tissue induction, hormonal regulation and cell type specification. *Development*, 144, 1382-1398.
- TOMLINS, S. A., RHODES, D. R., PERNER, S., DHANASEKARAN, S. M., MEHRA, R., SUN, X. W., VARAMBALLY, S., CAO, X., TCHINDA, J., KUEFER, R., LEE, C., MONTIE, J. E., SHAH, R. B., PIENTA, K. J., RUBIN, M. A. & CHINNAIYAN, A. M. 2005.

- Recurrent fusion of TMPRSS2 and ETS transcription factor genes in prostate cancer. *Science*, 310, 644-8.
- TYSON, D. R., INOKUCHI, J., TSUNODA, T., LAU, A. & ORNSTEIN, D. K. 2007. Culture requirements of prostatic epithelial cell lines for acinar morphogenesis and lumen formation in vitro: role of extracellular calcium. *Prostate*, 67, 1601-13.
- VALASTYAN, S. & WEINBERG, R. A. 2011. Tumor metastasis: molecular insights and evolving paradigms. *Cell*, 147, 275-92.
- VERHAGEN, A. P., RAMAEKERS, F. C., AALDERS, T. W., SCHAAFSMA, H. E., DEBRUYNE, F. M. & SCHALKEN, J. A. 1992. Colocalization of basal and luminal cell-type cytokeratins in human prostate cancer. *Cancer Res*, 52, 6182-7.
- VISAKORPI, T., HYYTINEN, E., KOIVISTO, P., TANNER, M., KEINANEN, R., PALMBERG, C., PALOTIE, A., TAMMELA, T., ISOLA, J. & KALLIONIEMI, O. P. 1995. In vivo amplification of the androgen receptor gene and progression of human prostate cancer. *Nat Genet*, 9, 401-6.
- VON ZGLINICKI, T. 2002. Oxidative stress shortens telomeres. *Trends in Biochemical Sciences*, 27, 339-344.
- WALLEN, M. J., LINJA, M., KAARTINEN, K., SCHLEUTKER, J. & VISAKORPI, T. 1999. Androgen receptor gene mutations in hormone-refractory prostate cancer. *J Pathol*, 189, 559-63.
- WANG, T., WEI, J. J., SABATINI, D. M. & LANDER, E. S. 2014. Genetic Screens in Human Cells Using the CRISPR-Cas9 System. *Science*, 343, 80-84.
- WANG, X., KRUIHOF-DE JULIO, M., ECONOMIDES, K. D., WALKER, D., YU, H. L., HALILI, M. V., HU, Y. P., PRICE, S. M., ABATE-SHEN, C. & SHEN, M. M. 2009. A luminal epithelial stem cell that is a cell of origin for prostate cancer. *Nature*, 461, 495-U61.
- WEBBER, M. M., BELLO, D., KLEINMAN, H. K. & HOFFMAN, M. P. 1997. Acinar differentiation by non-malignant immortalized human prostatic epithelial cells and its loss by malignant cells. *Carcinogenesis*, 18, 1225-1231.
- WEI, C., WANG, F., LIU, W., ZHAO, W., YANG, Y., LI, K., XIAO, L. & SHEN, J. 2018. CRISPR/Cas9 targeting of the androgen receptor suppresses the growth of LNCaP human prostate cancer cells. *Mol Med Rep*, 17, 2901-2906.
- WEIDONG, H. 2018. Study of CRISPR-Cas9 Mediated PD-1 and TCR Gene-knocked Out Mesothelin-directed CAR-T Cells in Patients With Mesothelin Positive Multiple Solid Tumors.
- WHITACRE, D. C., CHAUHAN, S., DAVIS, T., GORDON, D., CRESS, A. E. & MIESFELD, R. L. 2002. Androgen induction of in vitro prostate cell differentiation. *Cell Growth & Differentiation*, 13, 1-11.
- WIEDENMANN, B., FRANKE, W. W., KUHN, C., MOLL, R. & GOULD, V. E. 1986. Synaptophysin - a Marker Protein for Neuroendocrine Cells and Neoplasms. *Proceedings of the National Academy of Sciences of the United States of America*, 83, 3500-3504.
- WOODS, C., LEFEUVRE, C., STEWART, N. & BACCHETTI, S. 1994. Induction of Genomic Instability in Sv40-Transformed Human-Cells - Sufficiency of the N-Terminal-147 Amino-Acids of Large T-Antigen and Role of Prb and P53. *Oncogene*, 9, 2943-2950.
- WU, C. T., ALTUWAIJRI, S., RICKE, W. A., HUANG, S. P., YEH, S. Y., ZHANG, C. X., NIU, Y. J., TSAI, M. Y. & CHANG, C. S. 2007. Increased prostate cell proliferation and

- loss of cell differentiation in mice lacking prostate epithelial androgen receptor. *Proceedings of the National Academy of Sciences of the United States of America*, 104, 12679-12684.
- WYMENGA, L. F. A., WISMAN, G. B. A., VEENSTRA, R., RUITERS, M. H. J. & MENSINK, H. J. A. 2000. Telomerase activity in needle biopsies from prostate cancer and benign prostates. *European Journal of Clinical Investigation*, 30, 330-335.
- XIE, Q., LIU, Y. L., CAI, T., HORTON, C., STEFANSON, J. & WANG, Z. A. 2017. Dissecting cell-type-specific roles of androgen receptor in prostate homeostasis and regeneration through lineage tracing. *Nature Communications*, 8.
- XIN, L., LAWSON, D. A. & WITTE, O. N. 2005. The Sca-1 cell surface marker enriches for a prostate-regenerating cell subpopulation that can initiate prostate tumorigenesis. *Proc Natl Acad Sci U S A*, 102, 6942-7.
- XUE, Y., SMEDTS, F., DEBRUYNE, F. M. J., DE LA ROSETTE, J. J. M. C. H. & SCHALKEN, J. A. 1998. Identification of intermediate cell types by keratin expression in the developing human prostate. *Prostate*, 34, 292-301.
- YAO, J. C., PAVEL, M., PHAN, A. T., KULKE, M. H., HOOSEN, S., PETER, J. S., CHERFI, A. & OBERG, K. E. 2011. Chromogranin A and Neuron-Specific Enolase as Prognostic Markers in Patients with Advanced pNET Treated with Everolimus. *Journal of Clinical Endocrinology & Metabolism*, 96, 3741-3749.
- YE, R. S., PI, M., COX, J. V., NISHIMOTO, S. K. & QUARLES, L. D. 2017. CRISPR/Cas9 targeting of GPRC6A suppresses prostate cancer tumorigenesis in a human xenograft model. *Journal of Experimental & Clinical Cancer Research*, 36.
- YU, S. Q., YE, C. R., NIU, Y. J., CHANG, H. C., TSAI, Y. C., MOSES, H. L., SHYR, C. R., CHANG, C. S. & YE, S. Y. 2012. Altered prostate epithelial development in mice lacking the androgen receptor in stromal fibroblasts. *Prostate*, 72, 437-449.
- ZANONI, M., PICCININI, F., ARIENTI, C., ZAMAGNI, A., SANTI, S., POLICO, R., BEVILACQUA, A. & TESEI, A. 2016. 3D tumor spheroid models for in vitro therapeutic screening: a systematic approach to enhance the biological relevance of data obtained. *Scientific Reports*, 6.